2010

Influence of post-consumer recycled asphalt shingles on hot mix asphalt containing fractionated recycled asphalt pavement

Andrew Aaron Cascione
Iowa State University

Influence of post-consumer recycled asphalt shingles on hot mix asphalt containing fractionated recycled asphalt pavement

by

Andrew Aaron Cascione

A thesis submitted to the graduate faculty

in partial fulfillment of the requirements for the degree of

MASTER OF SCIENCE

Major: Civil Engineering (Civil Engineering Materials)

Program of Study Committee:
R. Christopher Williams, Major Professor
Vernon R. Schaefer
W. Robert Stephenson

Iowa State University

Ames, Iowa

2010

ACKNOWLEDGEMENTS

I would like to express thanks to Steve Gillen at the Illinois Tollway Authority, Ross Bentsen at the Bloom Companies, Jay Benke at STATE Testing, Brett Williams at Rock Road Companies, and Debra Haugen for their assistance in obtaining samples during the field demonstration project and serving as points of contact to discuss the project.

I would also like to thank my advisor Dr. Chris Williams for his support, guidance, and leadership throughout the course of my graduate studies and this research.

In addition, I wish to thank Dr. Schaefer and Dr. Stephenson for being part of my advisory committee. Their support and cooperation is very much appreciated.

I would also like to thank Chris Pross and Jianhua Yu who helped perform part of the lab work.

TABLE OF CONTENTS

LIST OF TABLES

LIST OF FIGURES

ABSTRACT

As the cost of construction materials continue to rise and place financial constraints on transportation agencies, engineers are looking for sustainable methods that minimize construction costs and optimize the selection of materials used in asphalt pavements. Two methods that are beginning to receive considerable attention for highway construction are adding post-consumer recycled asphalt shingles (RAS) to hot mix asphalt (HMA) and increasing the percentage of reclaimed asphalt pavement being added to HMA through the process of fractionation.

The objective of this research is to characterize the effects of post-consumer RAS on the laboratory performance of HMA and its compatibility with fractionated recycled asphalt pavement (FRAP).

In the summer of 2009, a field demonstration project was conducted by the Illinois Tollway on the Jane Addams Memorial Tollway (I-90). Eight mix designs containing zero or five percent RAS and varying percentages of FRAP were developed and placed in the pavement shoulder. Production and laboratory prepared samples of the mixes were obtained for dynamic modulus, flow number, moisture sensitivity, beam fatigue, and fracture energy tests in addition to binder extraction and subsequent characterization. From the dynamic modulus testing, master curves were constructed to characterize the stress/strain response of the HMA samples. From the extracted binders, a suite of Superpave tests was conducted at different temperatures and frequencies to build master curves for analyzing how the addition of RAS binder affected the rheological properties of the mix binder blend. A statistical analysis was performed on the dynamic modulus and flow number test results to determine how the behavior of the asphalt materials containing RAS differed from the behavior of the

asphalt materials not containing RAS when varying percentages of FRAP were a part of the mix designs.

Laboratory test results indicate that the mixes containing five percent RAS with less than 40 percent recycled materials exhibit an increased resistance to permanent deformation while maintaining satisfactory performance to fatigue stresses, low temperature cracking, and freeze-thaw durability. Although the low temperature binder performance grade increased with the addition of recycled materials, the mix performance test results did not follow that trend, indicating fibers in the RAS materials likely contributed to the performance of the mixtures.

CHAPTER 1: INTRODUCTION

1.1 Background

Transportation agencies are increasingly investigating new technologies that will reduce the cost of asphalt pavement materials while maximizing long-term performance. According to the American Society of Civil Engineer's (ASCE) 2009 Infrastructure Report Card, 186 billion dollars is needed annually for rehabilitation and maintenance of United State roadways, but only 70.6 billion dollars is spent annually. Since 96 percent of hard surfaced roadways in the United States are paved with asphalt, there is a strong need for lowering the cost of asphalt pavements that also meet superior performance standards of being safe, smooth, and structurally capable of supporting heavy traffic loads. The need for well performing asphalt pavements together with the rising prices of liquid asphalt and the scarcity of quality aggregates have placed additional pressure on agencies and owners to create effective economic solutions.

The cost of asphalt materials can be reduced by replacing the new (virgin) asphalt cement and mineral aggregates with recycled products derived from construction waste or byproducts that contain asphalt mix components. Using recycled products saves not only on the cost of asphalt materials, but also on the amount of construction waste since it is not being placed in landfills. Recycling products into asphalt pavement also means less energy is needed to produce the pavement, making it a more sustainable product that minimizes its impact on the environment. Furthermore, properly designed asphalt mixes that contain recycled products can exhibit no performance differences or even improved performance for certain applications compared to typical mixes (Al-Qadi et al. 2007).

The most common source for secondary materials comes from reclaimed asphalt pavement (RAP). RAP is old pavement that has been milled from the roadway, crushed into smaller aggregates sizes, and stockpiled. At the end of an asphalt pavement's service life, the pavement is still valuable since it contains mineral aggregates and asphalt cement that can be reheated and reincorporated with new hot mix asphalt (HMA). The Federal Highway Administration (FHWA) and the Environmental Protection Agency (EPA) report that of the 100.1 million tons of asphalt pavement removed each year, 80.3 million tons is reused as part of new roads, roadbeds, shoulders, and embankments, making asphalt America's number one recycled material (FHWA, 1993).

Most transportation agencies have a construction specification in place that allows asphalt producers to add RAP to HMA, but only up to a certain percentage, typically 25 percent. By increasing the amount of RAP usage, the cost of asphalt pavement can be even further reduced. Adding higher amounts of RAP to HMA reduces the amount of control engineers have when combining different crushed aggregate sizes to formulate a well-performing mixture. Since a typical RAP stockpile contains aggregate particles of varying sizes and binder contents, increasing the RAP content in pavements can increase the variability of the HMA end product (NCHRP 2001). To maintain quality and consistency of mixes when increasing the RAP percentage, RAP can be fractionated into stockpiles of different sizes similar to the processing of virgin aggregates. Thus, using fractionated reclaimed asphalt pavement (FRAP) allows for an increase in the level of quality control during the construction process, which in turn allows higher RAP mixes to be produced more consistently. Nationally, the concept of fractionating RAP is becoming recognized as an efficient way to lower the cost of a new mix and reduce the inconsistencies of the high RAP

mix properties without sacrificing quality (Vavrik et al. 2008). With this advancement in technology, research efforts of transportation agencies have focused on increasing RAP usage up to 50 percent.

Another source for secondary materials is recycled asphalt shingles (RAS). Asphalt shingles, like RAP, also contain mineral aggregates and asphalt cement, making RAS a candidate for product replacement in HMA. RAS comes from two difference sources, post-manufactured shingles and post-consumer shingles. Post-manufactured shingles are the waste products of the shingle manufacturing process, which include factory rejects and tab cut-outs, while post-consumer shingles are shingles that come directly from roofs of commercial and residential buildings after their service life including damage from severe weather. Historically, the vast majority of research on RAS has focused on post-manufactured shingles since government engineers and regulators have traditionally accepted post-manufactured shingles over post-consumer shingles in the development of construction materials specifications and environmental regulations. With more recent technological advances in processing asphalt shingles, research efforts are trending towards the utilization of post-consumer shingles. A major factor driving this interest is that ten million tons of post-consumer shingles are placed in landfills in the United States each year, while only one million tons of post-manufactured shingles are placed in landfills each year (FHWA and EPA 1993). With this large pool of post-consumer shingle resource, there is significant potential for cost savings in mix constituents and landfill space.

Recycling manufactured shingle scrap has been occurring for the last 25 years due to the many applications of RAS as a construction material (Krivit and Associates 2007). RAS has been used mostly as a secondary material for HMA in commercial and private

pavements. Recently, it has become more widely used in highway pavements by transportation agencies.

1.2 Problem Statement

One transportation agency evaluating options that minimize construction costs and optimize the selection of materials used in their asphalt pavements is the Illinois Tollway (Tollway). The Tollway is a user-supported system of public roadways. The Tollway receives no state or federal funding for maintenance and operation of its system, relying primarily on tolls paid by travelers on the roadway (Bentsen 2010).

Over the last few years, the Tollway has begun implementing an unprecedented rehabilitation/expansion program for its highway network. Due to financial constraints, economic demands, and the need to improve as much of the network as possible, it faces many challenges as it continues to update its system of roadways. Therefore, it is important for the Tollway to look to new technologies for solutions that answer the economic and performance challenges they face.

With more transportation agencies studying the options of adding RAS or using higher amounts of RAP through fractionation, the Tollway became interested in adopting these techniques in their construction specifications. In a partnership with the U.S. EPA, the Tollway and the U.S. EPA selected Iowa State University to conduct research investigating the performance of asphalt pavements with RAS that contain higher amounts of fractionated RAP. The results of this research project are presented herein for this thesis.

1.3 Objectives

In the summer of 2009, the Tollway conducted a field demonstration project on the applicability and feasibility of using RAS in asphalt mixes that contain an increased amount of fractionated RAP. The project took place on the Jane Addams Memorial Tollway (I-90) in the Rockford, Illinois area. From research previously conducted by the Tollway in 2007 (Vavrik et al. 2008), a new construction specification was developed that allowed asphalt mixes to have up to 40 percent FRAP on shoulder binder course mixes and up to 50 percent FRAP on shoulder base course mixes. The objective of this new research was to determine how replacing five percent of the FRAP in these new mixes containing higher amounts of FRAP with five percent post-consumer RAS would affect the performance of asphalt pavements. This was accomplished by evaluating the performance characteristics of field and laboratory produced samples of the asphalt mixtures containing either RAS or no RAS. Laboratory performance tests measured and analyzed the response of the mixtures to different loading and environmental conditions. The testing results were analyzed using statistical methods to determine differences among the sample means. The experimental plan was oriented at addressing the following:

1. Observe the effects of five percent RAS replacement and FRAP percentage on the low critical temperature and the high temperature grade of the final binder blend;
2. Observe the effects of five percent RAS replacement and FRAP percentage on the viscoelastic behavior of the binder and mixtures by modeling the materials properties with master curves;

3. Observe the effects of five percent RAS replacement and FRAP percentage on the dynamic modulus, flow number, fatigue performance, and freeze-thaw durability of the asphalt mixtures;
4. Observe the effects of low temperature fracture energy in the mixtures when the percentage of recycled products is increased; and
5. Compare the performance of laboratory mixed samples to field produced samples.

1.4 Scope of Laboratory Study

For the 2009 field demonstration project, eight different mixes were developed that contained various percentages of RAS and FRAP. Of the eight designs developed, there were three different types of mixes: a base course, a binder course, and a surface course as shown in Table 1-1. These mixes were placed as test strips in the shoulder of the highway in different sections of the pavement structure.

Table 1-1. Mixture design matrix

Mix ID	Mix Type	FRAP (%)	RAS (%)
1	Base Course	25	5
2	Base Course	35	5
3	Base Course	45	5
4	Base Course	50	0
5	Binder Course	35	5
6	Binder Course	40	0
7	Surface Course	20	5
8	Surface Course	25	0

The laboratory testing plan included a combination of empirical based tests and mechanistic based tests, which measured fundamental engineering properties on the asphalt mixture and the extracted asphalt binder from field produced samples and laboratory

produced samples. The performance tests selected for this study were based on the type of distresses the pavement would be subjected to during its service life. These distresses include rutting, fatigue cracking, thermal cracking, and freeze-thaw distresses and were evaluated by performing the tests outlined in Table 1-2. In order to fully characterize the pavement performance, each sample was tested for these distresses as they are considered to be the principle types of distresses for flexible (asphalt) pavement design in mechanistic-empirical methods (Huang 2004).

Table 1-2. Testing Equipment Matrix

Testing Equipment	Material Tested	Measured Response	Distress Mode
Dynamic Shear Rheometer	Extracted Binder (high temps)	Shear Modulus (G*) Phase angle (δ)	Rutting
	Extracted Binder (intermediate temps)	Shear Modulus (G*) Phase angle (δ)	Fatigue Life
Bending Beam Rheometer	Extracted Binder (low temps)	Creep Stiffness (s) Creep Rate (m)	Thermal Cracking
Hydraulic Powered Universal Testing Machine	Asphalt Mixture	Dynamic Modulus (E*)	Rutting
	Asphalt Mixture	Flow Number	Rutting
	Asphalt Mixture	Indirect Tensile Strength	Freeze-Thaw Damage
Beam Fatigue Apparatus	Asphalt Mixture	Flexural Stress	Fatigue Life
Disk Compact Tension[1]	Asphalt Mixture	Fracture energy at low temperatures	Thermal Cracking

[1]Conducted by University of Illinois Urbana-Champaign

In addition to the testing matrix, the rheological behavior of the blended asphalt binder was modeled by using the CAM model (Marasteanu et al. 1996) to develop a master

curve that fully characterizes its time-temperature dependency over a wide frequency range. Likewise, the viscoelastic behavior of the asphalt mixture under dynamic loading was modeled using the sigmoidal function as expressed by NCHRP 1-37A (2004) to construct master curves to characterize the stress-strain relationship of the total mixture (E*) at different temperatures and loading frequencies.

All tests were conducted at Iowa State University in the asphalt materials research laboratory except for the DC(T) fracture test which was conducted by the University of Illinois Urbana-Champaign.

1.5 Organization

This thesis is divided into five distinct chapters including this introductory chapter (Chapter 1). Summaries of the contents of the remaining chapters are provided as follows:

Chapter 2 provides a literature review on the use of RAS in HMA and subsequent research studies on the effect of FRAP and RAS on HMA.

Chapter 3 describes the materials and material properties evaluated in this study. In addition, the experimental laboratory performance test methodologies used to characterize and analyze HMA mixture performance are discussed.

Chapter 4 discusses the HMA characterization test results and related statistical analysis of the mixtures and asphalt binders evaluated in this study.

Chapter 5 states the summary and conclusions for the research work conducted under this study.

CHAPTER 2: LITERATURE REVIEW

2.1 Introduction

A literature search was conducted for this research project to prepare for the laboratory testing phase of the study. The purpose of this search was to understand the RAS and RAP materials used in the asphalt mixtures and to identify previous research on the use of these materials for roadway applications. Information regarding material characterization of RAS and RAP as well as studies conducted by states, universities, and private and public organizations was obtained. The summary of these findings are presented below.

2.2 Asphalt Shingles

Understanding the composition and properties of asphalt shingles is necessary for fully characterizing asphalt mixtures that incorporate their use. The American Society for Testing and Materials (ASTM) has specifications for their production. There are two different types of specifications, ASTM D225 which specifies asphalt shingles made with organic (cellulose or wood fiber) backing and ASTM D3462 which specifies asphalt shingles made with fiberglass backing. These specifications are fairly broad so the exact composition of shingles will vary among different manufacturers.

Shingles are manufactured by saturating and coating both sides of organic or fiberglass backing felt with liquid asphalt. The asphalt used to coat the felt material is different than asphalt used in paving materials. The asphalt used in roofing shingles is much harder and stiffer because the manufacturers use an “air-blown” process to increase the viscosity of the asphalt. The process infuses oxygen into the asphalt which changes the chemical make-up of the asphalt making it stiffer. The shingles are then covered with sand

and crushed-stone granules to increase their durability and resistance to weathering. The individual components of asphalt shingles are shown in Figure 2-1.

Figure 2-1. Components of Asphalt Shingles (Grzybowski et al. 2010)

The percentages of the individual component materials in asphalt shingles are different in shingles manufactured with organic felt compared to shingles manufactured with fiberglass felt. Brock (2007) summarized the composition of each type of shingles and his data presented in Table 2-1. The shingles manufactured with organic felt have substantially more liquid asphalt then shingles manufactured with fiberglass felt due to the different absorption of the materials. Since asphalt binder is the most valuable product in RAS for paving materials, RAS made from organic felt will have a high economic value. RAS made from post-consumer shingles (indicated as "Old" in Table 2-1) also has higher asphalt contents than RAS made from post-manufactured shingles due to the loss of a portion of the surface granules from weathering. McGraw et al. (2007) found similar asphalt contents as Brock in post-manufactured shingles and post-consumer shingles after conducting extractions on multiple samples.

Table 2-1. Asphalt Shingle Composition (Brock, 2007)

	Organic		Fiberglass		Old	
	(lbs. per 100 sq. ft.)	(%)	(lbs. per 100 sq. ft.)	(%)	(lbs. per 100 sq. ft.)	(%)
Asphalt	68	30	38	19	72.5	31
Filler	58	26	83	40	58	25
Granules	75	33	79	38	75	32
Mat	0	0	4	2	0	0
Felt	22	10	0	0	27.5	12
Cut-out	(2)	1	(2)	1	0	0
TOTALS	221		202		235	

The other components used in the manufacturing of shingles are also a valuable commodity in HMA. The crushed-stone granules for example can reduce the amount of manufactured sand needed for an asphalt mixture. Next to asphalt binder though, the component that is of particular interest to researchers and HMA producers is the fibers that come from the felt backing. Fibers are used as an additive in asphalt with a gap-graded or open-graded aggregate structure to prevent drain-down of the asphalt binder. Several studies conducted in the United States found that significant benefits can be gained from asphalt paving mixtures that incorporate fibers by increasing the tensile strength and toughness of the mixes (Newcomb et al. 1993).

2.3 Processing Roofing Waste

For shingles to be successfully used in asphalt paving mixtures they need to be shredded or ground down to relatively small particle sizes. Different types of crushers including rotary shredders and hammer mills are used to process the shingles. The 2006 AASHTO provisional standard on the use of RAS as an additive in HMA requires that 100

percent of the RAS passes a 12.5 mm (0.5 inch) sieve. Some state agencies that have a construction specification in place for RAS require an even smaller maximum particle size by specifying 100 percent of the RAS passes either the 9.5 mm (0.375 inch) sieve or the 4.75 mm (No. 4) size.

In order to maximize the benefits of RAS, past research has helped identify how the RAS gradation affects its performance in HMA. Research completed by Button et al. (1996) and Abdulshafi et al. (1997) found that a finer grind produced a more consistent and better performing mix. Button et al. (1996) also found that the mixes containing a finer ground post-consumer RAS increased the tensile strength more than a coarser grind.

The size of the recycled asphalt shingle can also be expected to affect the fraction of shingle asphalt binder that contributes to the final blended binder (Krivit and Associates 2007). A smaller RAS particle will have a larger surface area and more exposed binder. With more binder exposed on the surface of the RAS particle, more binder will be activated and fully blended with the virgin asphalt. Mix designs developed by the Iowa Department of Transportation (DOT) have revealed that not all of the RAS binder becomes activated in the asphalt mixture. Their mix designs revealed that approximately two-thirds of RAS binder behaves as liquid when heated and contributes to the final binder blend. The other third behaves as an aggregate that is coated with asphalt. Subsequently, the Iowa DOT only pays contractors for 67 percent of the asphalt binder that is measured in the RAS (Iowa DOT 2010).

As more recyclers gain experience processing shingles, better quality facilities and processes are being developed to solve the challenges faced during production. The continuing challenges in utilizing RAS are found to be in the quality control and quality

assurance of the final product along with identifying mix designs that meet the requirements of specifying agencies (Scholz 2010). When processing post-consumer shingles, construction debris must be removed from the shingle. This includes wood, nails, and other contaminates. Usually manual labor is utilized to separate the shingle from the wood. Removal of nails and other material removal is accomplished by using magnets at different locations on plant conveyer belts before and after the crushing process.

2.4 Asphalt Shingle Binder Properties

While using recycled products in HMA helps achieve a more economical asphalt pavement and lowers its impact on the environment, adding recycled products to HMA can also impact its performance due to the rheological behavior change of the final binder blend (NCHRP 2001). It has been well established that the rheological properties of the asphalt binder affect pavement performance (Roberts et al. 1996). Therefore, it is important to understand the behavior of asphalt binder to design and characterize HMA with RAS or higher amounts of RAP. Before understanding the implications of adding asphalt via recycled shingles to HMA, it is helpful to understand how RAP binder affects HMA properties since RAP has been researched extensively over the last 30 years and is commonly added to HMA.

When RAP is added to HMA, it contributes aggregate and asphalt binder to the final mixture. The final blend of recycled materials and virgin materials needs to meet certain physical properties for design and construction specifications. Asphalt binder from RAP is stiffer than virgin asphalt because during the construction and service life of the pavement from which the RAP came, the binder aged and hardened. If the asphalt binder from the RAP is very stiff or if much of it is added (more than 20%), the influence of the RAP binder

can have a large effect stiffening the final binder blend (NCHRP 2001). Asphalt mixtures containing stiffer asphalt binder can exhibit higher resistance to rutting but decreased resistance to low temperature cracking and fatigue cracking (SHRP-A-367 1994). Because the asphalt in post-consumer roofing shingles not only undergoes a stiffening process during production, but also has typically undergone years of oxidative aging, agencies are concerned RAS could have stiffening effects on the final binder blend (Scholz 2010) impacting pavement performance.

To counter the effect of adding a stiffer binder, a softer virgin asphalt is often used. Historically, blending charts have been used in designing HMA with two different grades of binder (The Asphalt Institute 2007). With the advent of Performance Graded (PG) binders, "grade bumping" is practiced by agencies as an easy method to account for the introduction of stiffer binder in the mixture matrix. When the percentage of reclaimed asphalt pavement exceeds a certain amount, the specified virgin binder performance is reduced one or two grades on the low temperature and/or high temperature side.

Because RAP only contains four to five percent asphalt content, adding 5, 10, or 15 percent RAP will not make a large reduction in the percentage of virgin binder added to the mix as compared to RAS. As a result, agencies have been accustomed to writing specifications for RAP by allowing a certain percentage of RAP. In contrast, when RAS is added to HMA, a much larger percentage of virgin asphalt is reduced because RAS can contain up to 30 percent asphalt. To help regulate the amount of recycled asphalt being added to HMA when RAS is used so the final blend is not too stiff, the concept of "percent binder replacement" has emerged (Bentsen 2010). Typical percent binder replacement specifications require a maximum of 20 to 40 percent in combination with grade bumping

requirements. The percent binder replacements of the mixes conducted in this study are between 25 and 65 percent.

2.5 Past Experience Using Asphalt Shingles in HMA

Literature associated with performance testing of asphalt pavements containing post-consumer RAS has increased over the last few years. A challenge for most states is to determine and integrate RAS properties into HMA mix design properties that must be taken into consideration when using post-consumer RAS. Monitoring the end product through well defined specifications helps ensure an owner/agency is receiving a quality final product that will lead to realizing the benefits of RAS.

Johnson et al. (2010) of the Minnesota Department of Transportation recently investigated the incorporation of RAS in HMA through a laboratory study and field investigation. Mixtures containing no RAS, post-consumer RAS, or manufactured waste RAS at three or five percent with either zero, 15, or 30 percent RAP were developed and tested in the laboratory for binder and mixture properties. The conclusions from the study included the following:

- Dynamic modulus laboratory tests revealed that the stiffness of mixtures containing RAS/RAP was significantly higher than mixtures containing no recycled materials at high temperatures/low frequencies suggesting an increased resistance to rutting;
- The low temperature binder grade was increased with the addition of RAP and/or RAS suggesting an increase in thermal cracking potential;
- The evaluation of a failed highway section revealed a high binder replacement ratio, which was shown to be related to the amount of recycled material;

- The use of a softer grade (from PG 58-28 to a PG 51-34) reduced the stiffness of the RAP/RAS asphalt mixtures;
- Post-consumer RAS or manufactured waste RAS can be used for MNDOT projects; and
- The current specification of 30 percent binder replacement can be maintained.

Scholz at Oregon State University (2010) conducted a study on asphalt mixtures containing five percent post-consumer RAS with 0, 10, 20, 30, 40, and 50 percent RAP to determine how the addition of these materials would affect the final binder blend. The control mixture used contained no recycled materials. The virgin binder grade for all mixtures was a PG 70-28. The results of the study revealed the following:

- Inclusion of five percent RAS and no RAP resulted in an increase in both the high and low temperature performance grades; and
- At RAP contents of 30 percent or more, in combination with five percent RAS, the low temperature grade exceeded that of the mixture containing only five percent RAS while the high temperature grade equaled that of the mixture containing five percent RAS.

2.6 Summary

The composition of RAS provides both an economical and engineering benefit that can enhance the performance of asphalt pavements. One of the primary engineering aspects of adding these recycled materials to HMA mixes is the rheological behavior change of the final binder blend. Because the asphalt in post-consumer roofing shingles not only undergoes a stiffening process during production, but also years of oxidative aging, it tends to have a higher performance grade in both the low and high temperatures than virgin

asphalts typically used in highways. Likewise, increasing the amount of RAP in asphalt mixes has a similar stiffening effect. Therefore, blending binder from recycled materials with virgin binder can increase the performance grade of the final blend at both the high and low temperatures. An increase in the high temperature performance grade can decrease the risk of permanent deformation, but an increase in the low temperature performance grade can increase the risk of low temperature cracking. However, when RAS is used in asphalt mixtures, fibers from the roofing shingles have the potential to increase the tensile strength and ductility of the mixture and counteract the adverse effects of using recycled products at low temperatures.

CHAPTER 3: MATERIALS AND METHODS

3.1 Experimental Plan

In July 2009, the Illinois Tollway (Tollway) began a field demonstration project on The Jane Addams Memorial Tollway (I-90) west of Chicago. Eight mix designs were developed for the project. The material study matrix for the different mix designs is outlined in Table 3-1. Each of the mix designs contained various amounts of FRAP. Five of the designs also contained five percent post-consumer RAS, while the other three contained no RAS. Of the eight designs, there are three different types of mixes: a base course, a binder course, and a surface course. These mixes were placed as test strips in the shoulder of the highway in different sections of the shoulder pavement structure.

Table 3-1. Material study matrix

ID	Mix Type	FRAP %	RAS %	Experiment ID	Field Sample	Lab Sample
1	Base	25	5	Experimental	X	X
2	Base	35	5	Experimental	X	X
3	Base	45	5	Experimental	X	X
4	Base	50	0	Control	X	N/A
5	Binder	35	5	Experimental	N/A	X
6	Binder	40	0	Control	X	X
7	Surface	20	5	Experimental	X	X
8	Surface	25	0	Control	X	N/A

The HMA shoulder pavement structure was six inches deep and comprised of a four-inch base layer and a two-inch surface layer. (The base and binder mixes both functioned as the four-inch base layer of the pavement structure.) Each of the base and binder course mixes were placed in alternating mile long test strips, four inches deep, and overlaid with

mile long test strips of surface course mixes, two inches deep. Figure 3-1 details the shoulder pavement structure layout.

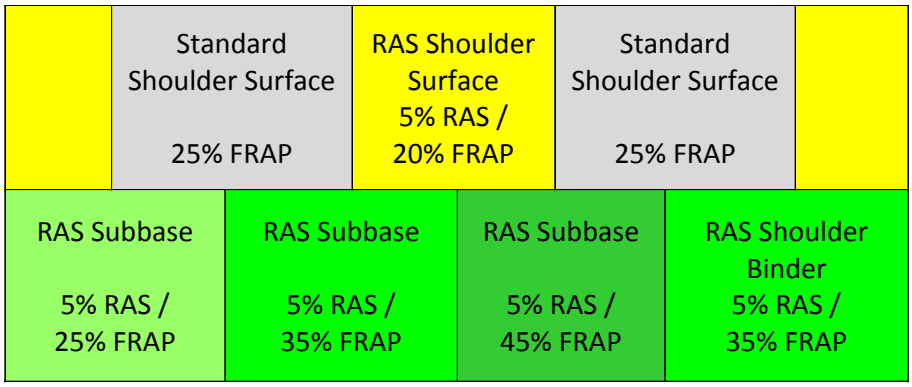

Figure 3-1. Shoulder pavement structure

The HMA was produced by Rock Road Companies at the Janesville/Beloit Plant in Wisconsin. For each experimental section, field and laboratory produced samples were obtained to determine if the performance characteristics of the field produced mix significantly deviated from performance characteristics of the laboratory produced mix as previously summarized in Table 3-1. For each control section, either a field or laboratory sample was obtained. Samples were obtained by Iowa State University with the assistance of the Rock Road Company. All together 13 mixes were collected from the project, seven field and six laboratory mixes.

From each sample collected, representative samples were reduced from the larger samples by following AASHTO T248 to obtain smaller size samples for testing. The tests performed on the samples and the number of samples made for each test is outlined in the experimental plan in Figure 3-2. All samples were specifically made for one test procedure with the exception of the dynamic modulus test and the flow number test which shared the same samples. All tests were conducted at Iowa State University with the exception of the

Disk Compact Tension test which was conducted by the University of Illinois Urbana-Champaign. Each test procedure was treated as an individual experiment and will be subsequently described and analyzed individually in this chapter.

Table 3-2. Experimental testing plan

Test Equipment	Measured Response	Sample Size	Failure Criteria
Dynamic Shear Rheometer	G*/Sin (δ)	1	Rutting
Bending Beam Rheometer	Creep Stiffness and Rate	2	Thermal Cracking
Universal Testing Machine	Dynamic Modulus (E*)	5	Rutting
	Flow Number	3	Rutting
	Tensile Strength Ratio	3	Freeze-Thaw
Beam Fatigue	Flexural Stress	6	Fatigue Cracking
Disk Compact Test*	Fracture Energy	4	Thermal Cracking

*Conducted by the University of Illinois Urbana-Champaign

Representative samples from each of the 13 sampled mixes were sent to the Minnesota Department of Transportation for binder extraction. The recovered binder samples were tested with Superpave binder equipment at Iowa State University in accordance with AASHTO M323 for testing in the Dynamic Shear Rheometer and the Bending Beam Rheometer and for subsequent determination of the performance grade of each blended binder.

3.2 Materials

The mix design summary is contained in Table 3-3. Mix design summary, and provides the characteristics of each mix design. Each mix used the same PG 58-22 virgin binder. The surface mix design had a nominal maximum aggregate size of 9.5mm (3/8 inch) and the base and binder mixes had a nominal maximum aggregate size of 19.0mm (3/4 inch). The base and binder course mixes are designed as asphalt-rich, fatigue resistant mixes for

layers of a perpetual pavement structure. The base mix was designed at two percent air voids while the binder mix was designed at three percent air voids.

Table 3-3. Mix design summary

Mix ID	Mix Type	FRAP	RAS	NMAS (mm)	% AV	N_{des}	VMA	% Total AC	% Virgin AC	% Binder Repl.	PG Grade
1	Base	25	5	19.0	2	50	11.5	5.3	3.0	43	58-22
2	Base	35	5	19.0	2	50	11.0	4.9	2.1	57	58-22
3	Base	45	5	19.0	2	50	11.0	5.0	1.7	66	58-22
4	Base	50	0	19.0	2	50	11.5	5.0	2.6	48	58-22
5	Binder	35	5	19.0	3	50	12.0	5.0	2.3	54	58-22
6	Binder	40	0	19.0	3	50	13.5	5.5	3.5	36	58-22
7	Surface	20	5	9.5	4	70	15.8	5.9	3.7	37	58-22
8	Surface	25	0	9.5	4	70	14.9	5.7	4.3	25	58-22

The properties of the recycled products used in the mix designs are presented in Table 3-4. The FRAP, as defined in Tollway specifications, is a Category 2, meaning it contained natural sand. The FRAP for each mix was comprised of two different RAP stockpiles. One stockpile contained the coarse portion RAP (primarily consisting of RAP above a number 4.75mm screen) and the other stockpile contained the fine portion RAP (consisting of the RAP below the 4.75mm screen). The fine portion RAP asphalt content of 6.0 percent is greater than the coarse portion RAP asphalt content of 3.3 percent. The difference between these two materials indicates that fractionating RAP into separate stockpiles will increase the control of the RAP during mix design and construction. With respect to the RAS gradation, approximately 100 percent of the RAS material passed the 9.5mm sieve.

Table 3-4. Gradations (percent passing by weight)

Sieve Size	Fine RAP (%)	Coarse RAP (%)	RAS (%)
25.0mm	100.0	100.0	100.0
19.0mm	100.0	100.0	100.0
12.5mm	100.0	100.0	99.9
9.50mm	100.0	93.0	99.6
4.75mm	94.0	35.0	96.4
2.36mm	70.0	20.0	92.3
1.18mm	52.0	16.0	74.0
0.60mm	39.0	13.0	51.8
0.30mm	23.0	9.0	43.5
0.15mm	15.0	7.0	33.8
0.075mm	10.9	5.0	24.0
% AC	3.3	6.0	28.1

The trend in binder contribution from the RAS and FRAP materials is shown in Figure 3-2. As the amount of FRAP is increased in the asphalt mixtures, with or without 5 percent RAS, the percent binder replacement linearly increases in the asphalt mixtures. Many agencies use the percent binder replacement concept to limit the amount of recycled materials in asphalt mixtures that contain RAS. These limiting ratios typically range from 20 to 40 percent, depending on the agency (Bentsen 2010). Several of the mixes used for this study are above this range allowing for a comparison of mixes with various amounts of binder replacement percentages.

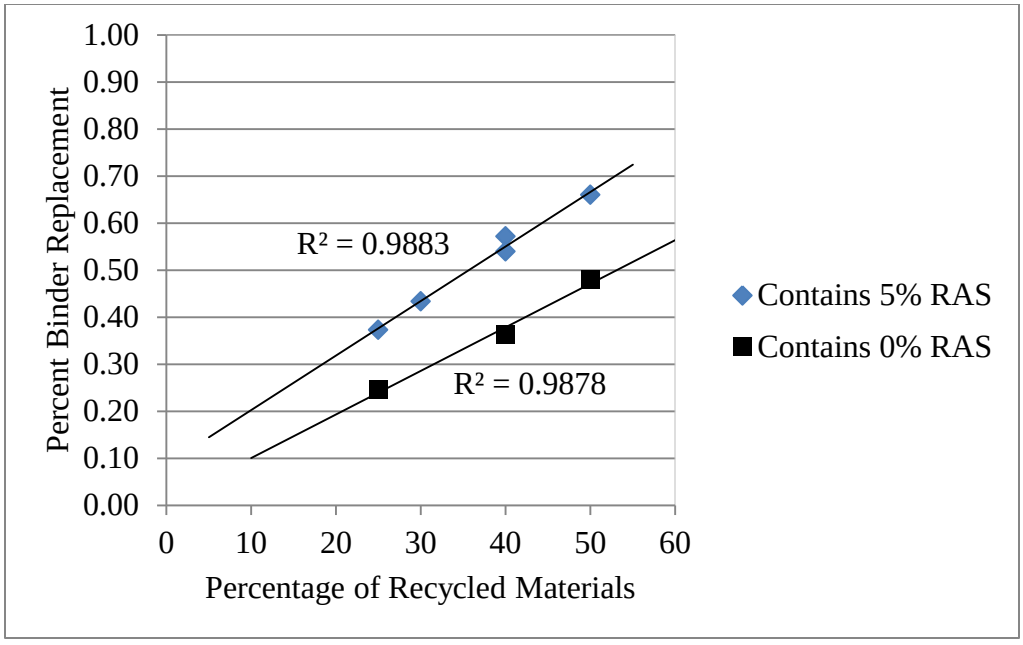

Figure 3-2. Contribution of FRAP and RAS to mix designs

The aggregate gradations for all the mixes are presented in Table 3-5. The aggregate gradation for base and binder course mixes (Mix ID 1-6) plot just below the maximum density line for material passing the 4.75 mm sieve, then cross the maximum density line for material retained on the 4.75 mm sieve. The aggregate gradation of the surface course mix (Mix ID 7-8) plots below the maximum density line which classifies this aggregate structure as being coarse graded. Figure 3-3 through Figure 3-5 plot each gradation on the 0.45 power chart.

Table 3-5. Aggregate gradations

Mix ID / Sieve Size	1	2	3	4	5	6	7	8
25.0mm	100	100	100	100	100	100	100	100
19.0mm	87	97	97	97	97	97	100	100
12.5mm	84	84	84	85	83	85	100	100
9.50mm	76	75	76	77	74	77	99	99
4.75mm	44	45	46	46	41	47	60	65
2.36mm	30	31	32	31	27	31	34	38
1.18mm	24	24	25	25	22	22	22	23
0.60mm	18	19	19	19	16	17	15	16
0.30mm	10	10	11	11	10	11	10	10
0.15mm	5	6	7	7	6	8	7	7
0.075mm	3.8	4.5	5.2	5.6	4.4	5.5	5.2	4.9

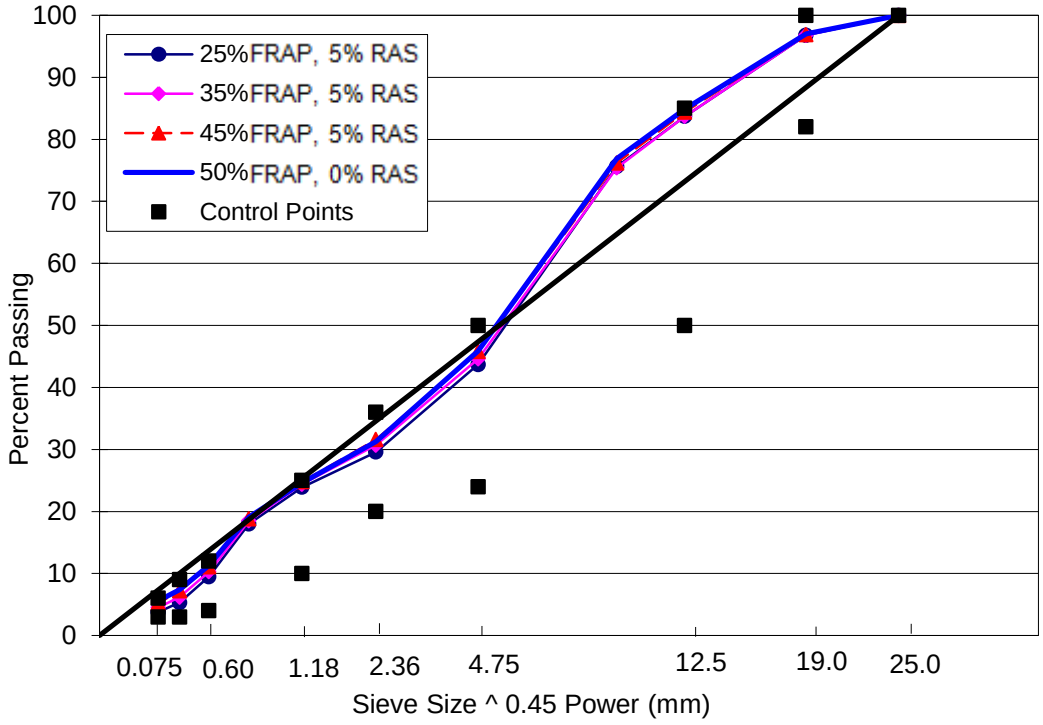

Figure 3-3. 0.45 Power chart for base course gradations

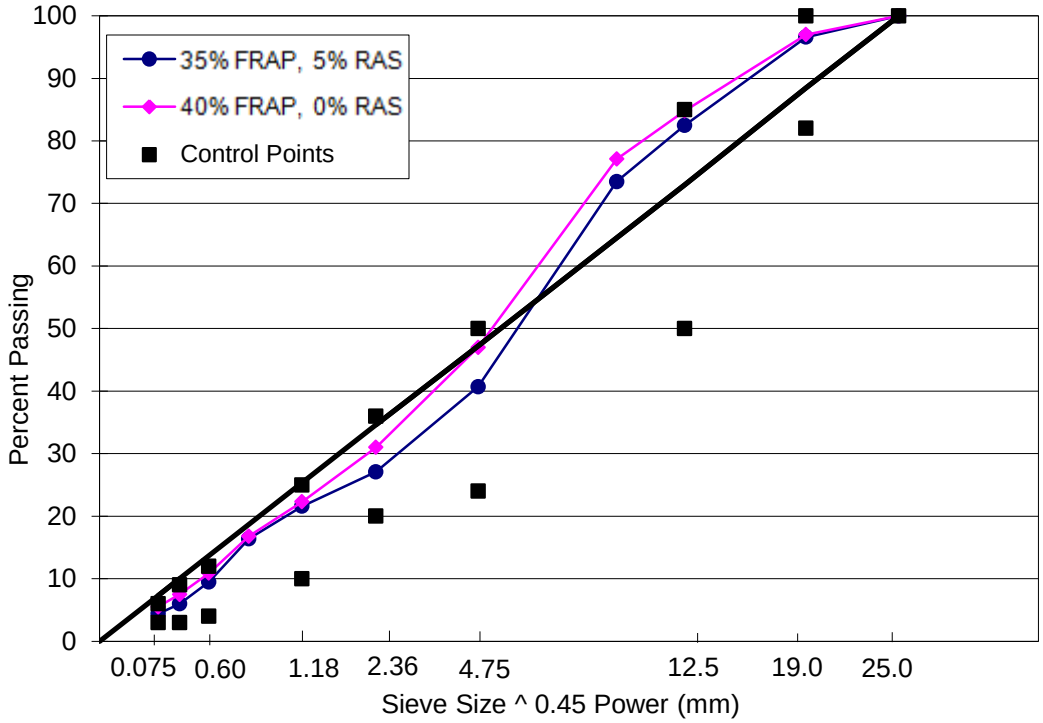

Figure 3-4. 0.45 Power chart for binder course gradations

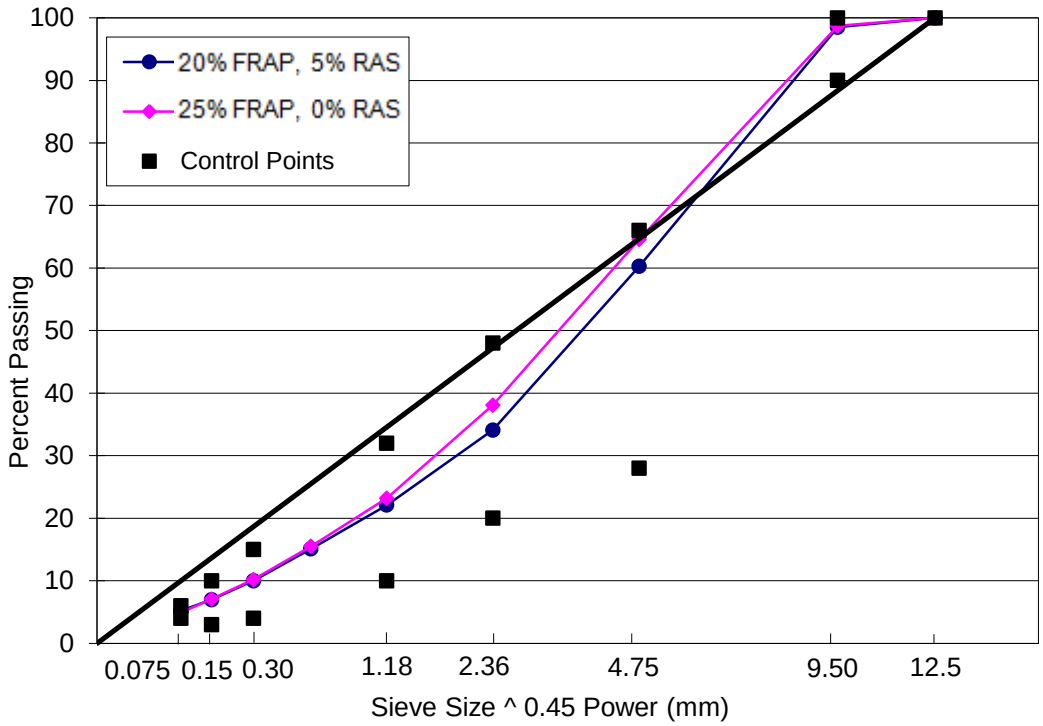

Figure 3-5. 0.45 Power chart for surface course gradations

3.4 Performance Graded Asphalt Binders

To understand the methodology of testing the extracted binders in the dynamic shear rheometer (DSR) and the bending beam rheometer (BBR), it is helpful to understand how asphalt binders are graded using performance graded (PG) specifications. The PG system relates the physical properties of the binders directly to field performance by taking into account three critical stages of an asphalt binders service life and the entire range of temperatures experienced at the project site. A series of aging simulations and tests is conducted on the binders to obtain a final binder grade which characterizes how it will perform at a given temperature and rate of loading.

The final grade is reported as two numbers, a high and a low temperature in degrees Celsius that are combined, including the minus sign (i.e., PG 64-22 is a grade commonly used in Iowa). As an example, a PG 64-22 grade binder is designed to sustain the conditions of an environment where the average seven-day maximum pavement temperature is 64 degrees Celsius and the minimum pavement design temperature is -22 degrees Celsius. The high temperature grade is obtained from testing an asphalt sample in the DSR at higher temperatures for the parameter $G^*/\sin(\delta)$ to give an indication of rutting resistance, and the low temperature grade is obtained from testing an asphalt sample in the BBR at lower temperatures for the parameters of creep stiffness and creep rate to give an indication of low temperature cracking susceptibility. Table 3-6 provides the different grade levels included in the PG binder specification.

Table 3-6. PG binder grades

High Temperature Grades	Low Temperature Grades
82	-10
76	-16
70	-22
64	-28
58	-34
52	-40
46	-46

In addition to the high and low temperature grades, an intermediate temperature parameter must be met for a given binder grade (G* x Sin(δ)). This parameter gives an indication of fatigue cracking resistance which occurs at intermediate pavement temperatures.

Because asphalt is comprised of hydrocarbons, it will react with oxygen during its service life and go through a process known as age hardening where its physical properties change. Therefore, the parameters obtained to grade the binder are tested after the sample has undergone a simulative aging process in the laboratory. Two types of equipment are used to simulate the aging processes, the rolling thin film oven (RTFO) and the pressure aging vessel (PAV). The RTFO is used to simulate short-term construction aging which occurs as the asphalt is heated in the hot mix asphalt plant, mixed with aggregate, and placed on the roadway. The PAV is used to simulate aging that occurs after ten or more years as the asphalt oxidizes on the roadway.

An asphalt binder is tested two different times in the DSR for the G*/Sin(δ) parameter, once before aging in the rolling thin film oven (RTFO) and once after. An unaged binder‘s G*/Sin(δ) parameter must be a minimum of 1.0 kPa to qualify for a grade level,

while a RTFO aged binder's G*/Sin(δ) parameter must be a minimum of 2.2 kPa to qualify for a grade level.

The low temperature cracking parameters of creep stiffness and creep rate obtained from the BBR are measured after the sample has been PAV aged. This is because pavements are the most prone to thermal cracking in the later stages of their service life as the binder hardens. The fatigue cracking parameter G* x Sin(δ) is also tested for in the DSR after PAV aging for similar reasons.

3.5 Dynamic Shear Rheometer

Asphalt binders are a viscoelastic material and behave partly as an elastic solid and partly as a viscous liquid. The DSR is able to quantify both elastic and viscous properties. The equipment measures a sample's complex shear modulus (G*) and phase angle (δ). The complex shear modulus is the ratio of total shear stress (τ_{max}-τ_{min}) to the total shear strain (γ_{max}-γ_{min}) and is considered to be the asphalt's total resistance to deformation when repeatedly sheared. The phase angle is also measured because asphalt is not a purely elastic material. The phase angle is a measure of the response time between the applied shear stress and the resulting shear strain. If asphalt were purely elastic, the phase angle would be zero degrees. If asphalt were a purely viscous newtonian fluid, the phase angle would be 90 degrees. Figure 3-6 illustrates the relationship between the factor of phase angle and time.

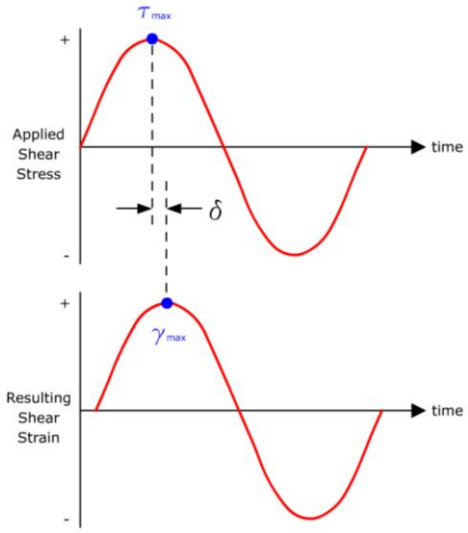

Figure 3-6. Relationship between phase angle and time (www.pavement interactive.org)

The complex shear modulus (G*) consists of two components, the storage modulus (G' the elastic component) and the loss modulus (G" the viscous component). The relationship between G' and G" as presented in Figure 3-7 formulate the phase angle of the asphalt. With these properties, rutting resistance and fatigue cracking resistance are measured.

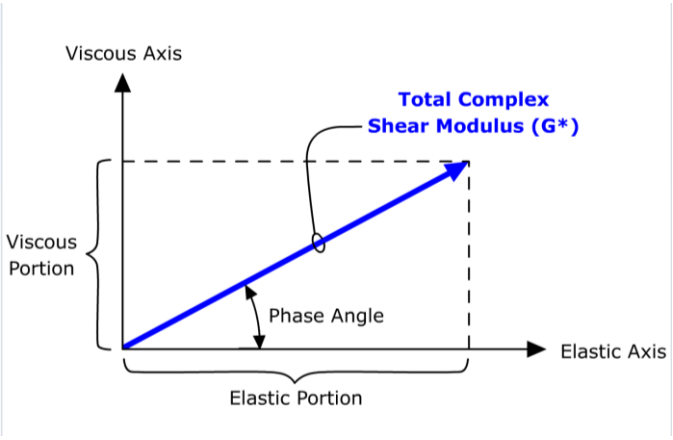

Figure 3-7. Relationship between storage modulus and loss modulus (www.pavementinteractive.org)

For asphalt binder to have rutting resistance, it must have high stiffness and elastic properties at high temperatures. Elasticity is defined as the property of being able to recover its original shape after being deformed by a load. The higher the G* value, the stiffer the asphalt binder is. Likewise the lower the δ value, the greater the elastic portion of G' is. Therefore as part of the PG binder specification system, the parameter G*/Sin(δ) is specified to be a minimum value (1.0 kPa for unaged binders and 2.2 kPa for RTFO aged binders).

ASTM D7175 was followed to test the asphalt binder in the DSR. A 25mm (for unaged or RTFO aged samples) or 8mm (for PAV aged samples) diameter sample of liquid asphalt was sandwiched between two parallel plates that load in a sinusoidal pattern at rate of 10 radians/second (1.59 Hz) while being submerged in a water bath. The specified DSR oscillation rate of 10 radians/ second (1.59 Hz) is used to imitate the shearing action related to a traffic speed of about 55 mph. Two parameters were measured at different water bath temperatures by following this procedure, G*/Sin(δ) and G*xSin(δ).

When testing the binders for the G*/Sin(δ) parameter, the binders extracted from field produced samples were not aged in the RTFO because the HMA was already subjected to short-term construction aging. Subsequently, the more stringent 2.2 kPa minimum value requirement for G*/Sin(δ) was used to grade these binders. The binders extracted from the laboratory samples were not aged in the RTFO either since the mix samples did undergo short term oven aging. To be consistent with the method for grading the binders extracted from the field produced samples and as an added factor-of-safety, the laboratory sample binders were also graded using the more stringent 2.2 kPa minimum required value for G*/Sin(δ).

3.6 Bending Beam Rheometer

Thermal cracking occurs primarily because of the existence of tensile stresses that build up within a pavement when it is subjected to progressively colder temperatures (Kim 2009). Thus it is a non-load associated distress. Low temperature cracks can occur from a single low temperature event or from repeated low temperature cycles. The asphalt binder plays a key role in low temperature cracking. If the stiffness modulus of the asphalt cement is too high at low temperatures, the pavement will be prone to cracking. To resist low temperature cracking, an asphalt binder must also possess a high stress relaxation ability at low temperatures in order to relieve stresses. Since previous studies (Johnson et al. 2010, Scholz 2010) have shown that adding RAS binders in HMA can increase the stiffness of the binder blend at low temperatures, this failure mechanism is a primary concern of the Tollway in this study.

Because asphalt binders at low temperatures are too stiff to reliably measure properties just using the DSR, the bending beam rheometer (BBR) is used to evaluate binder properties at low pavement temperatures. The BBR is a test for measuring how much a binder deflects under a constant load and temperature. The creep stiffness (S) and the rate of stress relaxation (m-value) are calculated from the results and used to determine an asphalt binder's critical cracking temperature and PG low temperature grade.

Before testing the extracted binders in the BBR, the samples were aged in a PAV. After PAV aging, the samples were molded into two beams of 127 x 12.7 x 6.4 mm in size for testing in a BBR. In the BBR machine, the beams were submerged in a subzero temperature bath and placed on top of a cradle that supported the ends of a beam. The center

of the beam was loaded with a 100 gram weight for 240 seconds. The procedure used to test the beams followed ASTM D6648 and is depicted in Figure 3-8.

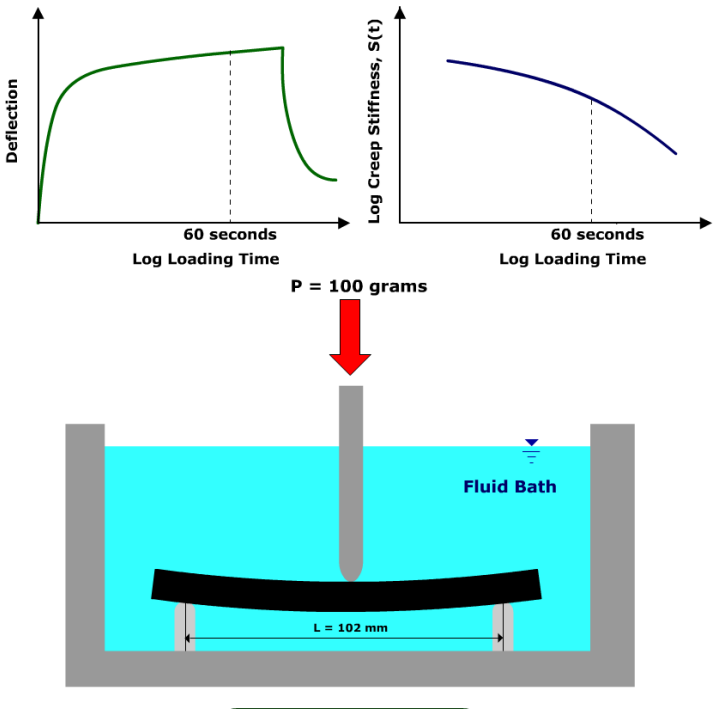

Figure 3-8. Bending beam rheometer test (www.pavementinteractive.org)

The BBR test was repeated on both beams at four different temperatures (0, -6, -12, and -18 degrees Celsius) with their resulting values at each temperature averaged to determine the critical low temperature. The creep stiffness of the beam was calculated using classic beam theory analysis using the following equation.

$$S(t) = \frac{PL^3}{4bh^3\delta(t)}$$

Where:

S(t) = creep stiffness (MPa) at time, t;

P = applied constant load, N;

L=distance between beam supports, 102 mm;

b = beam width, 12.5 mm;

h = beam thickness, 6.25 mm; and

δ = deflection (mm) at time; t.

If the creep stiffness is too high, the asphalt will behave in brittle manner and cracking is likely to occur (Asphalt Institute 2001). To limit the potential for cracking, PG specifications limit the stiffness to a maximum of 300 MPa for the low temperature binder grade.

The second parameter determined from the BBR is the m-value which represents the rate of creep stiffness. The m-value is the slope of the log stiffness versus the log time curve. A high m-value is desirable since the faster a pavement relieves tensile stresses, the less likely cracking will occur. The PG specifications limit the m-value to a minimum of 0.300 in addition to the creep stiffness specification for the low temperature grade.

The creep stiffness values and the m-values were plotted against the test temperatures for each binder sample. The temperature at which the creep stiffness exceeded 300 MPa or the m-value was lower than 0.300 was defined as the critical low temperature.

3.7 Asphalt Binder Master Curves

Since an asphalt pavement's performance is related to its rheological properties, it is important to understand a particular asphalt binder's response to loading at different temperatures and rates of loading. To model these rheological properties, master curves were constructed which plot the complex shear modulus (G*) over frequency at a given temperature. The master curve is constructed by using the time-temperature superposition principle which transforms temperature changes into frequency changes. With the master

curve, viscoelastic properties of an asphalt material can then be estimated over a wide frequency range, beyond the range in which actual measurements can be carried out.

The master curves were constructed using the testing data from the DSR and the BBR. This was accomplished by conducting frequency sweeps at different temperatures in the DSR to obtain shear modulus values (G*) and by testing all the binder samples in the BBR at the four different test temperatures. The BBR creep stiffness values were converted to shear modulus values through the following relationship:

$$G^* = S(t)/3$$

This relationship is valid since the asphalt binders are being tested in their linear viscoelastic range where the strains are small enough to have relatively no influence on modulus values. To ensure the linear viscoelastic assumption is valid, strain sweeps were conducted on each sample in the DSR before conducting the frequency sweeps.

The G* values from the BBR and DSR at each temperature were plotted against frequency. Each individual frequency curve is referred to as an isochrone. To create a master curve, the isochrones are shifted using the time-temperature superposition of asphalt materials to form one smooth curve as shown in Figure 3-9. The time-temperature superposition principle implies that the effects of low temperatures on asphalt materials cause them to behave the same way when loaded quickly. Likewise, the effects of high temperatures cause them to behave the same way when loaded slowly. An example of the time-temperature superposition in asphalt pavements is demonstrated through the rutting resistance as pavements are the most susceptible to rutting during the hot summer months and at intersections where traffic slows down.

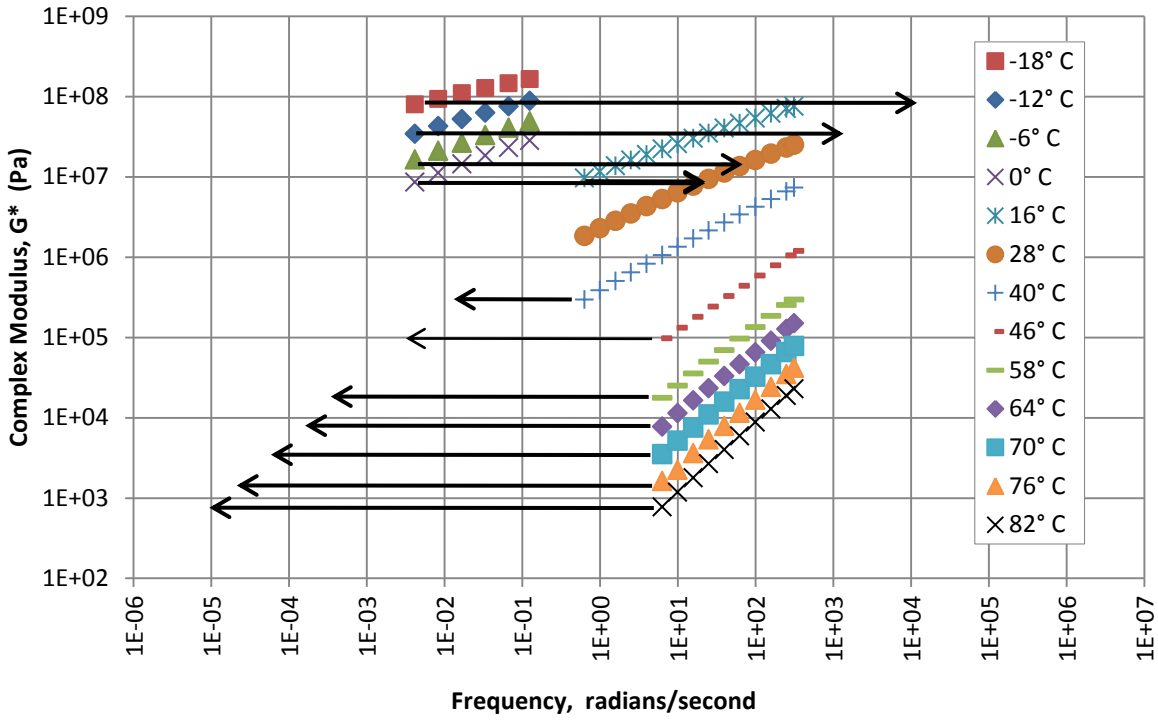

Figure 3-9. Master Curve Construction

The master curves formed in this manner describe the time dependency of the material with respect to a certain temperature. The amount of shifting at each temperature required to form the master curve describes the temperature dependency of the material. An example of a completed master curve is presented in Figure 3-10.

The overall shape of a master curve can be used to describe the performance characteristics of an asphalt binder. The G* values of a master curve at lower frequencies demonstrate how asphalt binder at high temperatures or low rates of loading behaves close to a Newtonian fluid where its shear strain is independent of its shear rate. At these low frequencies its phase angle approaches zero. The G* values at higher frequencies demonstrate how asphalt binder at low temperature or high rates of loading behaves close to an elastic solid where poisson's ratio equals 0.5. At these high frequencies its phase angle asymptotically approaches ninety degrees.

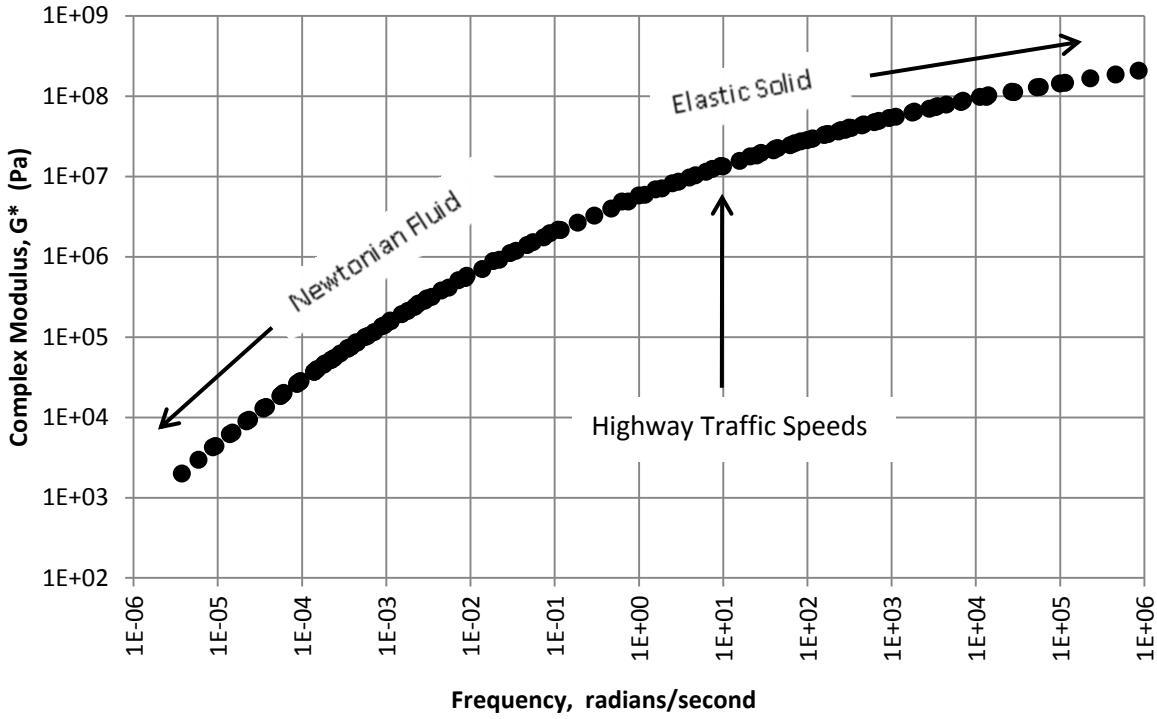

Figure 3-10. Example of Completed Master Curve Shifted at 28°C

The master curve can be mathematically modeled using the Christensen-Anderson-Marasteanu (CAM) model as it is considered an effective phenomenological model for unmodified asphalt binders whose properties are within the linear viscoelastic range (Kim 2009).

$$|G^*(\omega)| = G_g \left[1 + \left(\frac{\omega_c}{\omega}\right)^v\right]^{-\frac{w}{v}}$$

Where:

$|G^*(\omega)|$ = absolute value of complex modulus as a function of frequency ω (GPa);

G_g = glassy modulus (log [G_g] is considered fixed at 9.1); and

ω_c, v, w = model parameters.

To create the master curves, an Excel spreadsheet was used to fit the data to the CAM model at a reference temperature of 28 degrees Celsius.

3.8 Dynamic Modulus (E*)

The dynamic modulus was chosen as a material parameter to evaluate the pavement mixtures because it is a fundamental property that characterizes a pavement's response to loading conditions that simulate repeated traffic. This fundamental property is defined as the pavement stiffness. Just as Young's modulus is paramount for predicting the deflection of steel beams in a structure, the stiffness of asphalt concrete is critical for predicting the behavior of the material in pavement structures (Kim 2009). The stiffness of asphalt concrete depends on the temperature and the rate of loading. A higher stiffness indicates that for a given applied stress there will be a lower strain in the mixture. HMA mixes which have high stiffness modulus at high temperatures have a greater resistance to permanent deformation while HMA mixes which have a high stiffness modulus at low temperatures are very prone to cracking (Roberts et al. 1996). For HMA mixtures under constant strains at intermediate temperatures, a higher stiffness modulus can also result in a lower fatigue life.

During the dynamic modulus test, a cyclical load is applied vertically to a cylindrical sample in a sinusoidal wave form as presented in Figure 3-11. It is classified as an unconfined triaxial compression test with cyclical one-dimensional loading. The first triaxial compression tests that applied repeated loads to laboratory samples have their roots in soil mechanics. In the early 1960's Seed et al. introduced the concept of resilient modulus in the 1962 seminal paper titled "Resilience Characteristics of Subgrade Soils and Their Relation to Fatigue Failures in Asphalt Pavements."

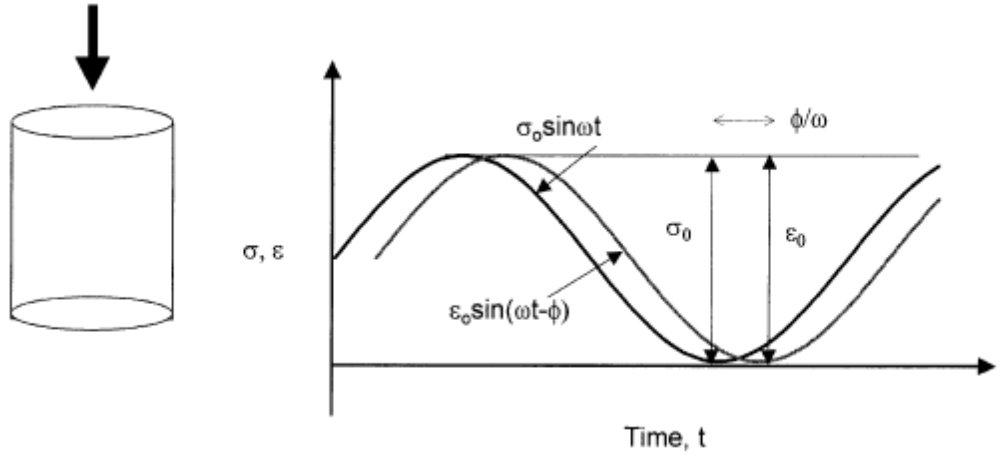

Figure 3-11. Haversine loading for the dynamic modulus test (NCHRP Report 547)

By applying a continuous sinusoidal load to asphalt materials, the viscoelastic behavior of the asphalt sample can be described through "complex" mathematics similar to the complex shear modulus (G*). For the dynamic modulus test, elastic as well as inelastic (viscous) deformations are measured. The dynamic modulus is mathematically defined as the maximum (i.e., peak) dynamic stress (σ_o) divided by the peak recoverable axial strain (ε_o).

$$|E^*| = \frac{\sigma_o}{\varepsilon_o}$$

The dynamic modulus (*E**) is the absolute value of the complex modulus E*. E* comprises of a storage modulus E' and a loss modulus E". The storage modulus refers to the elastic behavior of the material and the loss modulus refers to the viscous behavior of the material.

$$E^* = E' + iE^{"}$$

The proportions of the storage modulus and the loss modulus for a dynamic modulus value can be defined with the phase angle (θ) which can be described mathematical as:

$$E^* = |E^*|\cos\theta + i|E^*|\sin\theta$$

The phase angle describes the amount of time the strain responses occur after the stresses have been applied is defined by the following equation.

$$\theta = \frac{t_i}{t_p}(360)$$

Where:

t_i = time lag between a cycle of stress and strain (s);

t_p = time for a stress cycle (s); and

i = imaginary number.

For a pure elastic material, the phase angle is zero degrees and for a pure viscous material the phase angle is equal to 90 degrees.

The dynamic modulus test procedure used to test the asphalt pavement samples in this study followed AASHTO TP62 "Standard Test Method for Dynamic Modulus of Asphalt Concrete Mixtures". A gyratory compactor with a 100mm diameter mold was used to fabricate samples 150 mm in height by 100 mm in diameter at the design air void level. A batch of five samples was fabricated for each of the 13 HMA samples obtained in the study. A complete randomized factorial experiment was conducted on the samples in this procedure. The response was the dynamic modulus. This was measured by placing each sample in the hydraulically powered Universal Testing Machine (UTM) where an actuator applied the cyclical load to the sample. The resulting strains were measured from three linear variable differential transformers (LVDT's) that were attached to the sample. Each sample was tested at three temperatures (4^o, 21^o, and 37^oC) and nine frequencies of cyclical loading (0.1, 0.3, 0.5, 1, 3, 5, 10, 15, and 25 Hz) to capture the time and temperature dependency of the HMA mixes. The test procedures required that each sample was to be tested from the lowest temperature first to the highest temperature in combination with the highest frequency

first to the lowest frequency. Randomization of the batches and the samples within the batches was conducted to spread the effects of outside variables evenly across treatments. Before testing the batches at each temperature, the batches were placed in a random order, and before testing the samples in each batch, the samples were also placed in a random order.

3.9 Asphalt Mixture Master Curves

Similar to the data obtained from the binder testing, dynamic modulus values from frequency sweeps were used to construct master curves for the asphalt mixtures. Dynamic modulus master curves have become an important aspect for asphalt materials characterization and pavement designs that use a mechanistic-empirical approach. Through a master curve it is possible to integrate traffic speed, climatic effects, and aging for pavement response and distress models (Kim 2009). The use of the dynamic modulus master curve permits the elastic modulus of the HMA layers to be varied by temperature, speed, and layer depth in pavement designs. Master curves for asphalt mixtures can be mathematically modeled by the following sigmoidal function.

$$\text{Log}|E^*| = \delta + \frac{\alpha}{1 + e^{\beta+\gamma(log t_r)}}$$

Where:

tr = reduced time of loading at reference temperature;

δ = minimum value of *E**;

$\delta + \alpha$ = maximum value of *E**;

β, γ = parameters describing the shape of the sigmoidal function.

3.10 Flow Number

Rutting occurs in flexible pavements when small amounts of unrecoverable deformations build up under the wheel paths when traffic loads are applied (The Asphalt Institute 2001). This phenomenon can be the result of the consolidation of weak subgrade layers or a lack of shear strength in the asphalt materials. The internal friction of the aggregate structure must be high enough to withstand shear forces caused by traffic loads and the asphalt binder must be stiff enough to behave like an elastic solid at high temperatures. Lateral plastic flow of the asphalt materials can also occur in poorly designed mixtures if the asphalt content is too high or the void structure is too low (less than 3 percent).

The flow number test was used in this study to determine the deformation characteristics of each paving material by employing a repeated dynamic load for several thousand load cycles and plotting the cumulative permanent deformation versus load cycles. The procedure used for this test was derived from the testing protocol described in NCHRP Report 465 (Witzcak et al. 2002) and NCHRP Report 513 (Bonaquist et al. 2003).

The dynamic modulus samples were used as the material for this test since the dynamic modulus test is nondestructive. Three out of the five samples from each batch of dynamic modulus test specimens were randomly selected to be tested for flow number. The samples were placed in a UTM unconfined with a testing temperature of 37 degrees to simulate the climate conditions that cause pavement to be susceptible to rutting. An actuator applied a vertical haversine pulse load of 0.1 sec and 0.9 sec dwell (rest time) for the test duration of approximately 3 hours resulting in approximately 10,000 cycles applied to the specimen. The deviator stress applied by the actuator was 600 KPa. Three LVDT's were attached to each sample during the test to measure the cumulative strains. To determine the

order of testing batches of samples, the batches were placed in a random order. Before testing the samples in each batch, the samples were also placed in a random order.

3.11 Tensile Strength Ratio

Freeze-thaw damage or moisture–induced damage results in stripping which can be defined as the weakening or eventual loss of the adhesive bond in the presence of moisture between the aggregate surface and the asphalt cement in an asphalt mixture (Roberts et al. 1996). The strength of asphalt is derived from this cohesive asphalt/aggregate bond together with the internal frictional resistance of the aggregate structure. Forces caused by water freezing and thawing inside the asphalt mixture can reduce the cohesive strength and result in failure of the mixture.

The tensile strength ratio (TSR) is a value that indicates a pavement's susceptibility to damage caused by freezing and thawing cycles and traffic loading. The procedure used for this test was AASHTO T283. For this test, only the seven production samples of the asphalt pavement were tested. A batch of six specimens from each of the seven pavement samples was used as the material for this test. A gyratory compactor with a 100mm diameter mold was used to fabricate samples 62.5 mm in height by 100 mm in diameter at seven percent air voids. Three randomly selected samples in each batch were selected to be conditioned in a freeze-thaw environment while the other three were not. The samples were conditioned by saturating them with water, placing them in a plastic bag, and placing them in a freezer for 16 hours at -18 degrees Celsius. After 16 hours, the samples were placed in a 60 degree Celsius water bath for two hours. Following the two hour thawing environment, the conditioned samples were randomly tested for their indirect tensile strength in a UTM at 25 degrees Celsius along with the unconditioned samples. For a batch of six samples, the indirect tensile

strength of three conditioned samples was averaged and divided by the average indirect tensile strength of the unconditioned samples to obtain the TSR for that asphalt mixture. A higher TSR value indicates that good performance is expected in freeze-thaw environments.

The indirect tensile strength test (IDT) was performed in a UTM by placing a sample on its cylindrical side in a 25 mm wide loading strip. A static compressive load was applied to the loading strip with a magnitude that achieved a deformation rate of 2 inches/minute. During the test the static load increased to ensure the constant deformation rate. At some point, however, the sample began to crack and decrease in strength. As a result the applied static load also decreased for the remainder of the test. The maximum applied load during the test was used to calculate the horizontal tensile strength of the specimen.

3.12 Beam Fatigue

Fatigue cracking of flexible pavements is caused by repeated traffic loading at intermediate temperatures. It is the result of excessive horizontal tensile strains built up over time at the bottom of the asphalt pavement layers where the tensile strain is the highest under a wheel load. The pavement fails by developing micro cracks at the bottom of the asphalt layer that propagate to the surface over time. High severity fatigue cracking occurs when the cracks become a series of interconnected cracks that develop a pattern resembling chicken wire (alligator cracking). While fatigue cracking is mostly considered a function of several non-materials related causes such as heavy truck traffic or the end of a pavement's design life, it is also a function of pavement materials selection. The HMA must have a high enough tensile strength and be resilient enough to overcome repeated load applications without cracking (The Asphalt Institute 2001).

A repeated flexural test was conducted to evaluate the fatigue properties of the asphalt mixtures in the beam fatigue apparatus. The beam fatigue apparatus applies haversine loads at the third points of a beam specimen with dimensions 15 x 2.5 x 2 inches as shown in Figure 3-12. The load rate is applied at 10 Hz which produces a constant bending moment over the center of the beam. AASHTO T321 was followed for this test procedure.

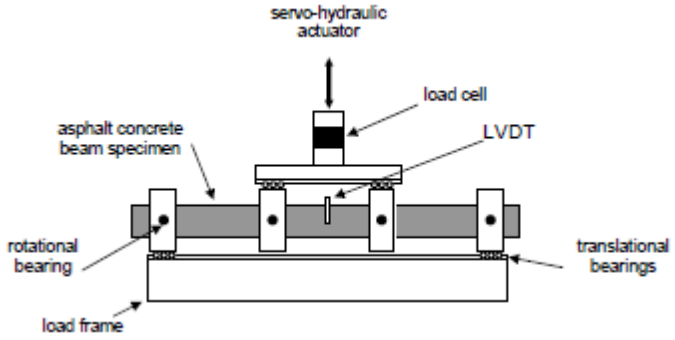

Figure 3-12. Third point loading mode fatigue test apparatus (from Diefenderfer 2009)

Six asphalt beams were fabricated for all 13 asphalt mixtures. The six beams for each mixture were saw cut from two slabs compacted in the linear kneading compactor, three beams from each slab. Beams from the laboratory produced samples were compacted to the laboratory air void levels of two percent for the base course mix, three percent for the binder course mix, and four percent for the surface course mix. Beams from the field produced samples were compacted to an air void level of three percent plus the laboratory design air void level (5%, 6%, and 7%) so fatigue properties of the field sampled mixes would be more representative of a typical field compaction level.

The beam fatigue apparatus was placed inside an environmental chamber set at 20°C to simulate the in-service temperature at which fatigue cracking is most likely to occur. The test was run in a constant strain mode. The six beams for each sample were tested at different strain levels to obtain the relationship between strain level and number of load

repetitions (cycles to failure). The strain and the number of load cycles to reduce the modulus by 50 percent were plotted on a log-log plot. The initial flexural modulus was measured at the beginning of the test at the 50^{th} load cycle. The six strain levels used in the tests ranged from 1000 micro strain to 250 micro strain. The relationship between strain levels and cycles to failure as plotted on a straight line were modeled using the following relationship.

$$N_f = K1\left(\frac{1}{\varepsilon_o}\right)^{K2}$$

Where:

N_f = number of cycles to failure;

εo = flexural strain; and

K1, K2 = regression constants.

The K1 and K2 coefficients were obtained from a best fit straight line of the data.

3.13 Disk Compact Tension

The testing of the Disk Shaped Compact Tension (DC(T)) fracture specimens was conducted by the University of Illinois Urbana-Champaign at the Advanced Transportation Research and Engineering Laboratory (ATREL) in Rantoul, IL. This test measures the fracture energy (G_f) of each mixture to predict thermal cracking resistance. The initial gyratory samples for the DC(T) fracture test were compacted by Iowa State University. The samples measured approximately 120mm in height by 150mm in diameter. DC(T) specimen fabrication and testing occurred in accordance with ASTM D7313. All DC(T) tests were conducted at -12^0C. This test temperature was chosen in order to comply with binder grade reliabilities in the northeast Illinois region where the mixes were placed.

Each gyratory sample yielded two 50 mm thick DC(T) specimens with smooth top and bottom faces. A crack mouth and a straight edge was cut into each specimen using a tile saw for the placement of a measuring gage. On each side of the crack mouth, two core holes were cut to place connections for the loading fixtures. A diagram of a completely cut DC(T) specimen with recommended dimensions is provided in Figure 3-13.

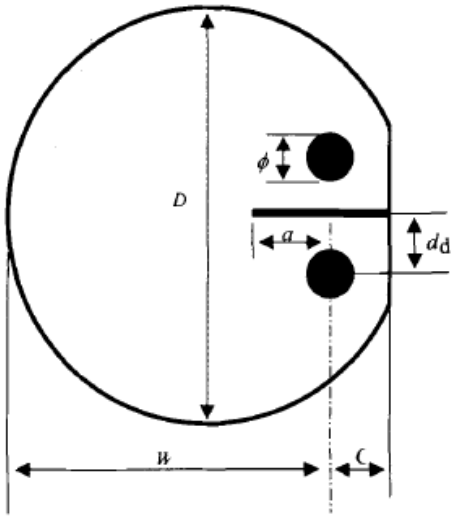

Recommended Dimensions (mm)	
D	150
W	110
ϕ	25
a	27.5
d	25
C	35

Figure 3-13. Completed DC(T) Specimen and ASTM-specified Dimensions (from Wagner 2005)

The fabricated DC(T) specimens were dried at room temperature for at least 24 hours to minimize the presence of moisture. After the drying period, the specimens were conditioned in an environmental cooling chamber at the chosen temperature of -12^0C for 2 hours prior to testing. To test the specimens, the loading connections placed in the core holes were spread apart in displacement control at an opening rate of 1mm/min. In order to determine the fracture energy (G_f) of each specimen, the area under the load vs. the crack

mouth opening displacement (CMOD) plot was calculated and normalized by the fractured surface area. The expression for fracture energy is presented as follows.

$$G_f = \frac{A_f}{l \cdot t}$$

Where:

A_f = Area under load vs. CMOD plot;

l = Length of fractured face; and

t = Specimen thickness.

An example of a load vs. CMOD plot is shown in Figure 3-14.

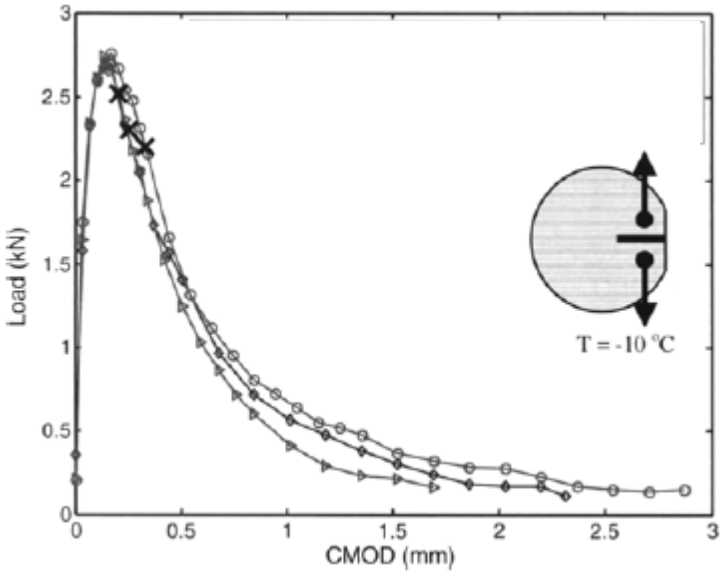

Figure 3-14. Load vs. CMOD plot (from Wagner 2005)

CHAPTER 4: RESULTS AND DISCUSSION

4.1 Performance Grades of the Extracted Binders

The performance grades of the extracted asphalt binders were determined from DSR and BBR test results. The high temperature performance grades are presented in Figure 4-1 and Figure 4-2. The results indicate the addition of recycled materials had a positive impact on the final binder high temperature performance grade as it increased several grades above the virgin asphalt's high temperature performance grade of 58. The increase of grade levels should improve these mixtures rutting resistance whether five percent FRAP was replaced with five percent RAS or not.

A comparison of the binders from field and laboratory samples indicate the binders from laboratory samples are stiffer than the binders from the field samples. Although AASHTO laboratory mixing protocols were followed, the stiffness of the binder in the laboratory mixes is high enough to conclude the samples were possibly aged too long and do not represent the true grade of the blended binder based on the properties/grades of the recovered field produced mixes. The results of the field mixes appear to better represent more reasonable changes in performance grade of the virgin binder when combined with binder from FRAP and/or RAS. The binders follow the general trend that as more recycled materials are added to the asphalt mixtures, the resulting high temperature performance grade of the binder blend will increase.

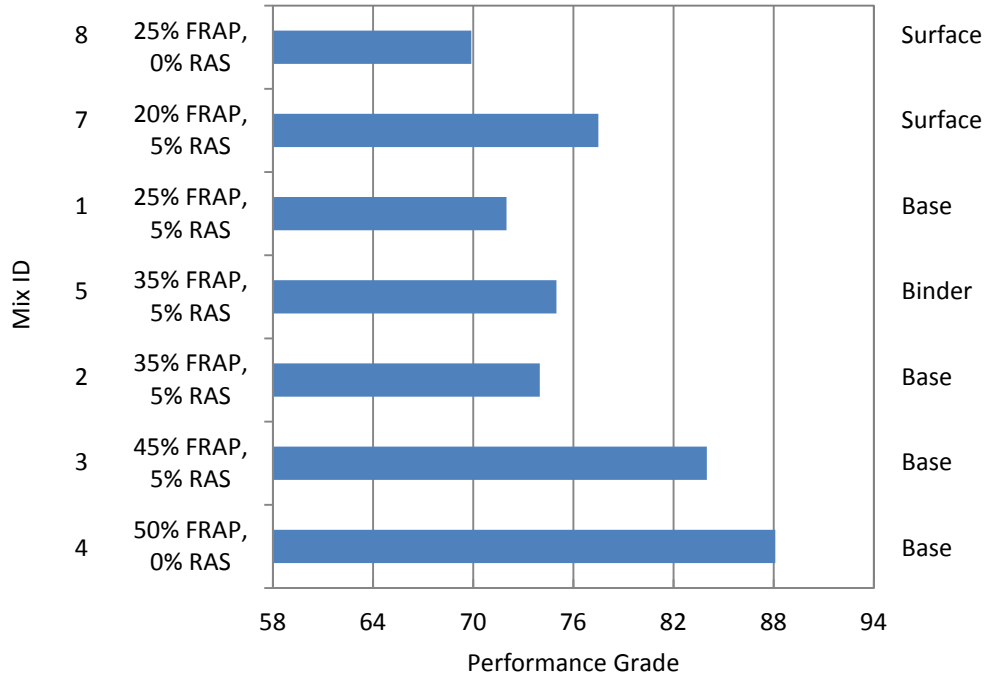

Figure 4-1. High temperature grade of binders extracted from field produced samples

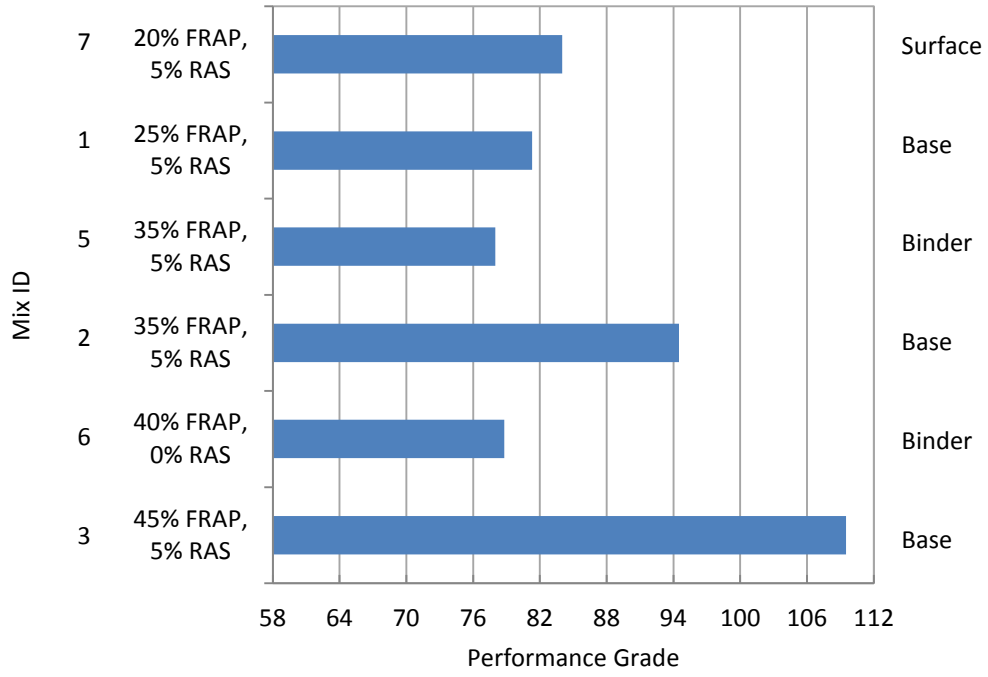

Figure 4-2. High temperature grade of binders extracted from lab produced samples

Figure 4-3 and Figure 4-4 present the low temperature performance grades of binders extracted from field and laboratory produced samples. In these results, binders from laboratory samples are also stiffer than the binders from field samples. Binders from the field samples appear to give more reasonable binder grades as the virgin low temperature grade was a PG-22. Accordingly, test results of binders from laboratory samples are used with more discretion in this analysis while results of the binders from field samples are given more credence.

In the binders from the field samples the low temperature grade did not change in mixes with 25% FRAP/0% RAS and 25%FRAP/5% RAS and only slightly increased in mixes with 20% FRAP/5% RAS and 35%FRAP/5% RAS. For mixes with 50 percent recycled materials, the increase was more substantial as the grades changed from -22 to -10. However, replacing five percent FRAP with RAS for the mix with 50 percent recycled materials had essentially no difference in the binder grade. While some increase in performance grade is expected with these percentages of recycled materials, the field mixes indicate adding up to five percent FRAS and 35 percent FRAP (40 percent total recycled materials) only increases the low temperature grade by one half a grade (3^{o} Celsius).

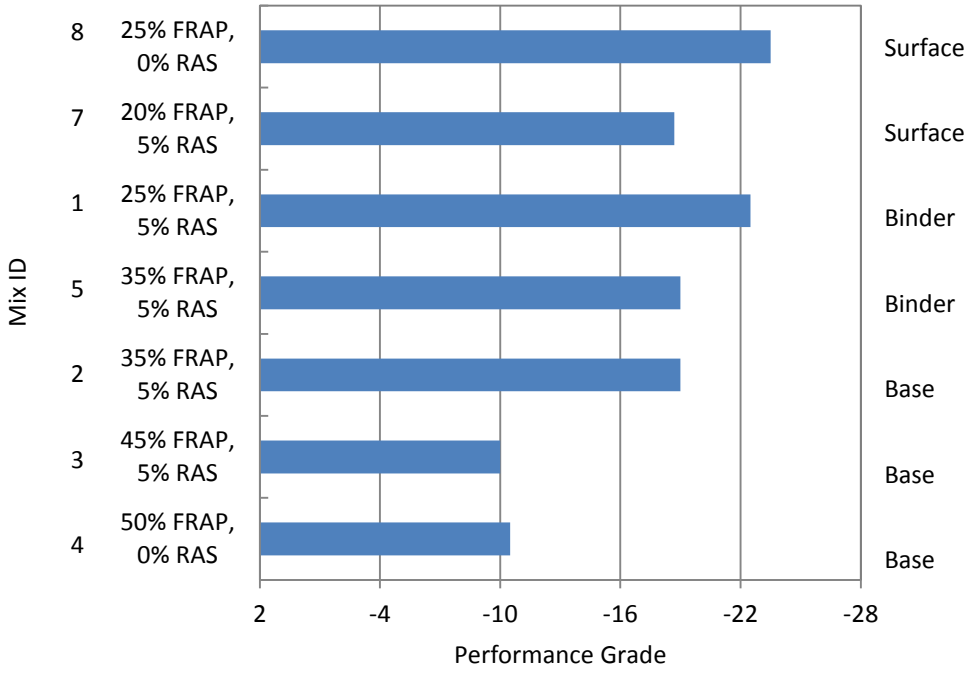

Figure 4-3. Low temperature grade of binder extracted from field produced samples

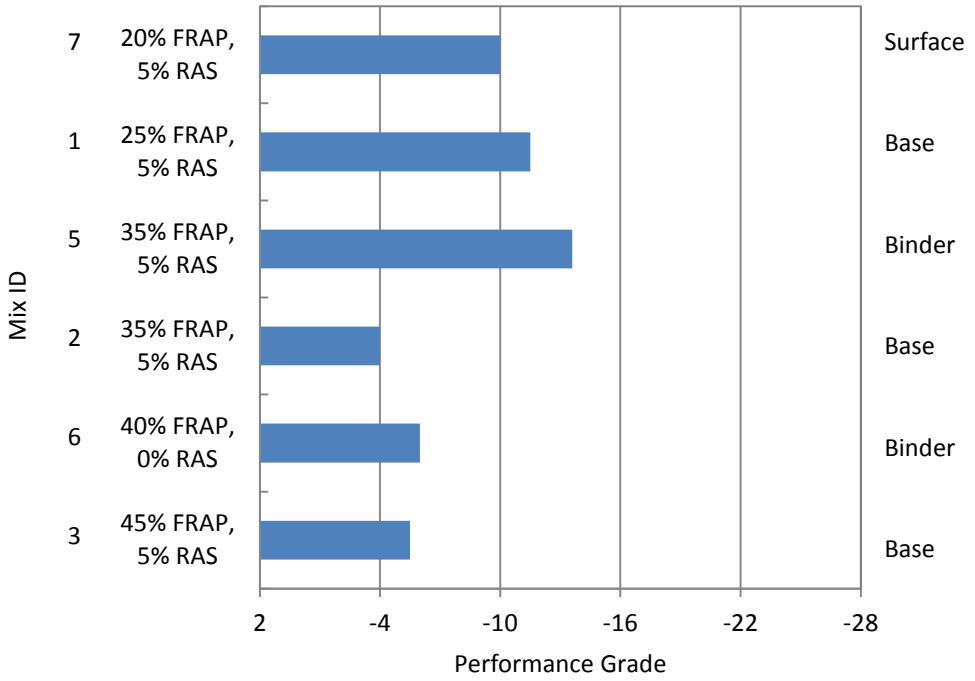

Figure 4-4. Low temperature grade of binders extracted from lab produced samples

4.2 Asphalt Binder Master Curves

The master curves characterizing the complex modulus (G*) of the recovered binder from the base course mixes at different loading frequencies are presented in Figure 4-5 and Figure 4-6. Figure 4-5 shows the master curves of the binder recovered from field samples, while Figure 4-6 shows the curves of the binder recovered from the laboratory samples. The master curves indicates that as more FRAP is added to the pavement mixtures, the curves shift upwards at the low frequency end of the curve with a slight upwards shift at the high frequency end of the curve. This trend indicates a stiffening of the binder at higher temperatures and/or lower frequencies as more FRAP is added to the pavement mixture which translates to an increased resistance to permanent deformation. The modest increase at the high frequency end of the curve indicates that as more FRAP is added to the pavement mixtures, the binder has the potential to become stiffer at lower temperatures for an increase in cracking potential. The master curves also indicate the binder from laboratory samples is much stiffer than the binder from field samples.

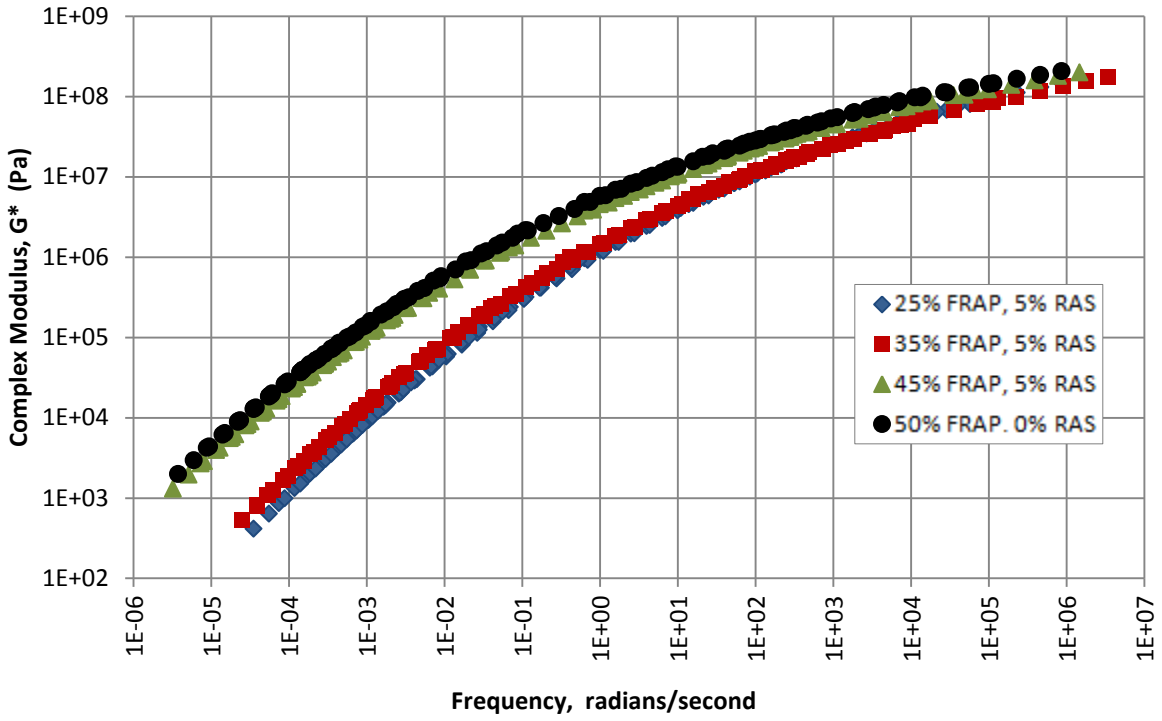

Figure 4-5. Master curves of recovered binder from field produced base course mixes

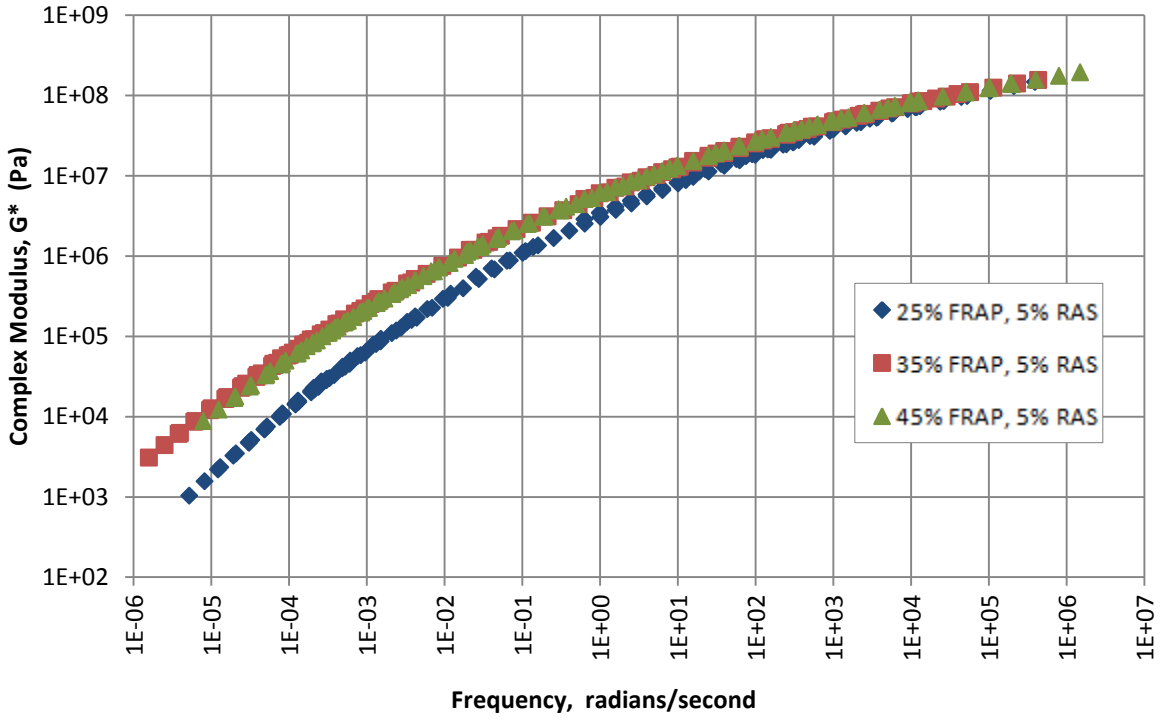

Figure 4-6. Master curves of binder from lab produced base course mixes

Figure 4-7 through Figure 4-9 display the base, binder, and surface course master curves for the recovered asphalt, respectively. When five percent RAS is replaced with five percent FRAP, the masters curves shift differently among the three binders. The affects of RAS appear to have less influence at higher FRAP percentages. For the master curves with binder containg 25 percent recycled materials, replacing five percent FRAP with RAS increases the stiffness of the binder at the high temperature/low frequency end but not at the low temperature/high frequency end. For binders with 40 to 50 percent percent recycled materials, there is no substantial shift in the master curves when five percent FRAP is replaced with five percent RAS.

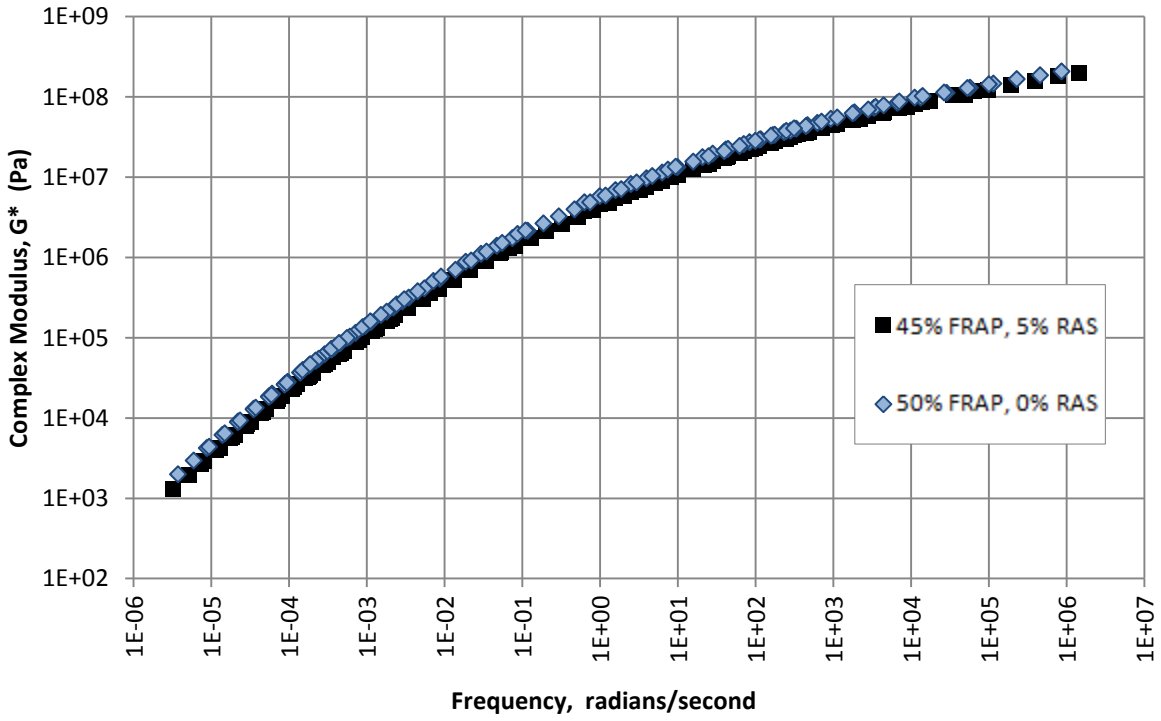

Figure 4-7. Master curves of binder from base course mixes with 50% recycled materials

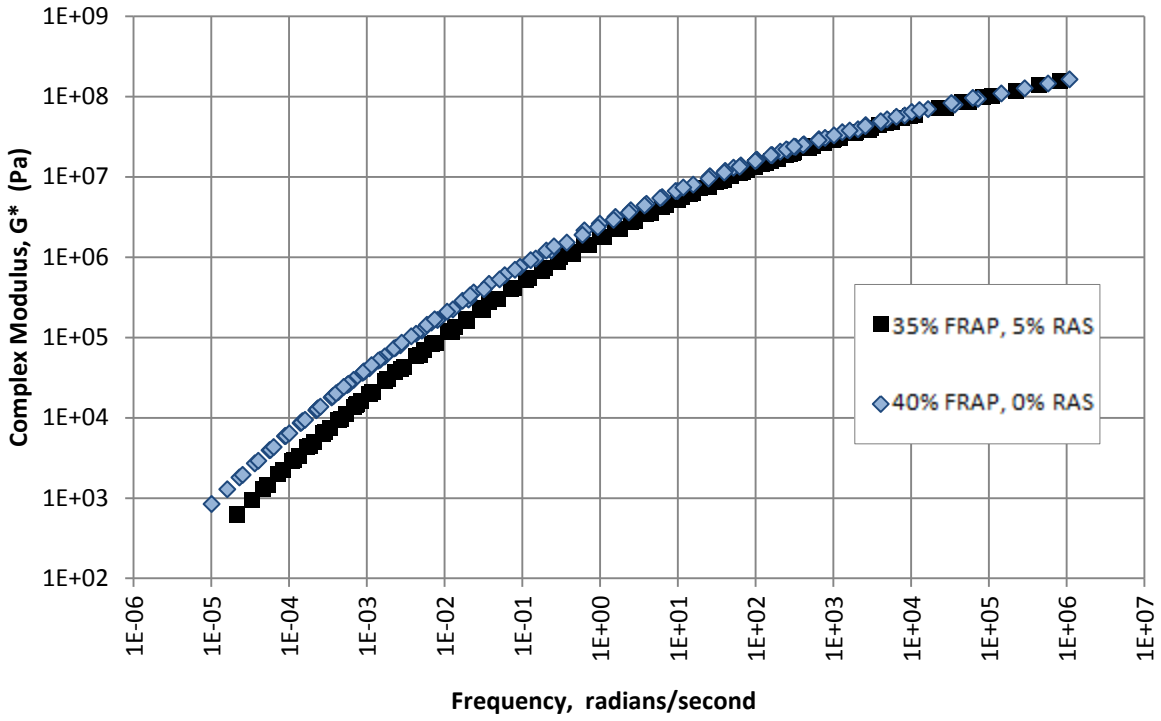

Figure 4-8. Master curves of binder from mixes with 40% recycled materials

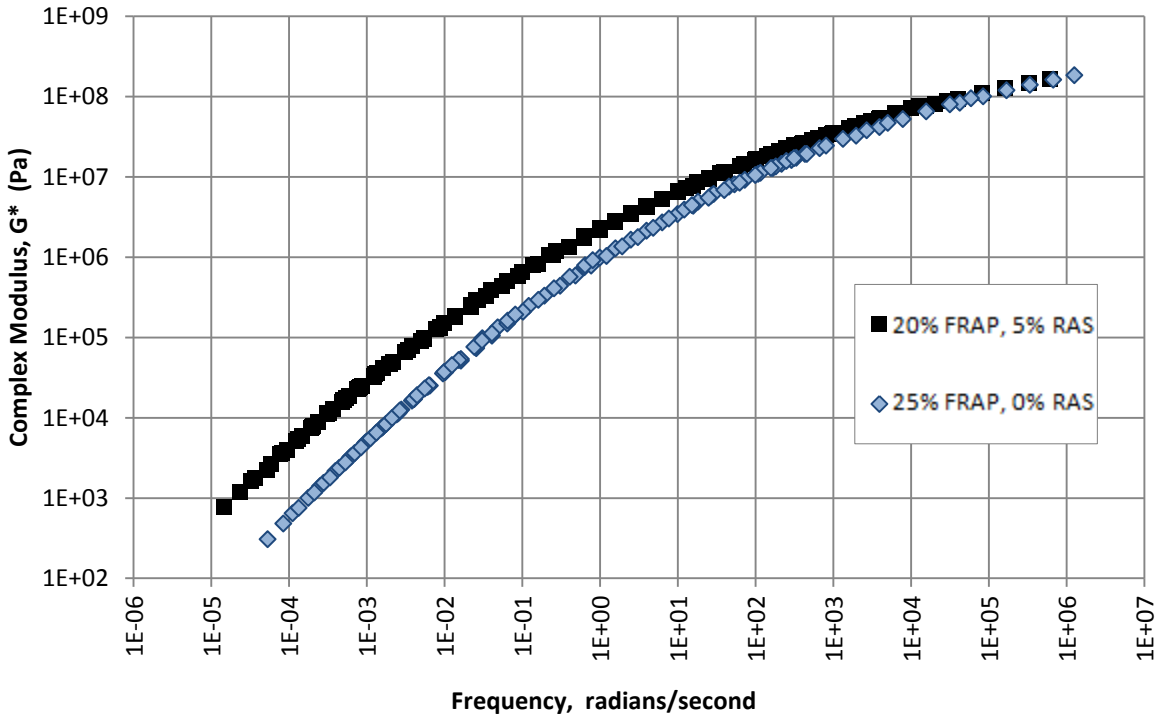

Figure 4-9. Master curves of binder from mixes with 25% recycled materials

In Figure 4-10 through Figure 4-14 a comparison is made between the master curves of binders from field and laboratory samples. All five master curves indicate the binders from laboratory produced samples are stiffer than the binders from field produced samples at all frequency ranges. This further supports the hypothesis that the AASHTO curing times when mixing laboratory samples may be too long for mixtures containing moderate amounts of recycled materials.

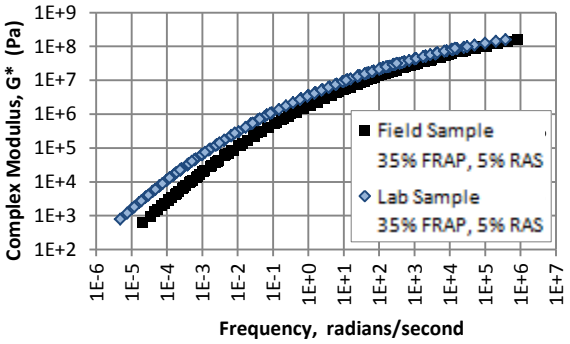

Figure 4-10. Binder course field vs. lab

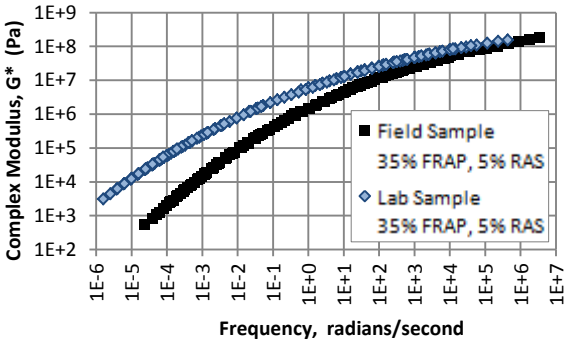

Figure 4-11. Base course field vs. lab

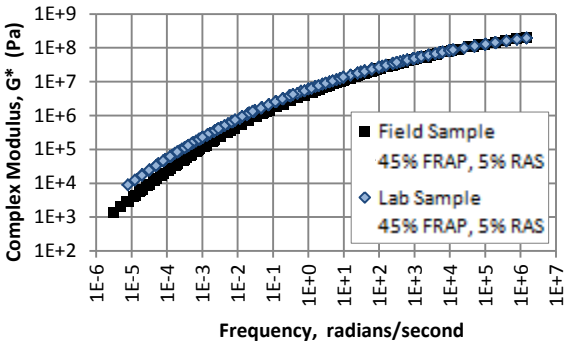

Figure 4-12. Base course field vs. lab

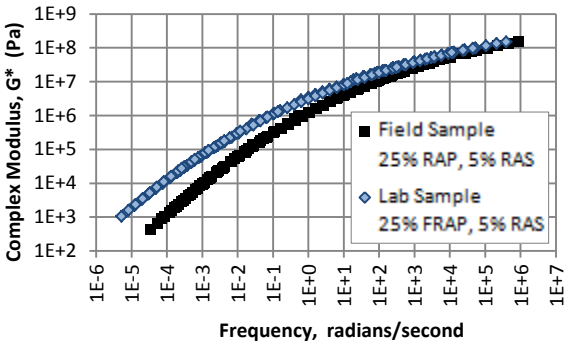

Figure 4-13. Base course field vs. lab

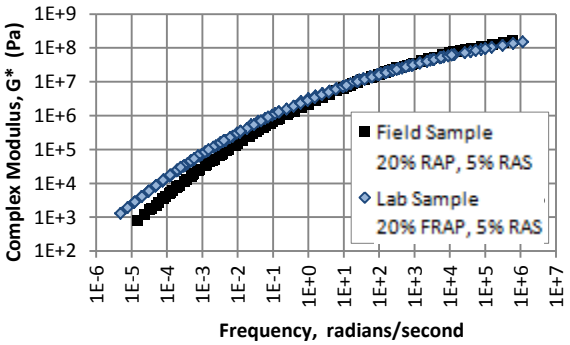

Figure 4-14. Surface course field vs. lab

The results of the binder tests indicate that increasing the percentage of FRAP in the Tollway mixes increases their rutting resistance as the performance grades of the field mixes with 50 percent recycled materials increased to a PG 88. The influence of RAS on the high temperature performance grade is exhibited by the shift in master curves for the binders from field samples. Only the master curve for the surface mix with 25 percent recycled materials displayed a visual increase in stiffness while the mixes with higher percentages of recycled materials (40% and 50%) did not. Therefore RAS may increase the rutting resistance of mixes with lower percentages of FRAP while not affecting mixes with higher percentages of FRAP.

The strongest trend in low temperature performance grades comes from analyzing the binders in terms of total percent recycled materials as RAS did not have any conclusive affects on the low temperature grade. Field samples with 25 to 30 percent recycled materials exhibited either no change or a half grade increase, field samples with 40 percent recycled materials exhibited a half grade increase; and field samples with 50 percent recycled materials exhibited the highest grade change of two full grade increases. Consequently, the binders with 50 percent recycled materials will be the most susceptible to thermal cracking in colder climates. However, binder properties alone do not determine the performance of an asphalt pavement as the aggregate/asphalt structure play a key role in HMA performance. As well, the RAS materials include fibers which may improve the low temperature ductility of the mix.

4.3 Dynamic Modulus Test Results

All the dynamic modulus (E*) test results are presented in Appendix A. E* values that appear to be outliers because they do not follow the trend in the testing data are shaded in gray. These values were omitted from the average E* values used to construct the master curve models but are taken into consideration in the statistical analysis by comparing the results before and after outlier removal. Only one outlier was encountered during the statistical analysis.

To analyze the tests results, first the individual master curves are compared followed by a statistical analysis of the dynamic modulus values obtained from the testing procedure. With the combination of three temperatures and nine frequencies, 27 E* values were measured for each sample. Rather than comparing all 27 values, three E* values were selected from each mixture as shown in Figure 4-15 to analyze its stiffness properties at high, intermediate, and low temperatures for the performance indicators of rutting, fatigue cracking resistance, and thermal cracking resistance. The statistical analysis conducted used two-way and one-way analysis of variance (ANOVA) to determine if any differences among the mean dynamic modulus values of each batch of five samples were significant or to due random error. The statistical software program JMP (2009) was used to conduct the analysis. A 95 percent significance level was used in the analysis for an alpha value of 0.05. The dynamic modulus values used were from the results of testing each mixture at 4°C at 25 Hz (high freq), 21°C at 10 Hz (med freq), and 37°C at 0.1 Hz (low freq).

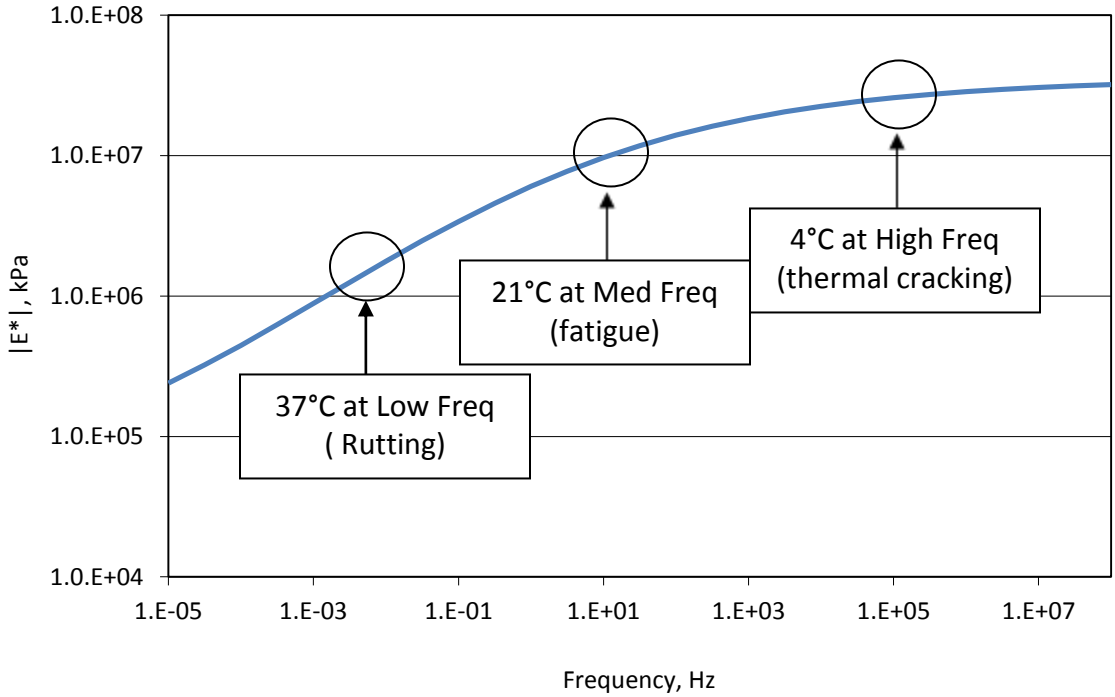

Figure 4-15. Dynamic modulus values used in statistical analysis

The first analysis conducted is to determine how increasing the percentage of FRAP in the base course mixes that contain five percent RAS affects their performance. The master curves from base course field and laboratory samples are presented in Figure 4-16 and Figure 4-17, respectively. Each mixture has the same amount of RAS (five percent) with different percentages of FRAP (25, 35, and 45 percent). In both the field and laboratory master curve models, there appears to be trend of increasing stiffness between when 45 percent FRAP is added to mixtures as opposed to only 25 percent FRAP. These observations correlate with the trends in the binder master curves.

The results of the ANOVA analysis are presented in Table 4-1 and Figure 4-18. For this analysis, a randomized basic factorial design was used to test if the sample type (laboratory or field) and percentage of FRAP in the base course mixes has significant effects on the E* results. The treatments used in the experiment are FRAP percentage and sample

type. The results indicate that at high temperatures/low frequencies, increasing the amount of FRAP from 25 percent to 35 percent significantly increases the E* due to the low p-value of 0.0006 and least significant difference (LSD) level change from A to B. At medium temperatures, increasing the amount of FRAP from 35 to 45 percent significantly increases the E* as well due to the low p-value of 0.0002 and change in LSD level from A to B. At high temperatures, the laboratory samples had significantly higher E* values than the field samples. There is also a significant interaction affect between the percent FRAP usage and sample type at intermediate temperatures.

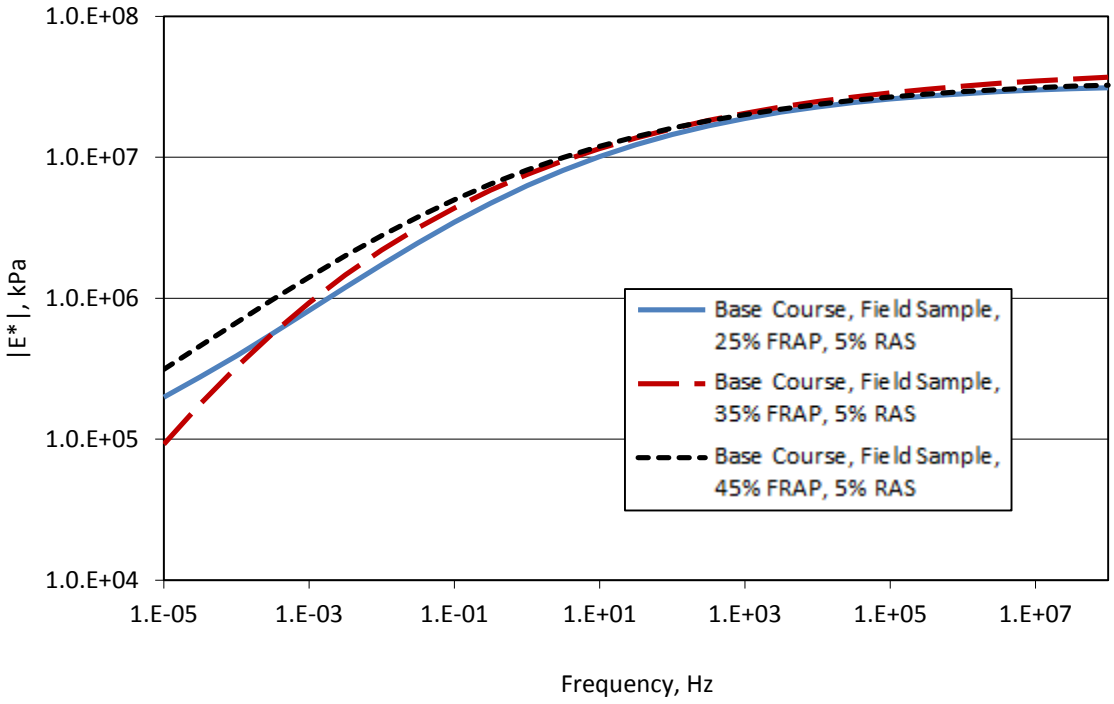

Figure 4-16. Master curves for base course mixes from field samples

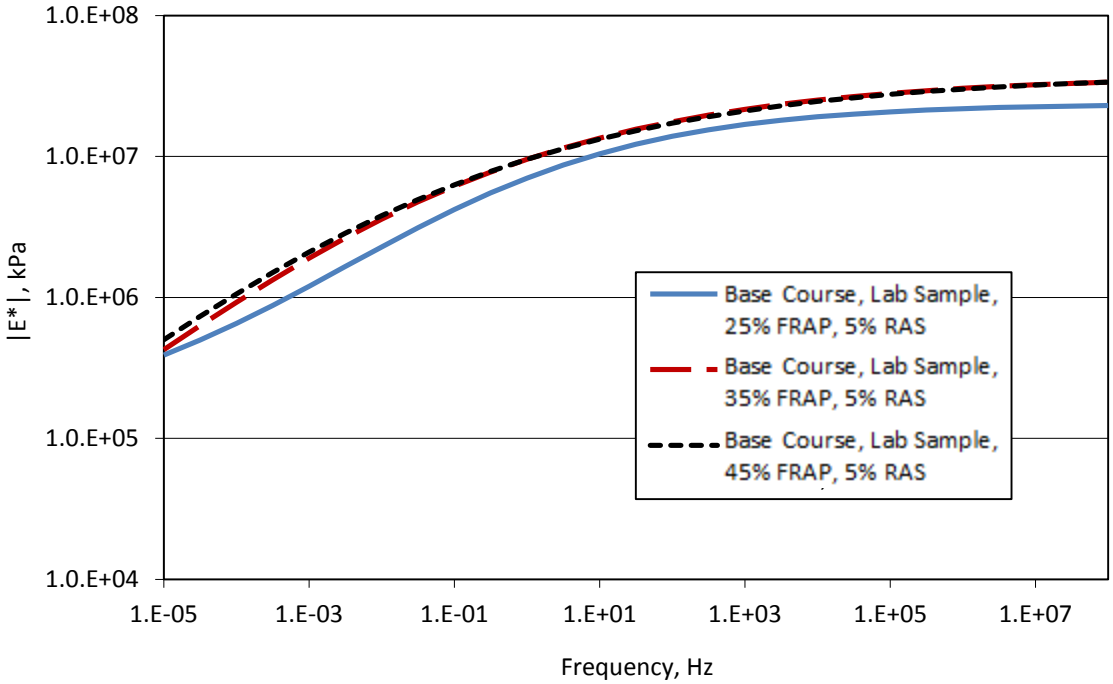

Figure 4-17. Master curves for base course mixes from laboratory samples

Table 4-1. ANOVA analysis for base course mixes

Dynamic modulus at 37°C at low frequency

Source	DF	Sum of Squares	Mean Square	F Ratio	Prob > F
Sample Type	1	2.563e+12	2.563e+12	23.7044	<.0001*
% RAP	2	2.2845e+12	1.142e+12	10.5643	0.0006*
Sample Type*% RAP	2	6.6507e+11	3.325e+11	3.0755	0.0655
Error	23	2.4869e+12	1.081e+11		
C. Total	28	8.006e+12			

Dynamic modulus at 21°C at medium frequency

Source	DF	Sum of Squares	Mean Square	F Ratio	Prob > F
Sample Type	1	2.1092e+11	2.109e+11	0.2360	0.6315
% RAP	2	2.278e+13	1.139e+13	12.7421	0.0002*
Sample Type*% RAP	2	8.479e+12	4.24e+12	4.7429	0.0184*
Error	24	2.1453e+13	8.939e+11		
C. Total	29	5.2922e+13			

Dynamic modulus at 4°C at high frequency

Source	DF	Sum of Squares	Mean Square	F Ratio	Prob > F
Sample Type	1	3.4064e+12	3.406e+12	0.8013	0.3796
% RAP	2	1.0486e+13	5.243e+12	1.2334	0.3091
Sample Type*% RAP	2	1.6488e+13	8.244e+12	1.9394	0.1657
Error	24	1.0202e+14	4.251e+12		
C. Total	29	1.324e+14			

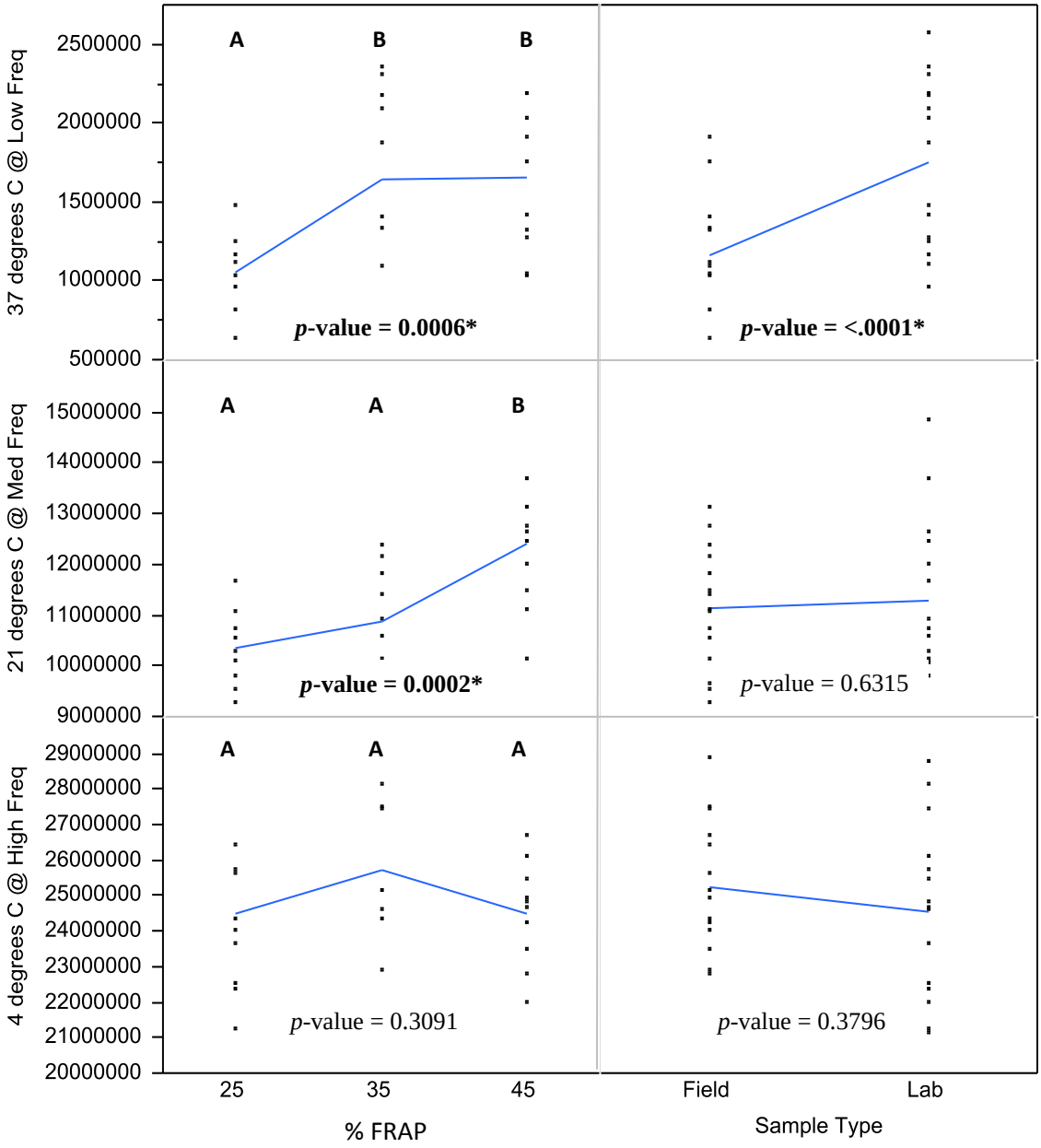

Figure 4-18. Least squared means plots with LSD levels

Based on the results of the analysis, increasing the amount FRAP can improve the rutting resistance of the base course mixes, but above 40 percent recycled materials (35% FRAP plus 5% RAS) there is no significant improvement. Above 40 percent recycled materials, the fatigue performance may be affected due to the increase in stiffness.

There are no statistical differences among the low temperature E* values in these mixes indicating that different percentages of FRAP (25% to 45%) have no effect on their low temperature performance. In contrast, a higher percentage of FRAP did effect the low temperature performance of the recovered binders by increasing the low performance grade. The negatives effects of FRAP on low temperatures may not be significant in the HMA samples is due to the fibers in the RAS which can increase the ductility and tensile strain of the mixture.

The interaction of E* values in Figure 4-19 shows that at intermediate temperatures the amount of FRAP affects the stiffness of the laboratory samples differently than the stiffness of the field samples. From 25 percent FRAP to 35 percent FRAP, the stiffness slightly decreased in the laboratory samples before increasing at 45 percent FRAP. Because FRAP materials are stiffer than virgin materials, a decrease in modulus is not expected. However, both laboratory and field produced samples did increase in stiffness when the percentage of FRAP increased from 25 percent to 45 percent which is the practical aspect of this data set.

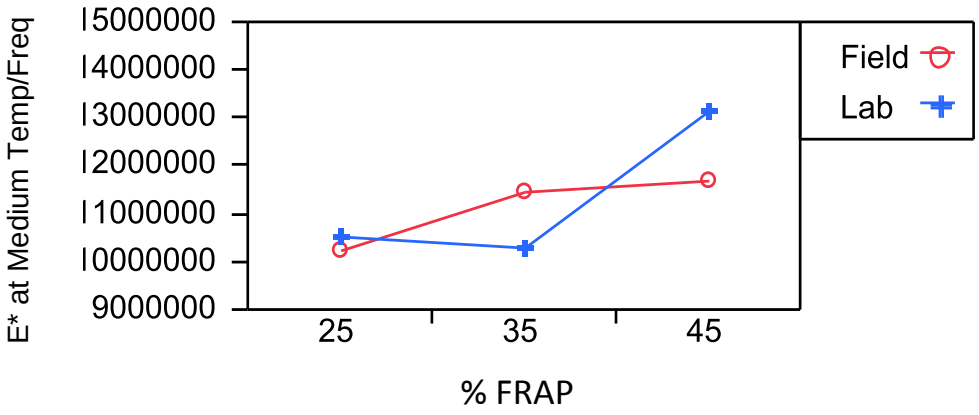

Figure 4-19. Interaction of E* values between %FRAP and sample type

The E* master curves that compare experimental mixes (5% RAS) to control mixes (0% RAS) for the base course, the binder course, and the surface course mixes are presented in Figure 4-20 through Figure 4-22. The RAS and no RAS master curves of the base course and binder course follow similar trends, while the master curve of the surface course mix containing RAS shifted substantia lly higher at low frequencies compared to the master curve of the surface course containing no RAS.

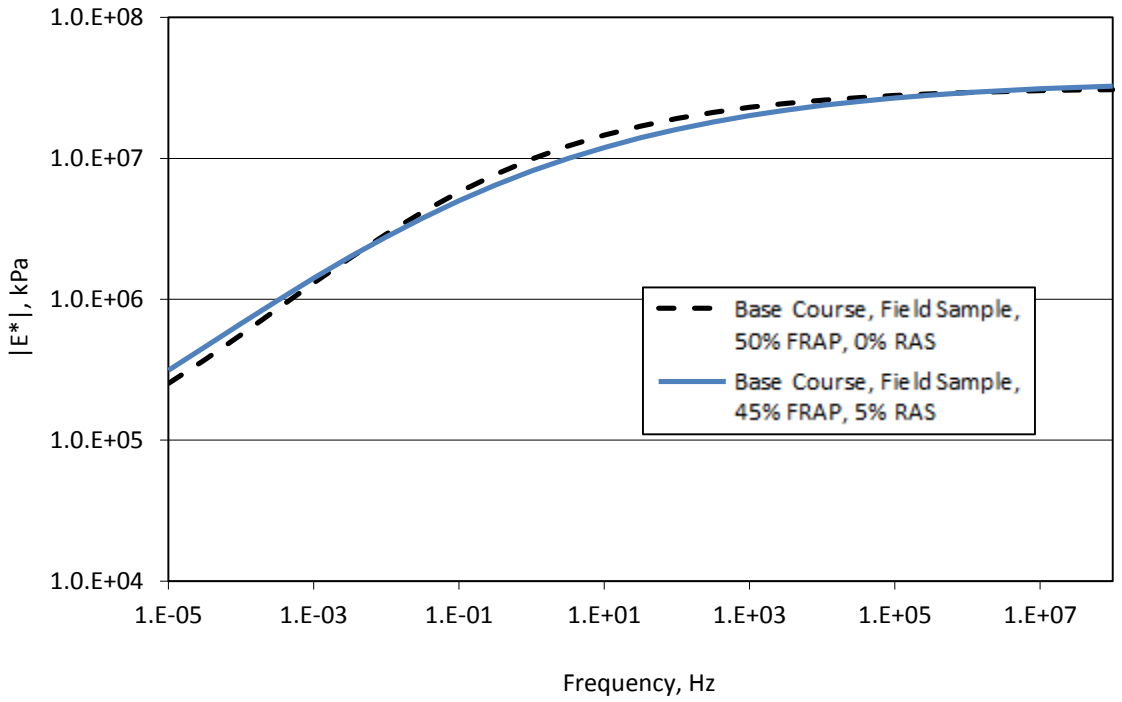

Figure 4-20. E* Master curves for base course field samples

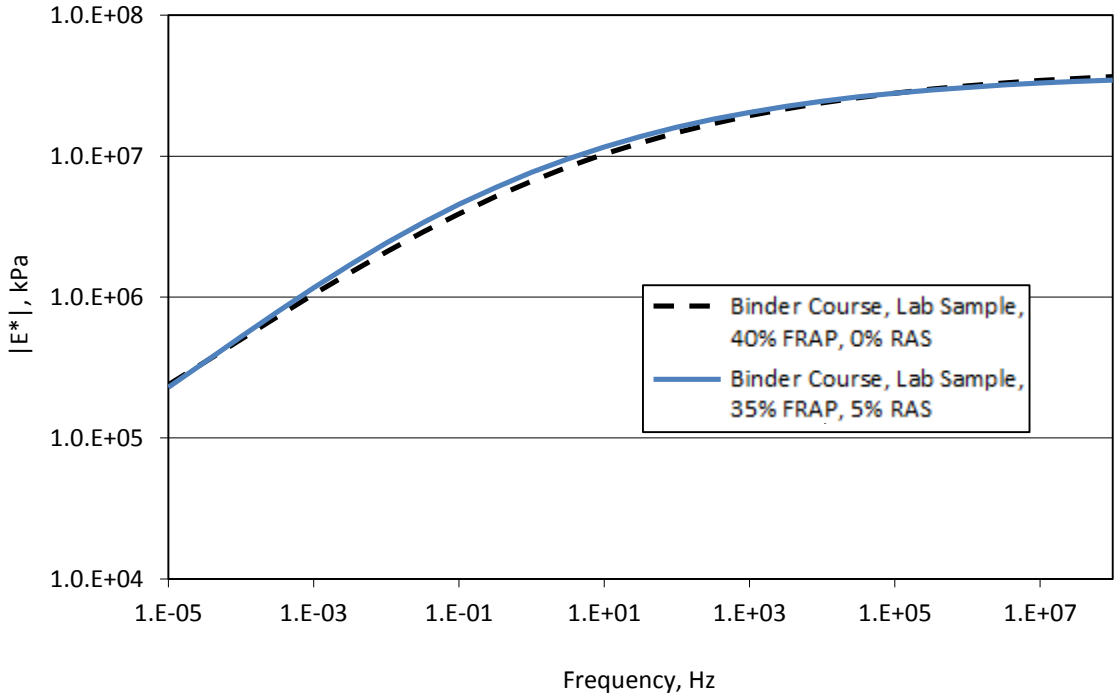

Figure 4-21 E* Master curves for binder course lab samples

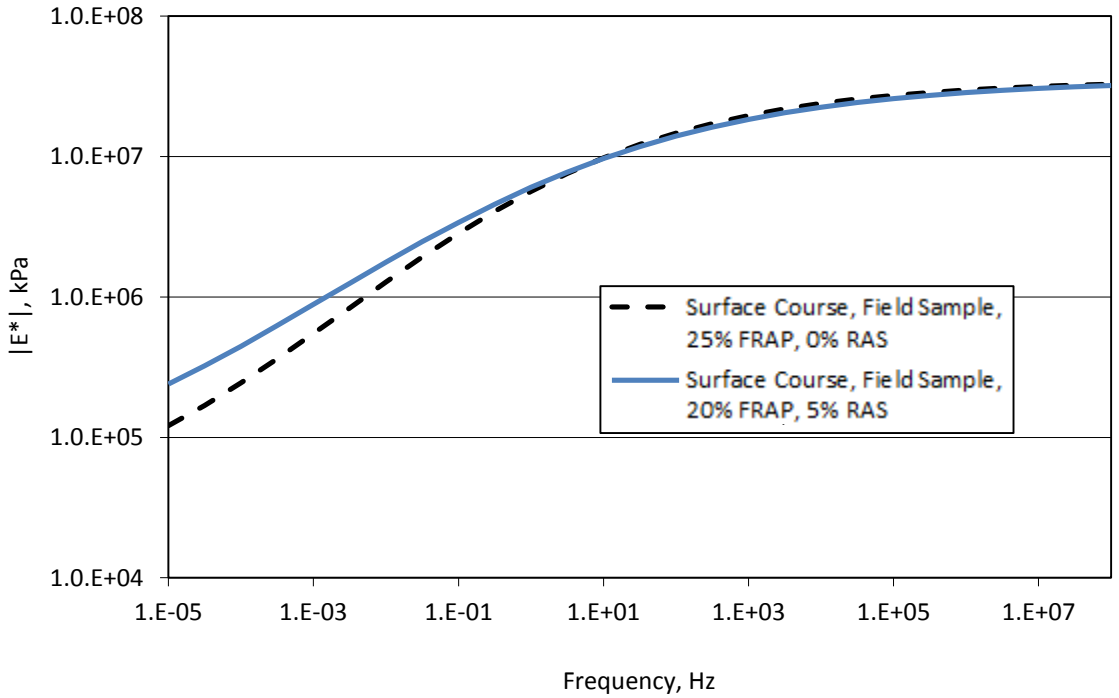

Figure 4-22. E* Master curves for binder course lab samples

Results of the one-way ANOVA tests conducted to compare the dynamic modulus values of the RAS mixes to the no-RAS mixes are presented in Figure 4-23. One-way ANOVA essentially reduces the analysis to a two sample t-test since a comparison is being made between two samples to test the null hypothesis if they came from the same population. The t-tests results indicate no significant differences between RAS and no-RAS mixtures at high temperature/low frequencies for all three mix types although the average E* values increased each time five percent RAS was replaced with five percent FRAP. In contrast, at intermediate temperatures and frequencies there are significant differences between RAS and no-RAS mixtures for all three mix types. The reason why the t-test detected differences at intermediate temperatures and not at high temperatures appears to be from the larger variation in test results at high temperatures. The larger variation in E* values at 37°C may be due to softening of the epoxy used to attach the LVDT metal holders on to each sample.

At low temperatures/high frequencies, the t-tests initially indicated there were no statistical differences for all three mix types. However, the base course mix with no RAS appeared to have one very low value that did not correspond with the overall trend in the data which can be seen in the values listed in Appendix A. After the removal of this suspected outlier, the p-value decreased to 0.026 resulting in a significant decrease in stiffness at low temperatures in the base course when RAS is used. The decrease in stiffness at low temperatures is an interesting observation since a larger percentage of the virgin binder in is being replaced when RAS replaces FRAP. The decrease in stiffness could be the result of fibers influencing the ductility of the mix.

While the dynamic modulus at low temperatures can give an indication of an asphalt pavements tendency to fracture or develop fatigue related distress, it does not directly

measure it. For a more accurate correlation between laboratory results with field performance for cracking and fatigue, the results from the disc shaped compact tension test and the flexural beam test will be used to evaluate the performance of the RAS mixtures under these distress criteria and further investigate the influence of the RAS fibers.

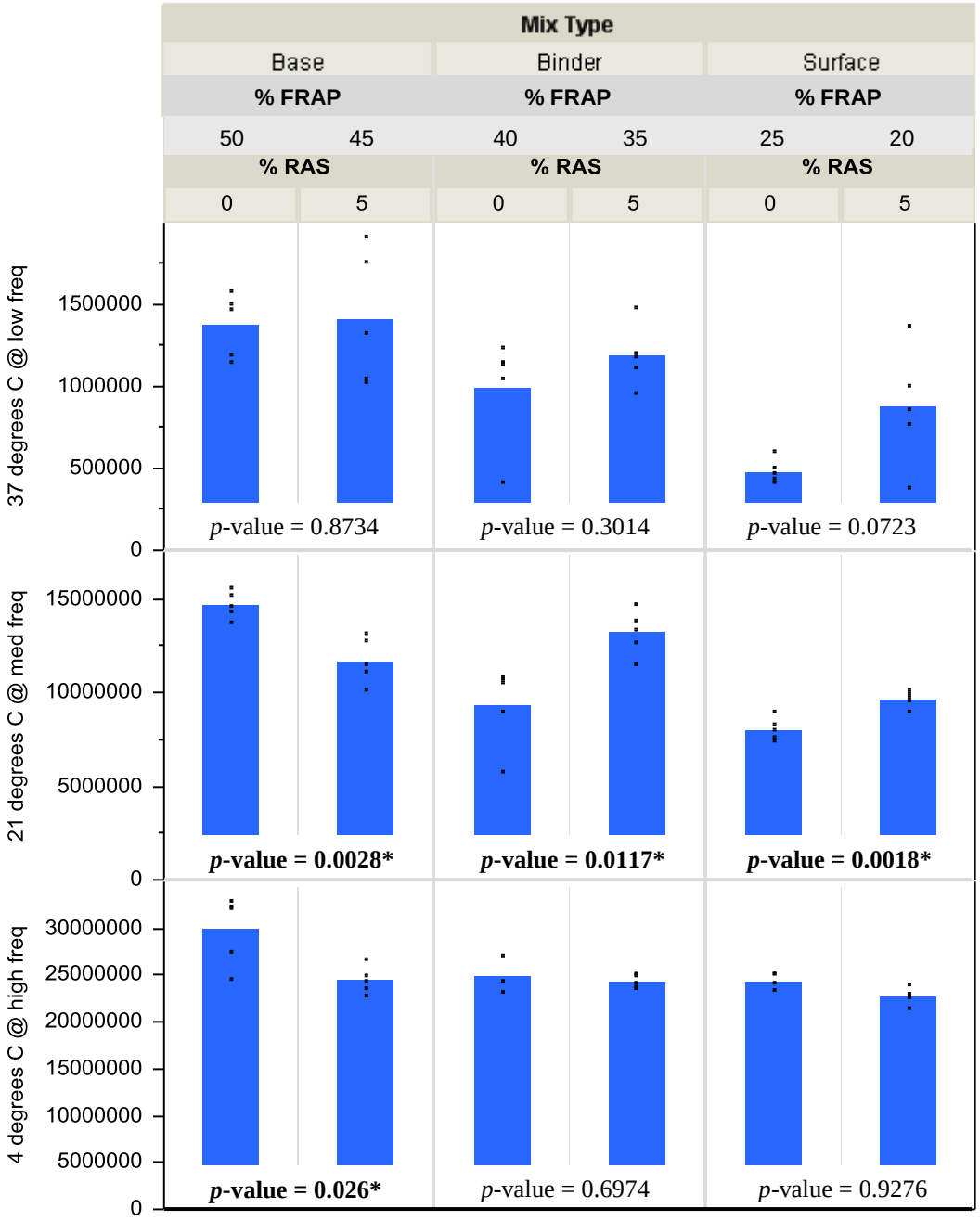

Figure 4-23. t-test results comparing E* values of mixes with RAS and no RAS

E* Master curves comparing field to laboratory produced mixes are presented in Figure 4-24 through Figure 4-28. They indicate the laboratory mixes are stiffer than the field mixes, especially at higher temperatures/lower frequencies. This provides further support that the laboratory oven curing times of recycled materials during mixing and compacting in the laboratory may be too long for mixtures containing moderate levels of recycled materials.

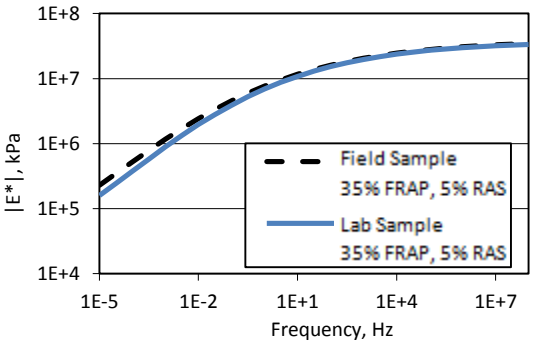

Figure 4-24. Binder course field vs. lab

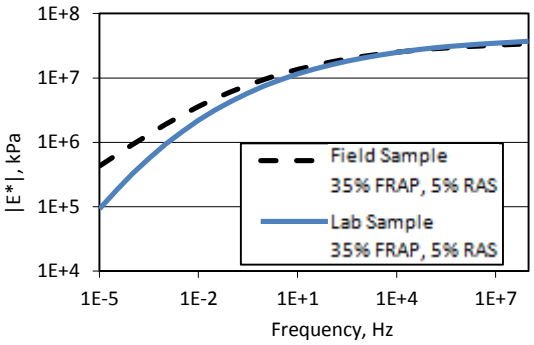

Figure 4-25. Base course field vs. lab

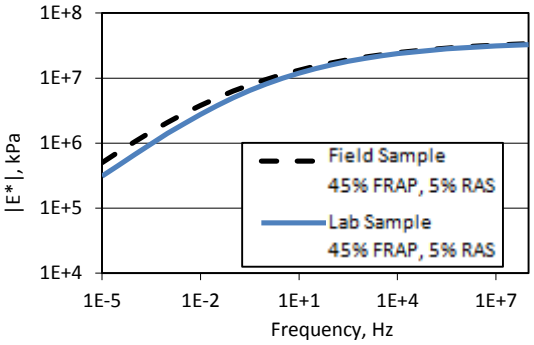

Figure 4-26. Binder course field vs. lab

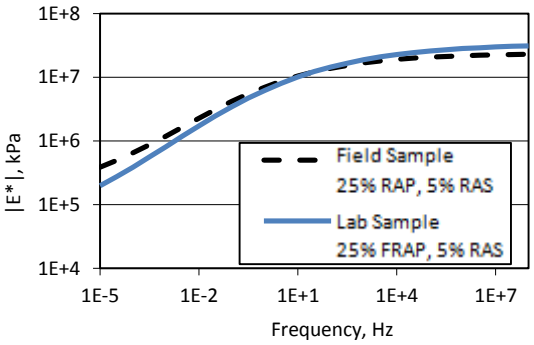

Figure 4-27. Base course field vs. lab

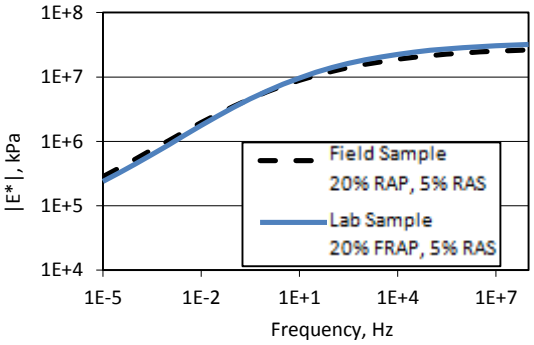

Figure 4-28. Binder course field vs. lab

4.4 Flow Number

The flow number of an asphalt mixture corresponds to the number of cycles needed to accumulate 0.5 percent strain in the sample tested. A higher flow number indicates a higher resistance to rutting. The test ends at 10,000 load cycles even if the sample has not accumulated 0.5 percent strain. A sample that reaches 10,000 load cycles is considered to be essentially rut resistant. Since all the samples tested reached 10,000 load cycles, the response measured in this test was the accumulated strain and is presented in Figure 4-29. The values are the average strain levels of the three samples in each batch. A lower strain level was interpreted as a higher resistance to rutting.

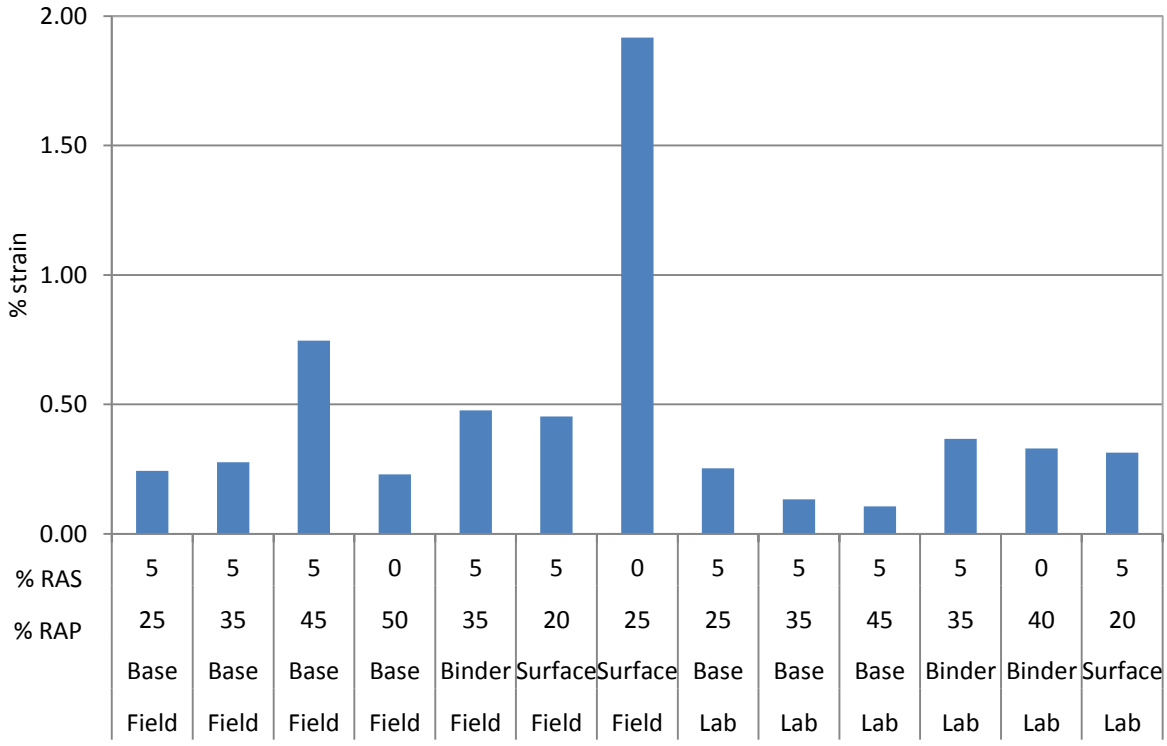

Figure 4-29. Percent strain after 10,000 cycles in flow number test

Statistical analyses using ANOVA tables and t-test analyses identical to the dynamic modulus statistical analyses were conducted to compare how FRAP percentage and sample type affect the rutting performance of the base course mixture and how replacing five percent FRAP with five percent RAS affects the rutting performance of all three mix types.

A summary of the ANOVA analysis to determine how FRAP percentage and sample type affect the rutting performance of the base course mixture is presented in Table 4-2 and Figure 4-30. The analysis indicates the percent strain accumulation in the base courses mixes correlates well with the base course mixes dynamic modulus tests at high temperatures. As the percentage of FRAP increases from 25 to 35 percent, the rutting resistance of the mixture significantly increases. From 35 to 45 percent FRAP, the rutting resistance does not change. The laboratory samples are also stiffer than the field samples.

The interaction between the field and laboratory samples indicates the effect of FRAP in laboratory samples is not the same as the effect of FRAP in field produced samples. The laboratory produced mixtures have a more consistent trend in percent strain accumulation versus FRAP percentage than the field produced samples. Nevertheless, both laboratory and field produced samples follow the same general trend of a decrease in strain with an increase in FRAP from the 25 percent level to the 45 percent level which is the practical aspect of this data.

Table 4-2. ANOVA table for % strain accumulation in the base course

Source	DF	Sum of Squares	Mean Square	F Ratio	Prob > F
Sample Type	1	0.29902222	0.2990222	56.4193	<.0001*
% FRAP	2	0.38443333	0.1922167	36.2673	<.0001*
Sample Type*% FRAP	2	0.12754444	0.0637722	12.0325	0.0014*
Model	5	0.81100000	0.162200	30.6038	<.0001*
Error	12	0.06360000	0.005300		

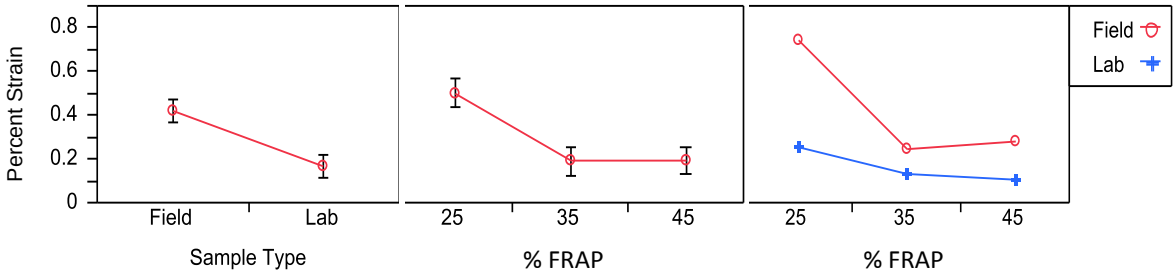

Figure 4-30. LSD means plots for % strain accumulation in the base course

Results of the t-tests tests conducted to compare the percent strain accumulation of mixtures containing RAS to mixes containing no-RAS are presented in Figure 4-31. The t-test flow number analysis is able to detect significant differences among mixtures with RAS and no-RAS where the t-test analysis for the dynamic modulus at high temperatures did not. From the t-test results, replacing five percent FRAP with five percent RAS significantly decreases the compressive strain accumulations in the binder and surface course mixes, but not the base course mixes.

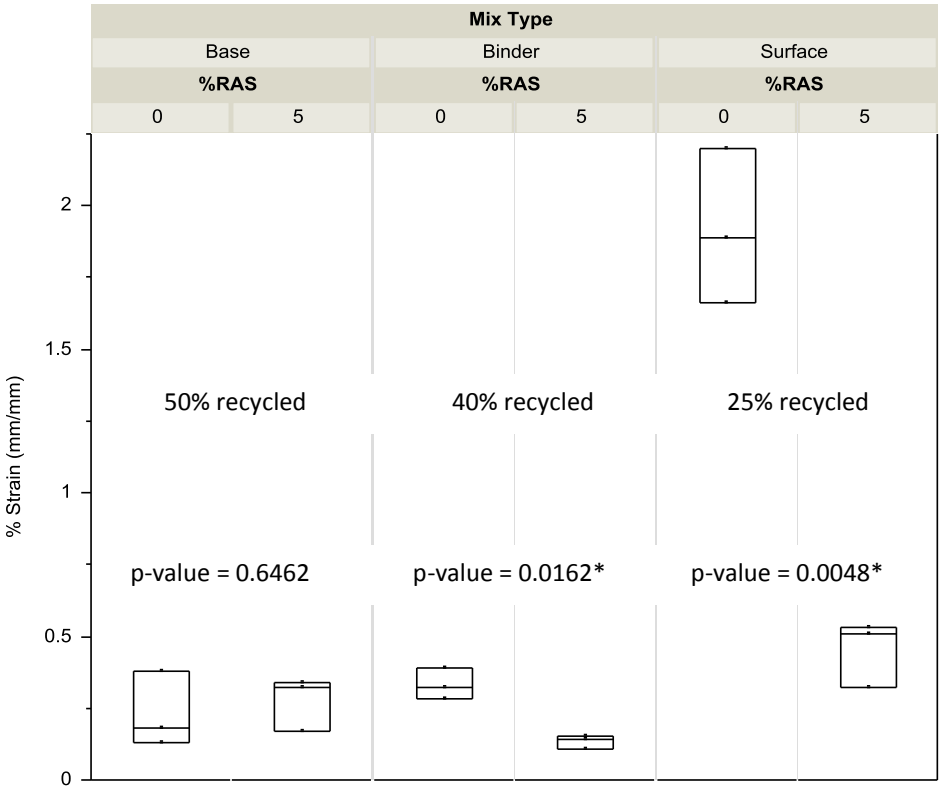

Figure 4-31. t-test results for strain accumulation in RAS mixtures

4.5 Tensile Strength Ratio Test Results

The tensile strength ratio test (TSR) results of the field produced mixtures are presented in Figure 4-32. Many transportation agencies require that an asphalt mixture have a TSR value of 0.80 or greater for good performance in a freeze-thaw environment. The results indicate good freeze-thaw performance can be expected for five of the seven mixtures as their TSR values are greater than 0.80. Although the other two mixtures did not meet the criteria, they come very close. Based on these results, mixtures that contain RAS and higher percentages of FRAP can have low moisture sensitivity and perform adequately in freeze-thaw environments.

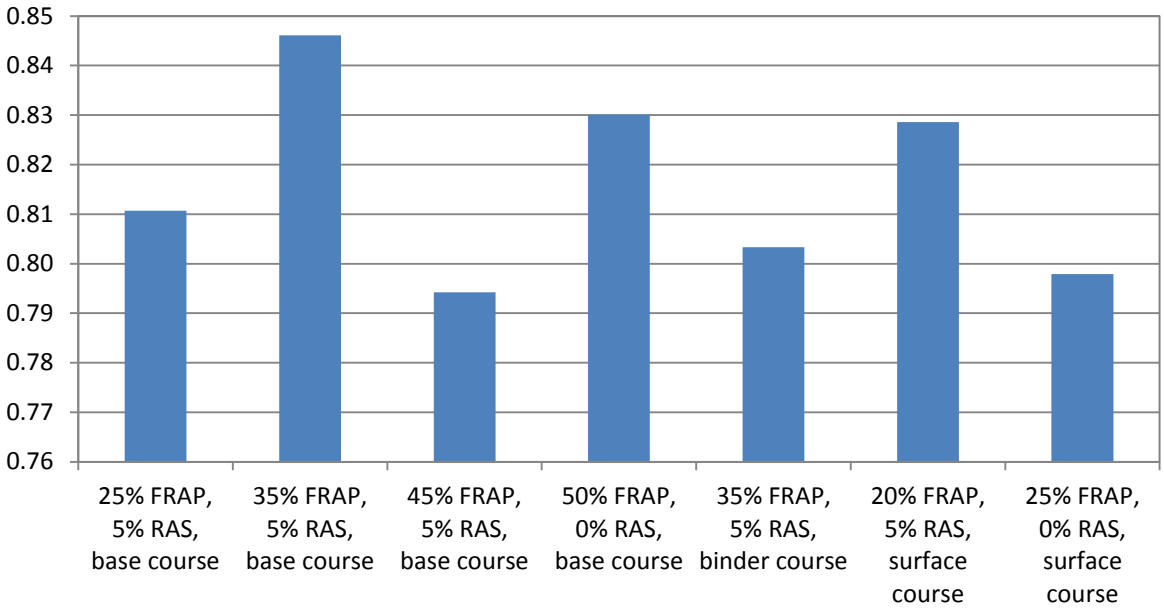

Figure 4-32. Tensile strength ratios of field produced mixes

4.6 Beam Fatigue Test Results

The fatigue data from the Tollway mixes was modeled using the following relationship to characterize their fatigue behavior.

$$N_f = K1\left(\frac{1}{\varepsilon_o}\right)^{K2}$$

The K1 and K2 coefficients are provided in Table 4-3. The K1 coefficient characterizes the flexural modulus, and the K2 coefficient indicates the rate of damage accumulation in a sample. When using this relationship as failure criterion for a pavement design, a lower K2 value is more conservative as it assumes faster accumulation of fatigue damage. Suggested values for K2 are 4.477 by The Asphalt Institute, 4.0 by Shell, and 3.571 by the University of Nottingham (Huang 2004). Carpenter (2006) recommended the Illinois Department of Transportation use a K2 value in the range of 3.5 to 4.5.

Table 4-3. Fatigue coefficients for Tollway mixes

Mix Type	% FRAP	% RAS	% Air Voids	K1	K2	R^2
Surface	25	0	7	6.486E-09	4.064	0.951
Surface	20	5	7	2.770E-10	4.163	0.989
Surface	20	5	4	2.497E-17	6.781	0.917
Base	25	5	5	1.338E-09	4.182	0.980
Base	25	5	2	3.077E-12	5.063	0.943
Base	35	5	5	6.669E-04	1.991	0.971
Base	35	5	2	4.820E-24	8.697	0.896
Binder	35	5	6	6.966E-08	3.605	0.860
Binder	35	5	3	6.123E-09	4.034	0.976
Binder	40	0	3	6.607E-12	4.980	0.913
Base	45	5	2	3.766E-06	2.907	0.662
Base	45	5	5	1.398E-07	3.460	0.803
Base	50	0	5	2.194E-16	6.158	0.972

By comparing the number of cycles to failure at the various strain levels the following observations can be made. With respect to the base course mixes in Figure 4-33, all the mixes exhibit reasonable levels of fatigue resistance except for the 35 percent/5 percent mix. This mix exhibits a steeper slope with a higher K2 value of 1.991 indicating quicker damage accumulation. The other three base course mixes appear to have reasonable K2 values between 3.5 and 6.2.

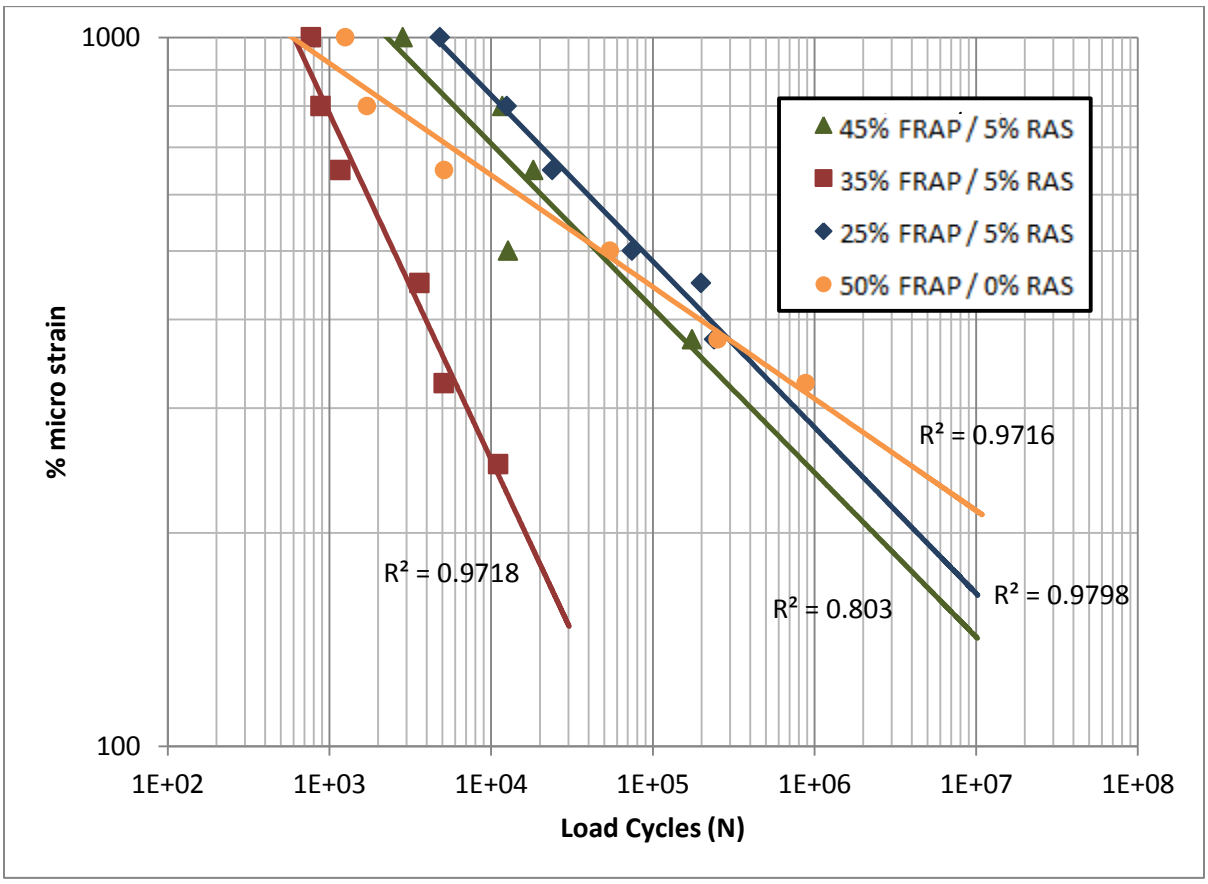

Figure 4-33. Field sampled base course mix fatigue curves

With respect to the binder course mix in Figure 4-34, both the mixes with RAS and no-RAS also have acceptable levels of K2 values. The binder course and base course mixes were designed as "binder rich" mixes with low air voids to resist fatigue cracking. Therefore, adequate fatigue life should be expected, yet the addition of RAS and FRAP materials introduces added variables. Based on the fatigue curves of the binder course mixes, replacing five percent FRAP with RAS when 40 percent recycled materials are used has no significant impact on its laboratory fatigue life.

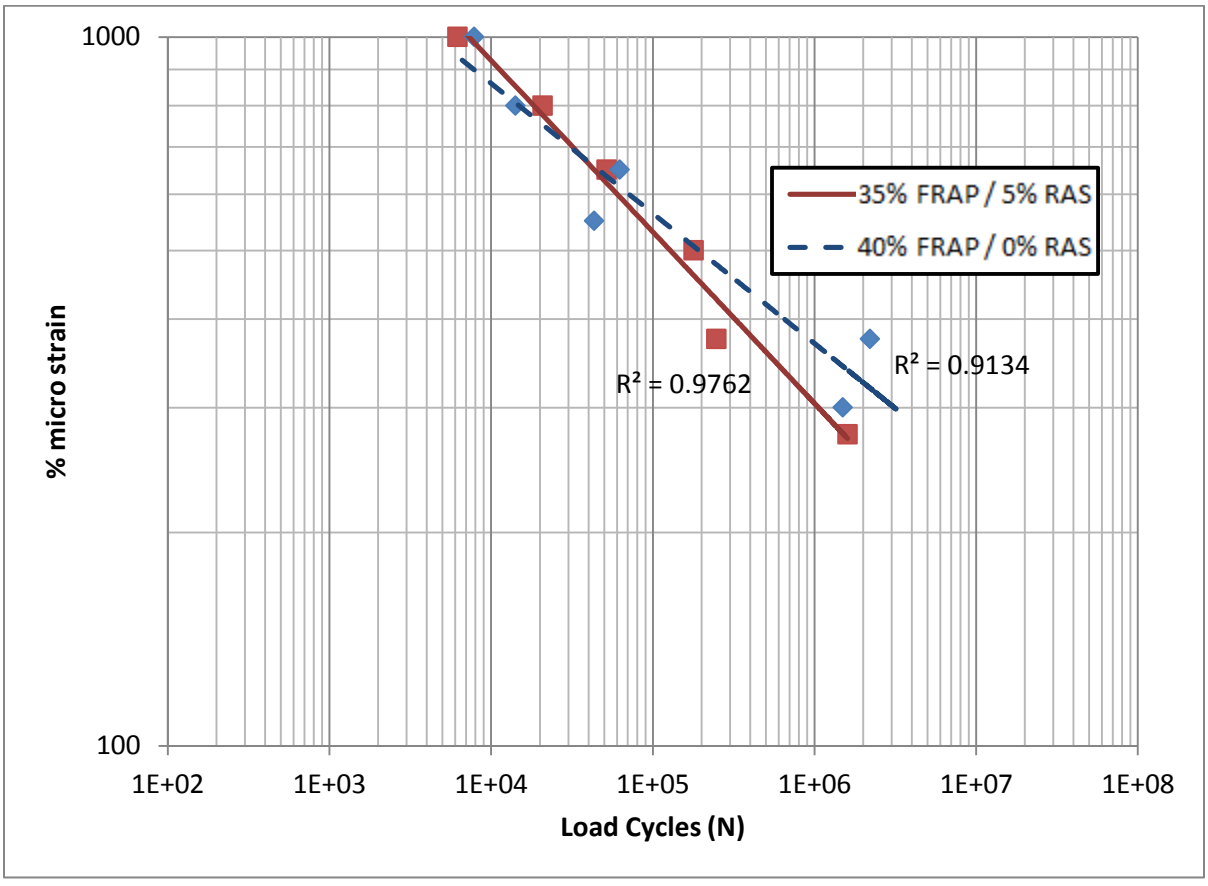

Figure 4-34. Laboratory produced binder course mix fatigue curves

With respect to the surface course mix in Figure 4-35, replacing five percent RAP with RAS does not change the rate of damage accumulation of the mix. However, the mix containing RAS has a lower K1 value which will reduce the fatigue life. Since this mix is intended for the surface of an HMA layer only, it will not incur tensile stresses as high as the binder and base course. Therefore, when this mix design is used in conjunction with the binder and base course mixes as part of a pavement design, there may be little fatigue performance difference between the mix with RAS and the mix without RAS.

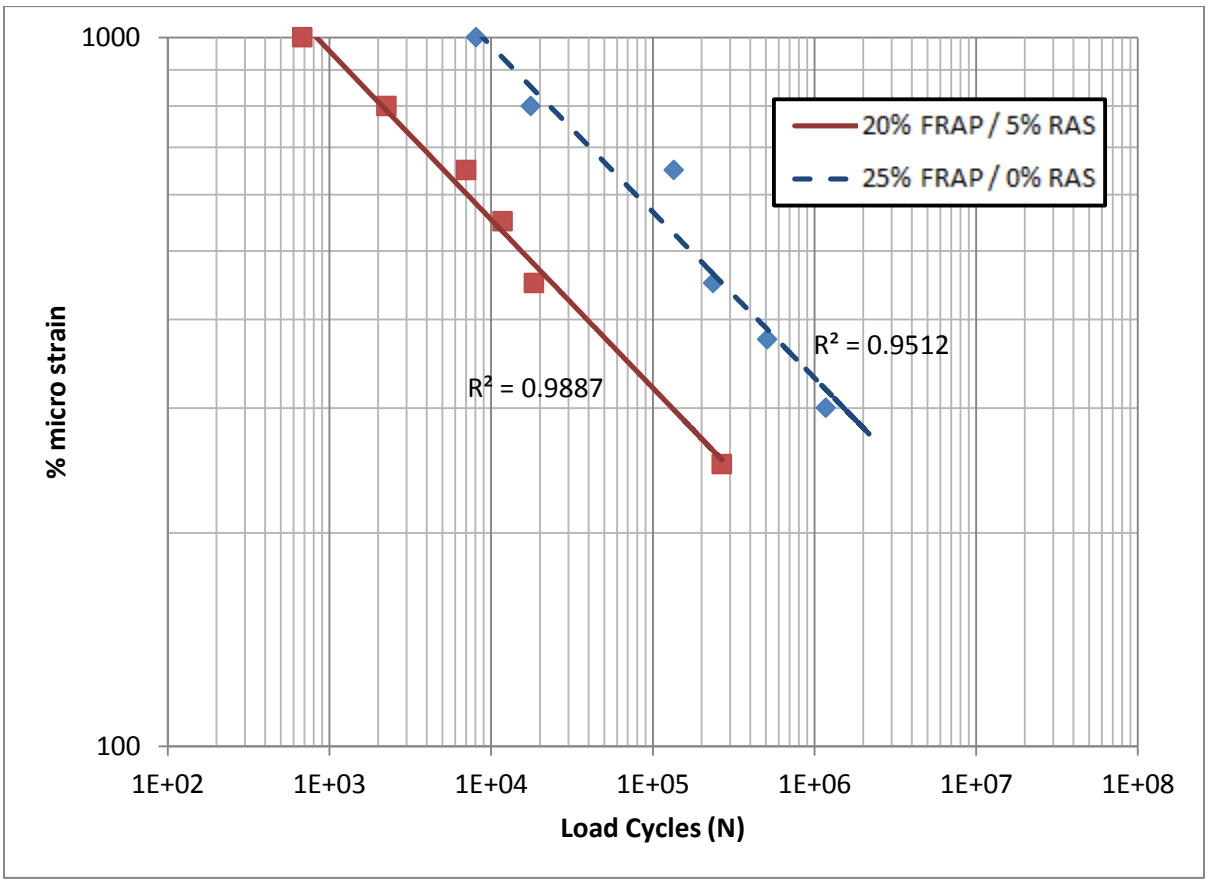

Figure 4-35. Field sampled surface course mix fatigue curves

K2 values for all the mixes are presented in Figure 4-36. The data does not appear to show any clear trends among the different mix types. Because there are many variables among the different beam mixtures, the analysis is somewhat clouded for all 13 mixtures. However, only two mixtures do not have K2 values greater than 3.5, indicating sufficient fatigue performance for most of the Tollway mixes. The one mix that may incur early fatigue cracking is the base course with 45 percent FRAP and 5 percent RAS since both the field and lab samples have relatively low K2 values of 3.5 and 2.9.

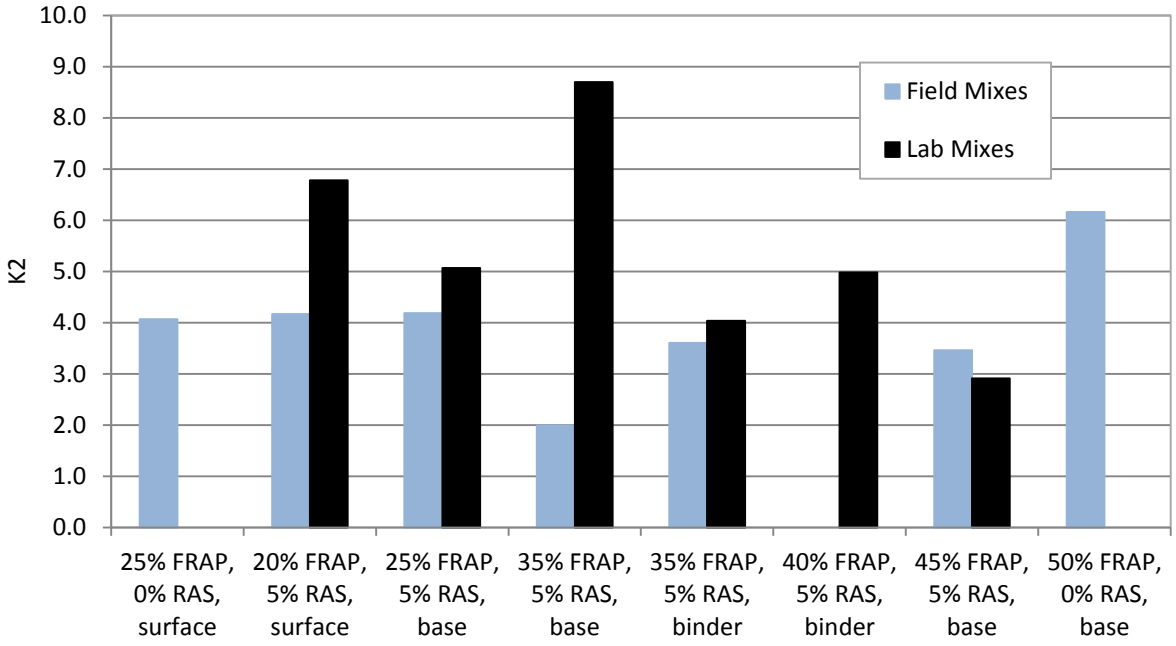

Figure 4-36. K2 values of Tollway mixes

For the Tollway mixes there is a strong correlation between the K1 and K2 values. In Figure 4-37, K1 and K2 are plotted on a semi-log plot and have an R^2 value of 0.99. This relationship is highly applicable for pavement design purposes since K1 coefficients have been modeled using mix properties (Carpenter 2006). If the correlation between K1 and K2 are known, K2 values could be predicted without performing fatigue tests.

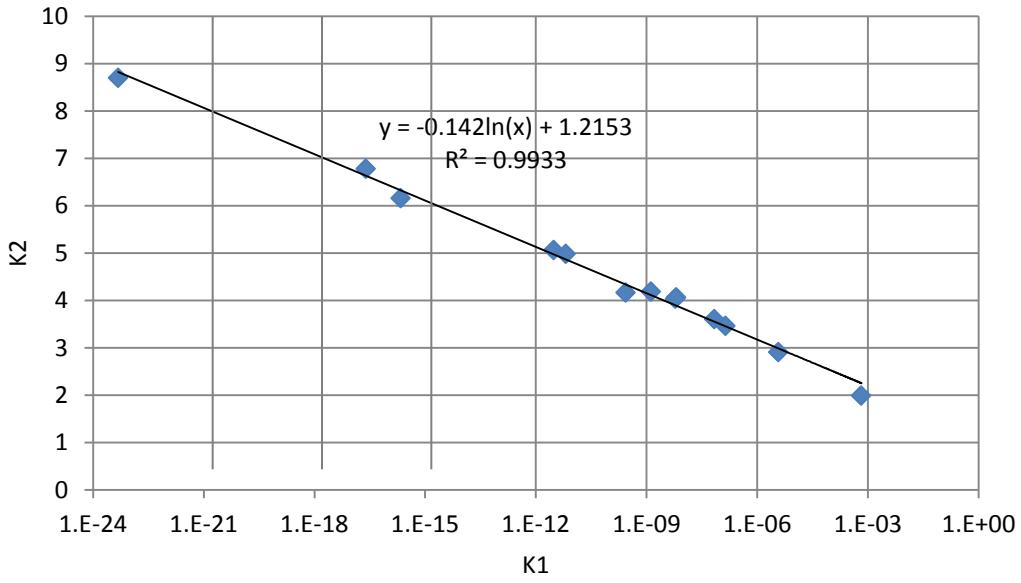

Figure 4-37. Relationship between K1 and K2

4.7 Disk Compact Tension Results

The DC(T) test results from the University of Illinois Urbana-Champaign for each of the 13 mixtures (4 replicates in each case) are presented in Table 4-4 and Figure 4-38. In addition, a plot of average CMOD fracture energy grouped according to the total percentage of recycled material (addition of RAS and FRAP) is displayed in Figure 4-39.

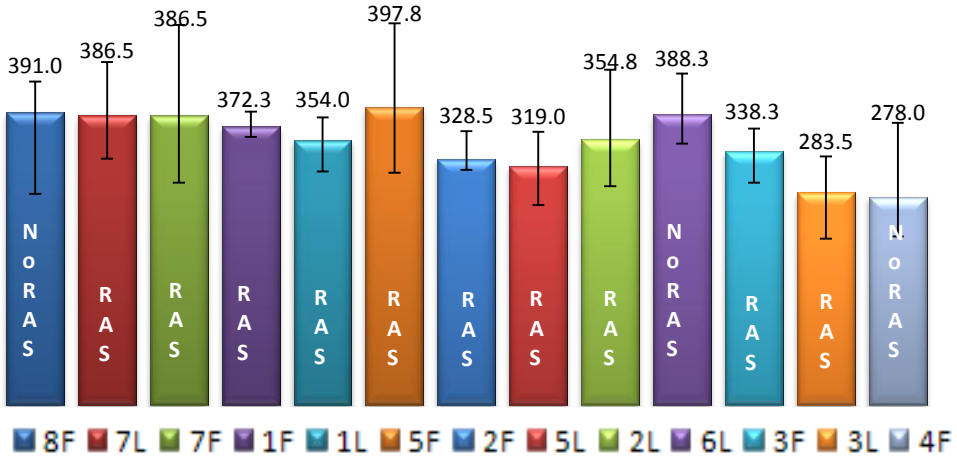

Figure 4-38. Disc compact tension DC(T) test results

Table 4-4. DC(T) mix ID's

Specimen ID	Sample Type	Mix Type	FRAP %	RAS %
4F	Field	Base	50	0
3L	Lab	Base	45	5
5L	Lab	Binder	35	5
2F	Field	Base	35	5
3F	Field	Base	45	5
1L	Lab	Base	25	5
2L	Lab	Base	35	5
1F	Field	Base	25	5
7L	Lab	Surface	20	5
7F	Field	Surface	20	5
6L	Lab	Binder	40	0
8F	Field	Surface	25	0
5F	Field	Binder	35	5

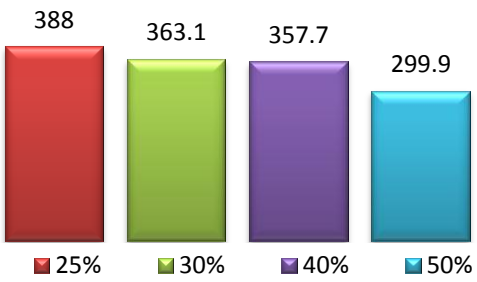

Figure 4-39. Average fracture energy sorted by % recycled materials

In general, a moderate threshold for a sufficiently resistant HMA mixture to thermal and reflective cracking lies between 350-400J/m^2 (Buttlar et al. 2010). Transverse cracking frequency is found to be minimal if the pavement core fracture energy average is greater than 400J/m^2 (Buttlar et al. 2010). Figure 4-39 shows a decreasing trend in fracture energy as the total percentage of recycled materials is increased. None of the Tollway mixtures produced fracture energies greater than 400J/m^2. Consequently, minor cracking will be the most likely result for these mixtures. Mixtures containing 40-50 percent recycled materials did not meet the lower recommended fracture energy limit of 350J/m^2 limit. Therefore, these mixtures may warrant the use of a slightly softer virgin binder grade in order to improve crack resistance.

For three mixes which five percent RAS was replaced with FRAP the average fracture energy value either increased or remained approximately the same. Considering that RAS replaces a larger percentage of the virgin binder than RAP, this is not necessarily an expected trend but can be explained by the presence of fibers in the RAS materials.

CHAPTER 5: SUMMARY AND CONCLUSIONS

This research was conducted to evaluate the laboratory performance of asphalt mixes that utilized RAS and higher percentages of fractionated RAP (FRAP) through their fundamental engineering properties. The mixes tested in this study were obtained from a field demonstration project conducted by the Illinois Tollway in the summer of 2009 for the purposes of developing a draft RAS specification that would allow HMA producers to replace five percent FRAP with RAS. In the study three different experimental mix types were produced and subsequently sampled: a 19.0 mm base course with two percent air voids at a Ndes of 50, a 19.0 mm binder course with three percent air voids at a Ndes of 50, and a 9.5 mm surface course with four percent air voids at a Ndes of 70. Four base course mixes, two binder course mixes, and two surface course mixes were sampled. The base course mixes contained 25, 35, and 45 percent FRAP mixes each with five percent RAS and a 50 percent FRAP mix with no RAS. The binder course mixes contained a 35 percent FRAP mix with five percent RAS and a 40 percent FRAP mix with no RAS. The surface course mixes contained a 20 percent FRAP mix with five percent RAS and a 25 percent FRAP mix with no RAS. Each mix used a PG 58-22 virgin binder. Field produced samples and laboratory mixed samples were obtained for each mix that contained RAS to compare field and laboratory mix performance. For the mixes containing no RAS, only field produced samples were obtained from the base and surface course mixes while only laboratory samples were obtained from the binder course mix.

To evaluate performance, physical and rheological tests were conducted on extracted asphalt binders and the HMA mixtures. The dynamic shear rheometer (DSR) and bending beam rheometer (BBR) tests were performed on the asphalt binders to characterize their

engineering properties. For the HMA mixtures, the dynamic modulus, flow number, tensile strength ratio, beam fatigue, and disk compact tension (DC(T) tests were conducted to evaluate permanent deformation, fatigue cracking, moisture sensitivity, and low temperature fracture energy. In addition, master curves for the asphalt binder and HMA mixtures were constructed to model their viscoelastic properties. A statistical analysis was performed on the dynamic modulus and flow number test results to determine if there were any significant differences in the material properties for mixes that replaced five percent FRAP with RAS and the base course mixes that utilized five percent RAS with 25, 35, and 45 percent FRAP. Based on the results of the laboratory tests, the following conclusions are drawn.

5.1 Comparison of Laboratory Mixed and Field Produced Samples

- Laboratory produced samples that utilized RAS exhibited higher modulus values than field produced samples in the dynamic modulus and binder test results. These findings are in agreement with Johnson et al. (2010). When using RAS in mix designs, the AASHTO mixing and/or curing procedures may need adjustment to ensure the aging of laboratory mixes compares with the amount of aging that occurs during production.

5.2 Rutting Resistance

- DSR tests results conclude that increasing the percentage of FRAP with or without RAS in the Tollway mixes increases their rutting resistance as the performance grades of the field mixes with 50 percent recycled materials increased to a PG 88. Similarly, the binder master curves indicate that as more FRAP binder is added to the total blend, the curves shift upwards at their low frequency end.

- RAS binders appear to have the most influence on the high temperature properties of an HMA mixture when lower percentages of FRAP are utilized. In the binder master curves for field samples, only the master curve with 25 percent recycled materials displayed a significant visual increase in stiffness while the mixes with higher percentages of recycled materials (40% and 50%) did not.
- Based on the statistical analysis of E* values at high temperatures, increasing the amount FRAP from 25 to 35 percent can improve the rutting resistance of the base course mixes, but above 40 percent recycled materials (35% FRAP plus 5% RAS) there is no significant improvement.
- Based on the flow number test results, very little rutting is likely to occur in the Tollway mixes since all samples accumulated strains less than five percent after 10,000 load cycles. The surface course mix with 25 percent FRAP and no RAS produced the greatest strain accumulation of 1.92 % indicating this mix has the least resistance to rutting. When five percent FRAP was replaced with RAS in the surface course and binder course the strain accumulation significantly decreased. As the percentage of FRAP increased from 25 to 35 percent in the base course, the strain accumulation also significantly decreased. From 35 to 45 percent FRAP, there was no significant change in the strain accumulation.

5.3 Fatigue Performance

- The beam fatigue test results indicate no clear trend in the data among the different mix types. However, only 2 of 13 mixtures had K2 coefficients below 3.5 while a majority of the mixes had K2 coefficients above 4.0 indicating sufficient fatigue resistance. The base course mix with 45 percent FRAP and 5 percent RAS had the

lowest K2 coefficients with values of 3.5 and 2.9 in the field and lab produced samples. Based on the beam fatigue test results, with the exception of the base course mix containing 45 percent FRAP and five percent RAS, utilizing FRAP and RAS at the percentages tested in the Tollway mixes is not detrimental to their fatigue performance.

- The lack of trend in the beam fatigue test results tends to agree with the dynamic modulus values measured at very similar intermediate temperatures and frequencies (20°C at 10 Hz) where fatigue cracking is the greatest concern. These E* values of the RAS and no-RAS mixtures for all three mix types had no statistical differences indicating no difference in fatigue cracking performance. Further, there was a statistical increase in stiffness in the base course mix above 40 percent recycled materials which corresponds to the low K2 values in the base course mixes with 45 percent FRAP and 5 percent RAS.

5.4 Low Temperature Cracking

- Using the BBR results, replacing five percent FRAP with RAS did not have any conclusive effects on the low temperature grade. Rather, by characterizing the binders in terms of total percentage of recycled materials, it is evident that increasing the percentage of recycled materials has an increasing effect on temperature grade. Field samples with total recycled material percentages between 25 and 30 percent exhibited either no increase in low temperature grade or a half grade increase at the most; field samples with 40 percent recycled materials exhibited a half grade increase; and field samples with 50 percent recycled materials exhibited the highest

grade change of two full grade increases. The binders with 50 percent recycled materials will be the most susceptible to thermal cracking in colder climates.

- The disk compact tension results demonstrated results similar to the BBR conclusions as the fracture resistance decreased in the Tollway mixes with the addition of recycled materials. The largest drop in fracture energy occurred at the addition of 50 percent recycled materials. All the mixtures produced fracture energies less than 400J/m^2 and consequently may exhibit minor cracking in the field. Mixtures containing 40 to 50 percent recycled materials did not meet the lower recommended energy limit of 350J/m^2 and therefore will have the greatest susceptibility to cracking.
- Dynamic modulus test results indicate there is no statistical effect of FRAP percentage in the low temperature E* values in the base course mixes while a higher percentage of FRAP did effect the low temperature performance of the recovered binders. The difference can be explained from the hypothesis that RAS contributes fibers (organic and fiberglass) to the stone-asphalt structure increasing the asphalt mixture's ductility. Furthermore, the low temperature stiffness of the base course with 50 percent FRAP was significantly reduced with the replacement of five percent RAS.
- Further evidence for the contribution of fibers is supported from the comparison of the RAS and no-RAS mixture performance in the disk compact tension test results. Although a larger percentage of the virgin binder is replaced when five percent RAS was used in lieu of FRAP, the average fracture energy value either increased or remained approximately the same.

5.5 Freeze-Thaw Durability

- The tensile strength ratios (TSRs) of all the field sampled mixes indicated no correlation between percent binder replacement or percentage or recycled materials with TSR values. However, five of seven mixes did exceed the 0.80 criteria. The two mixes that did not meet the minimum criteria of 0.80 were very close with values of 0.795 and 0.798. Based on these results, the Tollway mixes that utilized FRAP and RAS at the percentages tested should exhibit acceptable levels of durability performance in a freeze-thaw environment.

5.6 Recommendations for Future Research

The results of this study reveal several questions about RAS mixtures that should be addressed in future research to expand on the knowledge of their behavior and expected performance. In addition to the low air void RAS mixes tested in this study, more research is recommended on RAS mixes designed with more typical superpave design parameters that are used for pavements with higher traffic volumes. Further research should also be conducted on fibers found in RAS to verify their beneficial effects on HMA durability. Also, an in-depth investigation should be conducted on mix design procedures that utilize RAS and higher percentages of FRAP to understand why laboratory prepared samples are stiffer than field produced samples using current standard procedures. This includes developing a standardized procedure for handling, heating, and mixing RAS materials in the laboratory.

REFERENCES

AASHTO M323 "Standard Specification for Superpave Volumetric Mix Design," Standard Specifications for Transportation Materials and Methods of Sampling and Testing, Washington D.C., 2007

AASHTO T283 "Resistance of Compacted Bituminous Mixture to Moisture Induced Damage," Standard Specifications for Transportation Materials and Methods and Sampling and Testing, Washington D.C., 2007

AASHTO TP62 "Standard Test Method for Determining Dynamic Modulus of Hot-Mix Asphalt Concrete Structures," Standard Specifications for Transportation Materials and Methods of Sampling and Testing, Washington D.C., 2007

AASHTO T321 "Standard Method of Test for Determining the Fatigue Life of Compacted Hot-Mix Asphalt (HMA) Subjected to Repeated Flexural Bending," Standard Specifications for Transportation Materials and Methods of Sampling and Testing, Washington D.C., 2007

Abdulshafi, O., Kedzierski, B., Fitch, M., and Muhktar, H. "Evaluation of the Benefits of Adding Waste Fiberglass Roofing Shingle to Hot-Mix Asphalt," Report Number FHWA/OH-97/006m, Ohio Department of Transportation, July 1997

Al-Qadi, Imad L., M. A. Elseifi, and S. H. Carpenter, "Reclaimed Asphalt Pavement – A literature Review," Research Report FHWA-ICT_07_001, Illinois Center for Transportation, University of Illinois at Urbana-Champaign, Urbana, IL, 2007

Asphalt Institute "Asphalt Handbook" Manual Series No. 4, Asphalt Institute, Lexington, KY, 2007

Asphalt Institute "Superpave Mix Design" Superpave Series No. 2 (SP-02) Asphalt Institute, Lexington, KY, 2001

Asphalt Institute "Superpave Performance Graded Asphalt Binder Specification and Testing," Superpave Series No. 1 (SP-01) Asphalt Institute, Lexington, KY, 2001

ASTM D6648 "Standard Test Method for Determining the Flexural Creep Stiffness of Asphalt Binder Using the Bending Beam Rheometer," Annual Book of ASTM Standards. West Conshohocken, PA: ASTM International, 2001

ASTM D7175 "Standard Test Method for Determining the Rheological Properties of Asphalt Binder Using a Dynamic Shear Rheometer," Annual Book of ASTM Standards. West Conshohocken, PA: ASTM International, 2005

ASTM D7313 "Standard Test Method for Determining Fracture Energy of Asphalt-Aggregate Mixtures Using the Disk-Shaped Compact Tension Geometry," Annual Book of ASTM Standards. West Conshohocken, PA: ASTM International, 2003

Bentsen, R.A. "Illinois Tollway Authority Jump Starts Asphalt Shingle Recycling in the State," *C and D World*, May 21, 2010

Bonaquist, R. F., Christensen, D. W., and Stump, W. "Simple Performance Tester for Superpave Mix Design: First-Article Development and Evaluation," *National Cooperative Highway Research Program (NCHRP)*, Report 513, Washington D.C., 2003

Brock, Ben "Economics of RAS in HMA," Presentation at the 3rd Asphalt Shingle Recycling Forum, Chicago, Illinois, November 1-2, 2007

Buttlar, W.G., Ahmed, S., Dave, E. V. and Braham, A. F. "Comprehensive Database of Asphalt Concrete Fracture Energy and Links to Field Performance," Paper presented at the 89th Annual Meeting of the Transportation Research Board, Washington, D.C., January 2010

Button, J.; Williams, D.; and Scherocman, J. "Roofing Shingles and Toner in Asphalt Pavements," Texas Transportation Institute, Research Report 1344-2F, July 1996

Carpenter, S.H. "Fatigue Performance of IDOT Mixtures," Research Report FHWA-ICT-07-007, Illinois Center for Transportation, July 2006

Federal Highway Administration and Environmental Protection Agency, "Report to Congress, A Study of the Use of Recycled Paving Material," FHWA-RD-93-147, EPA/600/R-93/095, June 1993

Grzybowski, K., Lewandowski, L. "Multi-Disciplinary Characterization of Recycled Roofing Materials for Asphalt Pavement Applications," *Presentation by PRI Asphalt Technologies Inc. presented at the Pavement Performance Prediction Symposium*, Laramie, Wyoming, July 2010

Huang, Yang H. "Pavement Analysis and Design," Second Edition, Prentice Hall, New Jersey, 2004

Iowa Department of Transportation, "Developmental Specifications for Recycled Asphalt Shingles," DS-09038, February 2010

Johnson, E., Johnson, G., Dai, S., Linell, D., McGraw, J., Watson, M. "Incorporation of Recycled Asphalt Shingles in Hot Mixed Asphalt Pavement Mixtures," Minnesota Department of Transportation, St. Paul, MN, 2010

JMP, Version 8.02. SAS Institute Inc., Cary, NC, 1989-2009

Kim, Y. R. "Modeling of Asphalt Concrete," McGraw-Hill Professional, ASCE Press, Reston, VA, 2008

Longernecker, M., Ott, R. L. "An Introduction to Statistical Methods and Data Analysis," Fifth Edition, Duxbury, Pacific Grove, CA, 2001

Marasteanu, M., Anderson, D. "Time-Temperature Dependency of Asphalt Binders-An Improved Model," *Journal of the Association of Asphalt Paving Technologists,* Vol. 65, 408-448, 1996

McGraw, J., Zofka, A., Krivit, D., Schroer, J., Olson, R., and Marasteanu, M. "Recycled asphalt shingles in hot mix asphalt," *Journal of the Association of Asphalt Paving Technologists*, Vol. 76, 235-274, 2007

NCHRP. "Recommended Use of Reclaimed Asphalt Pavement in the Superpave Mix Design Methods: Guidelines," *National Cooperataive Highway Research Program Results Digest*, No. 253, Transportation Research Board of the National Academies, Washington, D.C., March, 2001

NCHRP 1-37A. "Guide for Mechanistic-Empirical Design of New and Rehabilitated Pavement Structures," Final Report, 2004

NCHRP Report 547 "Simple Performance Tests: Summary of Recommended Methods and Database," Transportation Research Board, National Highway Research Council, Washington D.C., 2005

Newcomb, D., Stroup-Gardiner, M., Weikle, B., Drescher, A. "Influence of Roofing Shingles on Asphalt Concrete Mixture Properties," Report MN/RC-93/09, University of Minnesota, Minnesota, 1993

Roberts, F. L., Kandhal, P. S., Brown, E. R., Lee, D., and Kennedy, T. W. "Hot Mix Asphalt Materials, Mixture Design, and Construction," 2nd Ed. National Asphalt Pavement Association Research and Education Foundation, Lanham, Maryland, 1996

Robinette, C. and Williams, R.C. "The effects of the testing history and preparation method on the superpave simple performance test," *Journal of the Association of Asphalt Paving Technologist*, Vol. 75, 297-317, 2006

Scholz, Todd "Preliminary Investigation of RAP and RAS in HMAC," Report Number OR-RD-10-12, Kiewitt Center for Infrastructure and Transportation, Oregon State University and the Oregon Department of Transportation Research Section, February 2010

Strategic Highway Research Program, "Binder Characterization and Evaluation, Volume 1: Physical Characterization," SHRP-A-367, National Research Council, Washington D.C. 1994

Wagoner, M.P., Buttlar, W.G., Paulino, G.H., and Blankenship, P. "Investigation of the Fracture Resistance of Hot-Mix Asphalt Concrete Using a Disk-Shaped Compact Tension Test," Journal of the Transportation Research Board, No. 1929, National ResearchCouncil, National Academy Press, Washington, D.C., pp. 183-192, 2005

Wagoner, M.P., Buttlar, W.G., Paulino, G.H., and Blankenship, P. "Investigation of the Fracture Resistance of Hot-Mix Asphalt Concrete Using a Disk-Shaped Compact Tension Test," Journal of the Transportation Research Board, No. 1929, National ResearchCouncil, National Academy Press, Washington, D.C., pp. 183-192, 2005

Witczak, M.W., K. Kaloush, T. Pellinen, M. El-Basyouny, "Simple Performance Test for Superpave Mix Design," *National Cooperative Highway Research Program (NCHRP),* Report 465, Washington D.C., 2002

Vavrik, R.W., Carpenter, S.H., Gillen, S., Behnke, J., Garrott, F., "Evaluation of Field-Produced Hot Mix Asphalt (HMA) Mixtures with Fractionated Recycled Asphalt Pavement (RAP)," Research Report ICT-08-030, Illinois Center for Transportation, October 2008

APPENDIX A: DYNAMIC MODULUS TEST RESULTS

Table A-1. Dynamic modulus test results, mix 5L

Temp	Freq	Dynamic Modulus (KPa) Binder Course, Lab Samples, 35% FRAP / 5% RAS						
(C)	(Hz)	Sample 1	Sample 2	Sample 3	Sample 4	Sample 5	Average	CV
4.0	25	24183998	23620963	23784852	24820457	25102486	24302551	2.65
4.0	15	22698025	23221336	23545402	23898941	23292657	23331272	1.90
4.0	10	21733953	21955150	22321844	21988235	22267861	22053408	1.10
4.0	5	20694705	20495560	20815535	21264323	20962307	20846486	1.39
4.0	3	19710475	20154571	20419348	20321383	19754634	20072082	1.62
4.0	1	17489591	17942081	18240929	18157674	17850356	17936126	1.65
4.0	0.5	16233016	16567871	17056735	16950712	16522491	16666165	2.02
4.0	0.3	15265183	15655363	15972889	15916450	15656226	15693222	1.79
4.0	0.1	13375420	13670223	13933906	13752145	13787851	13703909	1.51
21.0	25	13601266	15074553	14419423	13232964	13317249	13929091	5.70
21.0	15	12180592	13180734	12691851	11816573	11927822	12359514	4.61
21.0	10	11325689	12281241	11813326	10991572	11159381	11514242	4.58
21.0	5	10048046	10907502	10583046	9755415	10131139	10285030	4.45
21.0	3	8769637	9783847	9365502	8466770	8234452	8924042	7.18
21.0	1	7051095	7998941	7722500	7040120	6677332	7297998	7.46
21.0	0.5	6168229	7136445	6856308	6195710	6523549	6576048	6.39
21.0	0.3	5614784	6497477	6306345	5671758	6014103	6020893	6.41
21.0	0.1	4349931	5117805	5047042	4698755	4941444	4830995	6.46
37.0	25	5153369	5887228	6366952	5802492	5638843	5769777	7.60
37.0	15	4471951	5245978	5617901	5139878	5056830	5106508	8.12
37.0	10	3978721	4734834	5118170	4612961	4605033	4609944	8.89
37.0	5	3313248	3961978	4332417	3876579	3873884	3871621	9.42
37.0	3	2610016	3104701	3411252	3043936	3042619	3042505	9.40
37.0	1	1904416	2311254	2648979	2232770	2320713	2283626	11.63
37.0	0.5	1536752	1881569	2226535	1818760	1883283	1869380	13.13
37.0	0.3	1315047	1609762	1945260	1539754	1620209	1606006	14.07
37.0	0.1	961004	1172614	1472499	1116003	1201576	1184739	15.68

Table A-2. Dynamic modulus test results, mix 5P

Temp	Freq	Dynamic Modulus (KPa) Binder Course, Field Samples, 35% FRAP / 5% RAS						
(C)	(Hz)	Sample 1	Sample 2	Sample 3	Sample 4	Sample 5	Average	CV
4.0	25	22624894	24949755	23306143	24678466	21582206	23428293	6.02
4.0	15	21127400	23569244	22318308	23272154	20881250	22233671	5.47
4.0	10	20019172	21648738	21189529	22483252	19896964	21047531	5.22
4.0	5	18752081	20189710	19834803	21324657	18699288	19760108	5.53
4.0	3	18125881	19600997	19141267	20492566	17621894	18996521	6.04
4.0	1	15828854	17238075	16779137	18164104	15809427	16763920	5.94
4.0	0.5	14759601	16066380	15671958	16744373	14697677	15587998	5.60
4.0	0.3	13762986	14977970	14890520	16119506	13783481	14706893	6.67
4.0	0.1	11663404	12407504	12599687	13797025	11794660	12452456	6.82
21.0	25	12936768	11430412	13594784	14300421	12187983	12890074	8.77
21.0	15	11581746	10153596	11852212	12695054	11329275	11522377	8.00
21.0	10	10707636	9347983	10892824	11772297	10511941	10646536	8.18
21.0	5	9395460	8214646	9702415	10474210	9368516	9431049	8.62
21.0	3	8252037	7230305	8489556	9415185	8172370	8311891	9.40
21.0	1	6609728	5348729	6826895	7675339	6567455	6605629	12.61
21.0	0.5	5808358	4887924	5917272	6771620	5804568	5837949	11.43
21.0	0.3	5246087	4397127	5467937	6305298	5230297	5329349	12.79
21.0	0.1	3992052	3207082	4234267	4895926	4179826	4101831	14.76
37.0	25	5041376	4886262	5577331	5637128	5152148	5258849	6.32
37.0	15	4402027	4125589	4861028	4959481	4547732	4579172	7.42
37.0	10	3911877	3723034	4322382	4478196	4110049	4109108	7.40
37.0	5	3236637	3036452	3608098	3755963	3375299	3402490	8.43
37.0	3	2537263	2379753	2840941	3017018	2672804	2689556	9.29
37.0	1	1890174	1734187	2078528	2296283	2011001	2002035	10.50
37.0	0.5	1500928	1396850	1669304		1618067	1546287	7.89
37.0	0.3	1246679	1168695	1415370		1405470	1309053	9.27
37.0	0.1	903593	865234	1033310		1051339	963369	9.63

Table A-3. Dynamic modulus test results, mix 2L

Temp	Freq	Dynamic Modulus (KPa) Base Course, Lab Samples, 35% FRAP / 5% RAS						
(C)	(Hz)	Sample 1	Sample 2	Sample 3	Sample 4	Sample 5	Average	CV
4.0	25	21096386	24616707	28781381	27443974	28150542	26017798	12.22
4.0	15	21309047	25064419	28419026	26874207	19633676	24260075	15.27
4.0	10	19874691	23586809	26786081	23237532	27237433	24144509	12.41
4.0	5	19650148	22547341	25508969	24310558	25728078	23549019	10.70
4.0	3	18766193	21651874	24765740	23422176	25952082	22911613	12.29
4.0	1	17100977	20057032	22368819	21630832	23746320	20980796	12.13
4.0	0.5	14842113	18543395	21113850	20373577	22050768	19384741	14.69
4.0	0.3	18617292	17928309	20190537	19388033	21132814	19451397	6.50
4.0	0.1	18119518	16853298	18109842	17318099	19251294	17930410	5.10
21.0	25	13036125	14984662	16805167	15556191	17245543	15525538	10.72
21.0	15	12128987	13498953	15139843	14101283	15457300	14065273	9.51
21.0	10	11439004	12666969	13825538	13302700	14679084	13182659	9.27
21.0	5	10306952	11516732	12954413	12137226	13477500	12078565	10.29
21.0	3	9247010	10667801	11897591	11077877	12498771	11077810	11.25
21.0	1	7661457	8991448	10137093	9376375	10642003	9361675	12.26
21.0	0.5	6739721	8112693	9083203	8391778	9610134	8387506	13.02
21.0	0.3	6236566	7514948	8432490	7744851	8950618	7775895	13.26
21.0	0.1	5004619	6272171	7108701	6472720	7482101	6468062	14.71
37.0	25	9251209	7405257	8419864	7116915	8681458	8174941	10.92
37.0	15	8534316	6661415	7427113	6501740	7777665	7380450	11.30
37.0	10	7879908	6156916	6903425	6092484	7172542	6841055	10.89
37.0	5	6796481	5274039	5962509	5261947	6244719	5907939	11.12
37.0	3	5068411	4339801	4788212	4278498	5075271	4710039	8.16
37.0	1	3996132	3452823	3827686	3339643	4107969	3744851	8.97
37.0	0.5	3283938	2974468	3305647	2855380	3459860	3175859	7.91
37.0	0.3	2845564	2678040	2965825	2559549	3141013	2837998	8.10
37.0	0.1	2167214	2082682	2299572	1872776	2351418	2154733	8.82

Table A-4. Dynamic modulus test results, mix 2P

Temp	Freq	Dynamic Modulus (KPa) Base Course, Field Samples, 35% FRAP / 5% RAS						
(C)	(Hz)	Sample 1	Sample 2	Sample 3	Sample 4	Sample 5	Average	CV
4.0	25	25130152	22910237	27450128	24331286	27484205	25461201	7.84
4.0	15	25097594	22860623	26206494	24630399	25994921	24958006	5.36
4.0	10	23271101	21511197	24655975	22459409	24739260	23327388	5.99
4.0	5	22197898	20016829	23573581	22351041	23413551	22310580	6.37
4.0	3	21279511	19573906	22612685	21404193	22433204	21460700	5.64
4.0	1	18877296	17300438	20413290	19502838	20074394	19233651	6.39
4.0	0.5	17797915	15733437	19176279	18440151	18561749	17941906	7.40
4.0	0.3	16702638	14951854	17817338	17410075	17743543	16925090	7.02
4.0	0.1	14518974	12538546	15511607	15383728	15474238	14685418	8.63
21.0	25	13375726	11649733	14823535	14702620	14385556	13787434	9.60
21.0	15	12158428	10390424	13035752	13334104	12561216	12295985	9.40
21.0	10	11386781	9640709	12387589	12154726	11802890	11474539	9.52
21.0	5	10153932	8525710	11048864	11269611	10616869	10322997	10.58
21.0	3	9082248	7591994	10053808	10187890	9515781	9286344	11.25
21.0	1	7422737	5958785	8138101	8310559	7735520	7513141	12.45
21.0	0.5	6512494	5169452	7193263	7376339	6823543	6615018	13.22
21.0	0.3	5931198	4628759	6719990	6759442	6216748	6051228	14.34
21.0	0.1	4565326	3462297	5643994	5293446	4830231	4759059	17.56
37.0	25	6645664	5239498	7006837	6592994	6292709	6355540	10.60
37.0	15	5913599	4573144	6158484	5873088	5611102	5625884	11.01
37.0	10	5191254	4042258	5530818	5355517	5092836	5042537	11.57
37.0	5	4314743	3367826	4667203	4541027	4301987	4238557	12.05
37.0	3	3383133	2576894	3754418	3611518	3365101	3338213	13.65
37.0	1	2487152	1856952	2754861	2671466	2460805	2446247	14.38
37.0	0.5	2016224	1479459	2265006	2252992	2036845	2010105	15.86
37.0	0.3	1614698	1229191	1913413	1956291	1678727	1678464	17.33
37.0	0.1	1084694	809161	1332708	1396906	1090092	1142712	20.43

Table A-5. Dynamic modulus test results, mix 3L

Temp	Freq	Dynamic Modulus (KPa) Base Course, Lab Samples, 45% FRAP / 5% RAS						
(C)	(Hz)	Sample 1	Sample 2	Sample 3	Sample 4	Sample 5	Average	CV
4.0	25	24811140	26081762	24644244	25453355	21990949	24596290	6.36
4.0	15	24095576	24195117	24169785	24434482	21840089	23747010	4.52
4.0	10	23096994	23885623	23197339	21959214	21248102	22677454	4.66
4.0	5	21951614	23213783	22322289	22539268	10163164	20038024	27.64
4.0	3	20964921	22544225	20455010	20907983	19640847	20902597	5.07
4.0	1	18270095	20594881	19118081	10487080	18260795	17346187	22.78
4.0	0.5	15858464	19314429	18011562	16887795	17546244	17523699	7.34
4.0	0.3	16507084	17615604	17483098	9986228	16838172	15686037	20.52
4.0	0.1	14909098	16738350	16430769	16833082	15411260	16064512	5.34
21.0	25	13731033	15125364	16915051	15962844	14510211	15248900	8.13
21.0	15	12723197	13489508	15541685	14229518	13143269	13825435	8.01
21.0	10	11982963	12614860	14836918	13685734	12439659	13112027	8.76
21.0	5	10651959	11347375	13720902	12787453	11582868	12018111	10.19
21.0	3	9388361	10217506	12761229	11974821	10764469	11021277	12.27
21.0	1	7750986	8455344	11098164	10293081	9206864	9360888	14.45
21.0	0.5	6833094	7470106	10108841	9458462	8426828	8459466	16.02
21.0	0.3	6344225	6829139	9453845	8858259	7841605	7865414	16.70
21.0	0.1	5003460	5456217	7954846	7295012	6552163	6452340	19.09
37.0	25	6364667	6429075	8234243	7311963	6938851	7055760	10.84
37.0	15	5648462	5883190	7568329	6588558	6329576	6403623	11.68
37.0	10	5102409	5338221	7041243	6119213	5835728	5887363	12.90
37.0	5	4298306	4543154	6137634	5322612	5131019	5086545	14.17
37.0	3	3265007	3462800	5140864	4558804	4280965	4141688	18.78
37.0	1	2430521	2649110	4174869	3593147	3382364	3246002	21.91
37.0	0.5	2029565	2205711	3610932	3134868	2946656	2785546	23.66
37.0	0.3	1735848	1938476	3289621	2820618	2645714	2486056	25.80
37.0	0.1	1271168	1412439	2569708	2182532	2029652	1893100	28.67

Table A-6. Dynamic modulus test results, mix 3P

Temp	Freq	Dynamic Modulus (KPa) Base Course, Field Samples, 45% FRAP / 5% RAS						
(C)	(Hz)	Sample 1	Sample 2	Sample 3	Sample 4	Sample 5	Average	CV
4.0	25	24226009	22762650	23485138	26694803	24906905	24415101	6.17
4.0	15	23350340	22051628	19419875	25932617	24234124	22997717	10.64
4.0	10	21232438	18839997	21587507	25238744	22826501	21945038	10.66
4.0	5	19499306	19826490	20888626	24013151	21890715	21223657	8.58
4.0	3	19721917	19334828	19278299	22436782	20573545	20269074	6.50
4.0	1	16949820	17366905	18013845	20568855	19125248	18404935	7.94
4.0	0.5	15494194	15883178	16500622	19101697	17576938	16911326	8.61
4.0	0.3	14602747	14855249	16129048	18551001	16691173	16165844	9.84
4.0	0.1	13199338	13281804	14572785	17234808	15603629	14778473	11.47
21.0	25	13563934	11980009	13702776	15278705	15846189	14074323	10.88
21.0	15	11863670	10955275	12419424	13628955	14040934	12581652	10.06
21.0	10	11113371	10104775	11468171	12738248	13100975	11705108	10.45
21.0	5	9893614	9081890	10463448	11475913	11909175	10564808	10.89
21.0	3	8603911	8051762	9437093	10772628	10887964	9550671	13.28
21.0	1	6986207	6563946	7802919	8996621	9121334	7894205	14.61
21.0	0.5	6159878	5887145	7009549	8092405	8184315	7066658	15.04
21.0	0.3	5592473	5361585	6458615	7447074	7538101	6479569	15.61
21.0	0.1	4334375	4348963	5173004	6120905	6084767	5212403	16.90
37.0	25	5239767	5078180	6269622	7197230	7191601	6195280	16.47
37.0	15	4643625	4497837	5590113	6536473	6426377	5538885	17.30
37.0	10	4187174	3995973	5139008	5960394	5866623	5029835	18.21
37.0	5	3519547	3334841	4355327	5138171	5020531	4273683	19.44
37.0	3	2703267	2671465	3423390	4238327	4040178	3415325	21.36
37.0	1	2005589	1959019	2554055	3292873	3090853	2580478	23.62
37.0	0.5	1663661	1644278	2158216	2807677	2625427	2179852	24.56
37.0	0.3	1436801	1433682	1880774	2513467	2355667	1924078	26.16
37.0	0.1	1025737	1042033	1317927	1909787	1754497	1409996	28.81

Table A-7. Dynamic modulus test results, mix 1L

Temp	Freq	Dynamic Modulus (KPa) Base Course, Lab Samples, 25% FRAP / 5% RAS						
(C)	(Hz)	Sample 1	Sample 2	Sample 3	Sample 4	Sample 5	Average	CV
4.0	25	22354484	25733720	22488820	21206297	23647309	23086126	7.42
4.0	15	13254170	10996491	21281043	20529541	17804249	16773099	26.87
4.0	10	17865226	12282643	16178113	16843048	11711328	14976071	18.65
4.0	5	18590746	22447951	18452844	18276476	19743718	19502347	8.94
4.0	3	10078041	20921694	17558332	17462309	18875299	16979135	24.16
4.0	1	15961511	18527394	16076179	15702613	17249953	16703530	7.07
4.0	0.5	14965920	17509920	15057659	13704376	16265703	15500716	9.31
4.0	0.3	14195584	16679339	13190719	13533707	15540776	14628025	9.96
4.0	0.1		9214939	12544261	12368934	14053751	12045471	16.88
21.0	25	7948269	13904601	11968456	12706397	12644338	11834412	19.28
21.0	15	10096107	12491388	10958904	11093827	11527302	11233506	7.78
21.0	10	9770534	11669416	10075003	10266521	10703736	10497042	7.03
21.0	5	8651606	10320068	8792433	9268896	9606106	9327822	7.21
21.0	3	7632836	9214203	7750300	8135277	8603376	8267198	7.88
21.0	1	6230627	7682625	6376325	6644077	7054046	6797540	8.61
21.0	0.5	5452537	6881464	5641244	5872631	6336885	6036952	9.55
21.0	0.3	4961564	6307250	5137464	5357019	5794793	5511618	9.85
21.0	0.1	3893987	5097991	4110152	4238148	4595582	4387172	10.76
37.0	25	4438171	6030732	4791918	5212288	5346826	5163987	11.67
37.0	15	3970252	5458736	4269399	4626563	4797372	4624464	12.23
37.0	10	3614105	5011926	3852247	4238110	4386545	4220587	12.75
37.0	5	3026756	4301568	3274358	3604728	3727505	3586983	13.53
37.0	3	2305245	3480901	2537826	2847858	2914515	2817269	15.79
37.0	1	1747890	2675024	1926178	2181690	2160187	2138194	16.33
37.0	0.5	1477377	2283399	1647487	1842184	1818746	1813839	16.59
37.0	0.3	1285473	1996772	1453748	1647750	1590501	1594849	16.59
37.0	0.1	962834	1474179	1103294	1244773	1156147	1188245	15.97

Table A-8. Dynamic modulus test results, mix 1P

Temp	Freq	Dynamic Modulus (KPa) Base Course, Field Samples, 25% FRAP / 5% RAS						
(C)	(Hz)	Sample 1	Sample 2	Sample 3	Sample 4	Sample 5	Average	CV
4.0	25	26397187	24346621	23991285	25640384	28853033	25845702	7.51
4.0	15	23688887	21818745	18331576	13201771	24913738	20390943	23.17
4.0	10	22889113	10923165	21632375	21487644	22961393	19978738	25.57
4.0	5	21731263	20189073	20387218	19602878	23079049	20997896	6.67
4.0	3	20922250	20460111	18931681	18903334	21865276	20216530	6.38
4.0	1	18241725	10706869	16674699	17055330	19886510	16513026	21.07
4.0	0.5	16952684	16357559	15285320	15649929	18867754	16622649	8.48
4.0	0.3	15790568	15135897	14417802	13847446	17647269	15367796	9.56
4.0	0.1	13548496	12469445	12154815	11240774	14167410	12716188	9.10
21.0	25	11721830	11229582	8900622	11743730	12201126	11159378	11.73
21.0	15	11603133	10375348	9638206	11254973	11970343	10968401	8.66
21.0	10	10704838	9523902	9264544	10516867	11046607	10211352	7.59
21.0	5	9308011	8287720	8087049	9514766	9739345	8987378	8.34
21.0	3	7905497	7107855	6801514	8224291	8505742	7708980	9.45
21.0	1	6194626	5597403	5302986	6619223	6758013	6094450	10.38
21.0	0.5	5316540	4838666	4791047	5773350	5936364	5331193	9.82
21.0	0.3	4759447	4344588	4396178	5173078	5356548	4805968	9.43
21.0	0.1	3462182	3204829	3203751	3890285	4009138	3554037	10.65
37.0	25	4839979	4348654	3984266	5145410	5820392	4827740	14.75
37.0	15	4074847	3685148	3437093	4502223	4949622	4129786	14.79
37.0	10	3565674	3292735	3060459	3988524	4387804	3659039	14.60
37.0	5		2689182	2529010	3304468	3690489	3053287	17.70
37.0	3		2033947	1848581	2556939	2925602	2341267	21.00
37.0	1		1505865	1308322	1878429	2153613	1711557	22.07
37.0	0.5		1236491	1047215	1585235	1779505	1412112	23.45
37.0	0.3		1067529	885833	1325994	1523838	1200799	23.41
37.0	0.1		809253	627565	1028857	1108131	893451	24.37

Table A-9. Dynamic modulus test results, mix 7L

Temp	Freq	Dynamic Modulus (KPa) Surface Course, Lab Samples, 20% FRAP / 5% RAS						
(C)	(Hz)	Sample 1	Sample 2	Sample 3	Sample 4	Sample 5	Average	CV
4.0	25	14900369	13954071	20852212	23941139	22006198	19130798	23.24
4.0	15	13803250	12554903	21136436	22979439	20522095	18199225	25.78
4.0	10	13692053	16272760	20107684	21736907	19213931	18204667	17.63
4.0	5	13188938	17124661	18983328	20372273	18147489	17563338	15.48
4.0	3	11549307	15944481	18370562	19536269	17655016	16611127	18.75
4.0	1	10436972	14662406	16201534	17218744	15514773	14806886	17.67
4.0	0.5	9555848	13154291	15199100	16133574	14606700	13729903	18.73
4.0	0.3	9049311	12413970	14473408	15176839	13544072	12931520	18.60
4.0	0.1	8129446	10989979	12400506	13256156	11717619	11298741	17.34
21.0	25	7736207	9907312	11061528	11578665	11234670	10303676	15.20
21.0	15	7367794	8986232	10109302	10269775	10274151	9401451	13.38
21.0	10	6948396	8480600	9481561	9643775	9595549	8829976	13.08
21.0	5	6163788	7480608	8457373	8486128	8583492	7834278	13.22
21.0	3	5329990	6720596	7621176	7565111	7649965	6977367	14.32
21.0	1	4328024	4933247	6224113	6212915	6228001	5585260	16.07
21.0	0.5	3846330	5016547	5548411	5683293	5518739	5122664	14.78
21.0	0.3	3532587	3833231	5055179	5588196	5032563	4608351	19.10
21.0	0.1	2831103	3222355	4050731	4205144	4012380	3664343	16.45
37.0	25	3908550	4673117	4919338	2513614	2283852	3659694	33.14
37.0	15	3565455	4114238	4321671	2137464	1989042	3225574	34.03
37.0	10	3283103	3740899	3908923	1904282	1803471	2928136	34.41
37.0	5	2805903	3166413	3364446	1541548	1467192	2469101	36.59
37.0	3	2123560	2419535	2752039	1234867	1008493	1907699	39.60
37.0	1	1658597	1864053	2159222	931278	754899	1473610	41.10
37.0	0.5	1346893	1537681	1853196	736630	583094	1211499	44.39
37.0	0.3	1176740	1341630	1663897	641232	496342	1063968	45.82
37.0	0.1	889404	1046995	1283123	415253	374295	801814	49.56

Table A-10. Dynamic modulus test results, mix 7F

Temp (C)	Freq (Hz)	Dynamic Modulus (KPa) Surface Course, Field Samples, 20% FRAP / 5% RAS Sample 1	Sample 2	Sample 3	Sample 4	Sample 5	Average	CV
4.0	25	23010188	22469469	21473676	23829150	22728155	22702128	3.77
4.0	15	21516497	20499346	21984965	20539554	20392236	20986519	3.43
4.0	10	19956690	19591274	19490376	21735365	20840117	20322764	4.68
4.0	5	18754486	18189195	18623371	20071629	19355351	18998806	3.84
4.0	3	18123521	17440718	17566479	19684604	18776612	18318387	5.07
4.0	1	15762669	14973609	15182699	17252304	16324015	15899059	5.80
4.0	0.5	14675404	13850687	14042686	15928230	15536810	14806763	6.14
4.0	0.3	13667167	12837210	13291767	14935545	14518211	13849980	6.25
4.0	0.1	11576308	10721094	11126665	12681596	11986930	11618519	6.55
21.0	25	11423614	10677840	11222195	11126754	11720396	11234160	3.43
21.0	15	10464705	9637349	10161585	10729928	10650380	10328789	4.30
21.0	10	9710239	8958079	9487965	10078031	9868949	9620653	4.46
21.0	5	8556863	7764432	8251821	8870928	8708650	8430539	5.18
21.0	3	7439749	6625174	7180053	7823210	7729074	7359452	6.55
21.0	1	5940167	5205014	5704345	6293976	6181046	5864910	7.39
21.0	0.5	5188852	4524711	4971536	5569117	5437650	5138373	8.04
21.0	0.3	4669254	4063768	4455892	5069215	4955354	4642697	8.69
21.0	0.1	3564484	3002298	3417775	3940015	3821460	3549206	10.39
37.0	25	4785414	4351310	4374924	5083551	2283852	4175810	26.36
37.0	15	4250298	3622429	3799084	4468972	1989042	3625965	26.92
37.0	10	3829930	3175164	3410189	4007866	1803471	3245324	26.84
37.0	5	3259437	2653870	2814348	3357056	1467192	2710380	27.85
37.0	3	2820357	2068672	2214060	2611569	1008493	2144630	32.77
37.0	1	1918628	1510942	1684255	1941181	754899	1561981	31.03
37.0	0.5	1530955	1216408	1331409	1568168	583094	1246007	31.92
37.0	0.3	1398938	1070592	1138911	1349724	496342	1090901	32.99
37.0	0.1	1369159	771441	851212	997716	374295	872764	41.36

Table A-11. Dynamic modulus test results, mix 8F

Temp	Freq	Dynamic Modulus (KPa) Surface Course, Field Samples, 25% FRAP / 0% RAS						
(C)	(Hz)	Sample 1	Sample 2	Sample 3	Sample 4	Sample 5	Average	CV
4.0	25	23350806	24986546	24097916	25105828	15038405	22515900	18.83
4.0	15	22164558	23007888	21856987	22543201	21356587	22185844	2.85
4.0	10	19500276	20554837	21732852	22381674	14611766	19756281	15.59
4.0	5	17807766	19493130	20000382	20590927	19881311	19554703	5.38
4.0	3	17510247	17756055	19169042	18894079	18515621	18369009	3.90
4.0	1	14843752	15101640	16081788	16370947	15619418	15603509	4.11
4.0	0.5	13298705	13663744	14995600	14742496	13913415	14122792	5.11
4.0	0.3	12534155	12726053	12736109	13958217	12870849	12965077	4.38
4.0	0.1	10138556	10346680	11162409	11538331	10200375	10677270	5.93
21.0	25	9198290	10177166	9885009	10876259	8984968	9824338	7.77
21.0	15	8278218	9122133	8729842	9956649	8225153	8862399	8.04
21.0	10	7551647	8224340	7954998	8931554	7403879	8013284	7.58
21.0	5	6487597	7015031	6783136	7723235	6254697	6852739	8.25
21.0	3	5401393	5860152	5619822	6429738	5136561	5689533	8.66
21.0	1	3989815	4415041	4282465	4896870	3800321	4276902	9.87
21.0	0.5	3308299	3711779	3588193	4183408	3181956	3594727	10.89
21.0	0.3	2872650	3246660	3147942	3659245	2748275	3134954	11.34
21.0	0.1	1922983	2191957	2157515	2513243	1809801	2119100	12.84
37.0	25	3725570	3156852	3362430	3738671	2964572	3389619	10.12
37.0	15	3124017	2602258	2792872	3130725	2400807	2810136	11.43
37.0	10	2720246	2260546	2411325	2694262	2027976	2422871	12.11
37.0	5	2168926	1780400	1914747	2149904	1619662	1926728	12.29
37.0	3	1555260	1281157	1397314	1638267	1157315	1405863	13.94
37.0	1	1076970	863331	976231	1189765	838714	989002	14.88
37.0	0.5	824968	649057	766928	930807	639913	762335	16.09
37.0	0.3	707135	531807	628083	800432	551097	643711	17.36
37.0	0.1	497160	429275	471800	603673	414418	483265	15.51

Table A-12. Dynamic modulus test results, mix 4F

Temp (C)	Freq (Hz)	Dynamic Modulus (KPa) Base Course, Field Samples, 50% FRAP / 0% RAS Sample 1	Sample 2	Sample 3	Sample 4	Sample 5	Average	CV
4.0	25	32345274	24541332	27496272	32002875	32857397	29848630	12.27
4.0	15	29747635	12935683	18539884	27964104	30403367	23918135	32.52
4.0	10	20858295	24165221	16828554	19375654	29936412	22232827	22.75
4.0	5	29636643	25650356	25147245	28379672	28830569	27528897	7.28
4.0	3	26503444	24606561	22718991	27399504	25258269	25297354	7.13
4.0	1	26173027	22980688	21001337	22642067	25935394	23746503	9.42
4.0	0.5	23075007	21884385	19166540	20333095	23599488	21611703	8.59
4.0	0.3	21876167	20611326	18498216	19763959	19745515	20099036	6.20
4.0	0.1	20221277	18585179	16982470	18109762	21082732	18996284	8.68
21.0	25	18289721	16887113	16190518	17347866	17684411	17279926	4.60
21.0	15	16691114	15105587	14431621	15575376	15991743	15559088	5.52
21.0	10	15572196	14247814	13724889	14625907	15202422	14674646	5.02
21.0	5	14073784	12753334	12414524	13172439	13825131	13247842	5.28
21.0	3	12819220	11496909	10964086	11724988	12131901	11827421	5.89
21.0	1	10408363	9415657	8922284	9516209	9960095	9644522	5.85
21.0	0.5	9150022	8408768	7977971	8562439	8914326	8602705	5.28
21.0	0.3	8482745	7705926	7267021	7856990	8244158	7911368	5.99
21.0	0.1	6571498	6067944	5600487	6115887	6461708	6163505	6.20
37.0	25	7802847	7181997	7318377	8114958	7774478	7638531	5.00
37.0	15	6730491	6654926	6459182	7097015	6967714	6781866	3.74
37.0	10	6067190	6082379	5859379	6381645	6269834	6132085	3.28
37.0	5	5061856	5175551	4869259	5296042	5293339	5139209	3.49
37.0	3	4019534	4129648	3711788	4164016	4053179	4015633	4.47
37.0	1	2966964	3091837	2670758	3033368	2006435*	2753873	16.27
37.0	0.5	2454121	2564521	2180039	2479840	2195973	2374899	7.39
37.0	0.3	2111650	2205156	1828072	2164551	1956039	2053094	7.66
37.0	0.1	1469834	1575847	1193359	1495081	1148367	1376498	13.98

Table A-13. Dynamic modulus test results, mix 6L

Temp	Freq	Dynamic Modulus (KPa) Binder Course, Lab Samples, 40% FRAP / 0% RAS						
(C)	(Hz)	Sample 1	Sample 2	Sample 3	Sample 4	Sample 5	Average	CV
4.0	25		26998192		23099608	24378113	24825304	8.01
4.0	15		26137138		22395762	23835693	24122864	7.82
4.0	10		23955009		21156783	22477368	22529720	6.21
4.0	5		22106841		20094653	21069964	21090486	4.77
4.0	3		21862243		19512355	20273129	20549243	5.83
4.0	1		19220042		16304598	18056387	17860342	8.22
4.0	0.5		17657622		16009322	16899781	16855575	4.89
4.0	0.3		16498835		15085650	15927704	15837396	4.49
4.0	0.1		14018916		12868342	13758434	13548564	4.45
21.0	25	10694294	12627251	12564557	13428171	13248886	12512632	8.67
21.0	15	9628119	11665463	11400990	12052500	11757614	11300937	8.53
21.0	10	8900273	10734165	10483845	5777004	10792208	9337499	22.88
21.0	5	7763542	9395565	9325652	8800467	9515017	8960049	8.06
21.0	3	6820961	8346432	8291943	8711287	8596717	8153468	9.38
21.0	1	5453771	6609728	6649740	7061903	6921603	6539349	9.72
21.0	0.5	4718734	5786120	5865346	6196600	6141580	5741676	10.42
21.0	0.3	4378299	5288121	5308626	5630934	5609442	5243084	9.72
21.0	0.1	3362221	4031153	4081000	4349786	4351302	4035093	10.02
37.0	25	5277616	5763442	4772838	5563250	5396702	5354769	6.97
37.0	15	4655850	5055095	4276525	4790579	4783420	4712294	6.02
37.0	10	4162463	4465993	3867934	4285264	4349336	4226198	5.40
37.0	5	3474129	3708689	3227346	3562341	3597729	3514047	5.15
37.0	3	2748332	2913736	2461052	2728995	2786959	2727815	6.07
37.0	1	2133565	2151045	1955828	2136795	2208139	2117074	4.49
37.0	0.5	1737887	1838414	1658572	1834193	1847927	1783399	4.64
37.0	0.3	1561821	1554863	1441007	1631490	1644540	1566744	5.17
37.0	0.1	1231480	407931	1045898	1135002	1142515	992565	33.58